AD-A033 440 CONSTRUCTION ENGINEERING RESEARCH LAB (ARMY) CHAMPAI--ETC F/G 13/2
STUDY OF ARTICULATED CONCRETE REVETMENT MATTRESS: TEST AND ANAL--ETC(U)
NOV 76 F KEARNEY, J PRENDERGAST

UNCLASSIFIED CERL-TR-M-194 NL

| OF |
AD A033440

END

DATE FILMED
2-77

construction
engineering
research
laboratory

TECHNICAL REPORT M-194
November 1976

STUDY OF ARTICULATED CONCRETE REVETMENT MATTRESS: TEST AND ANALYSIS—RESULTS OF FY 1975 PROGRAM

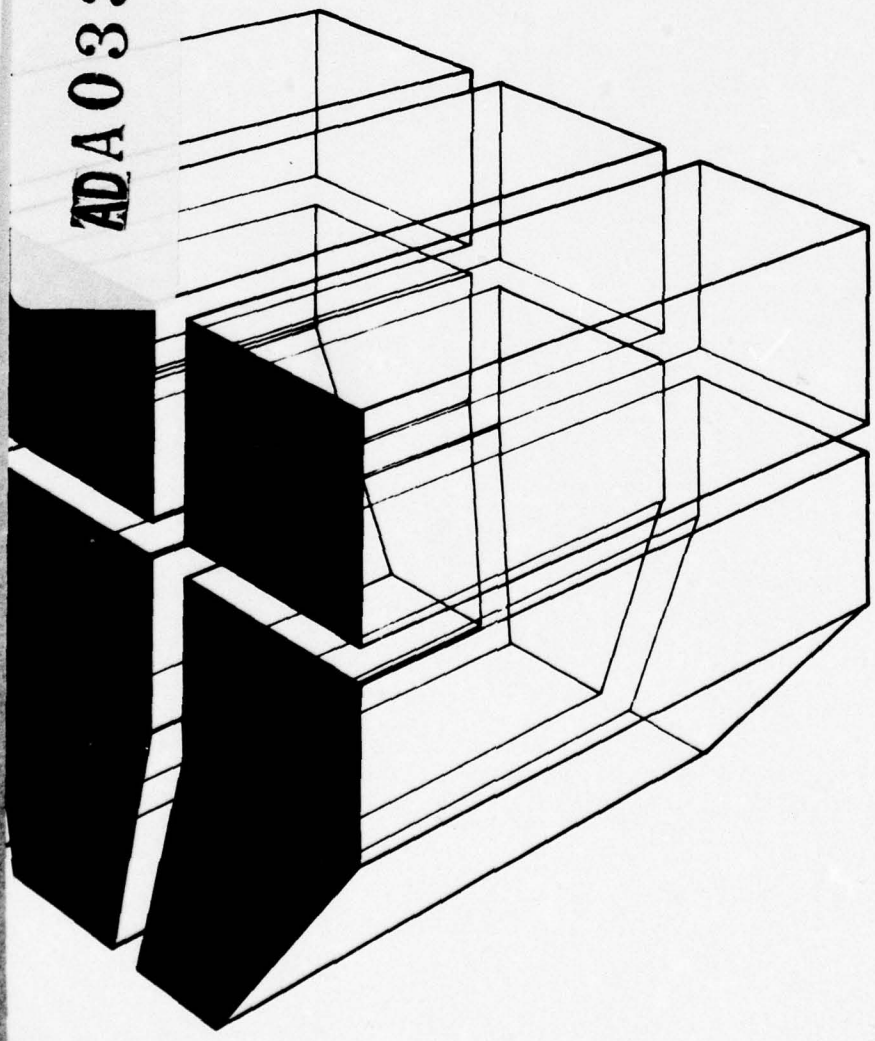

by
F. Kearney
J. Prendergast

CERL

The contents of this report are not to be used for advertising, publication, or promotional purposes. Citation of trade names does not constitute an official indorsement or approval of the use of such commercial products. The findings of this report are not to be construed as an official Department of the Army position, unless so designated by other authorized documents.

DESTROY THIS REPORT WHEN IT IS NO LONGER NEEDED
DO NOT RETURN IT TO THE ORIGINATOR

UNCLASSIFIED

SECURITY CLASSIFICATION OF THIS PAGE *(When Data Entered)*

REPORT DOCUMENTATION PAGE

READ INSTRUCTIONS BEFORE COMPLETING FORM

1. REPORT NUMBER: CERL-TR-M-194	2. GOVT ACCESSION NO.
3. RECIPIENT'S CATALOG NUMBER	
4. TITLE (and Subtitle): STUDY OF ARTICULATED CONCRETE REVETMENT MATTRESS: TEST AND ANALYSIS--RESULTS OF FY 1975 PROGRAM.	5. TYPE OF REPORT & PERIOD COVERED: FINAL rept.
	6. PERFORMING ORG. REPORT NUMBER
7. AUTHOR(s): F. Kearney, J. Prendergast	8. CONTRACT OR GRANT NUMBER(s): IAO LMMDC-FA-75-2
9. PERFORMING ORGANIZATION NAME AND ADDRESS: CONSTRUCTION ENGINEERING RESEARCH LABORATORY, P.O. Box 4005, Champaign, IL 61820	10. PROGRAM ELEMENT, PROJECT, TASK AREA & WORK UNIT NUMBERS
11. CONTROLLING OFFICE NAME AND ADDRESS	12. REPORT DATE: November 1976
	13. NUMBER OF PAGES: 65
14. MONITORING AGENCY NAME & ADDRESS *(if different from Controlling Office)*: 66p.	15. SECURITY CLASS. *(of this report)*: Unclassified
	15a. DECLASSIFICATION/DOWNGRADING SCHEDULE

16. DISTRIBUTION STATEMENT *(of this Report)*

Approved for public release; distribution unlimited.

17. DISTRIBUTION STATEMENT *(of the abstract entered in Block 20, if different from Report)*

18. SUPPLEMENTARY NOTES

Copies are obtainable from National Technical Information Service
Springfield, VA 22151

19. KEY WORDS *(Continue on reverse side if necessary and identify by block number)*

revetments
articulated concrete mattresses
structural analysis

20. ABSTRACT *(Continue on reverse side if necessary and identify by block number)*

This report presents results of the fiscal year 1975 (FY 75) portion of a program to determine the magnitude and distribution of forces developed during launching of articulated concrete mattresses on the banks of the lower Mississippi River and to provide guidance for design changes in the mat structure. The FY 75 work involved monitoring the launching of some of the approximately 10,000 experimental squares cast with two 4000-lbf (17.8 kN) breaking strength longitudinal wires instead of three. Results indicate that the two-longitudinal-wire mat will have adequate strength. Results also confirm conclusions

(cont on p 1473B)

DD FORM 1 JAN 73 1473 A EDITION OF 1 NOV 65 IS OBSOLETE

405 279

UNCLASSIFIED

SECURITY CLASSIFICATION OF THIS PAGE *(When Data Entered)*

Block 20 continued.

drawn from earlier work in the program (F. Kearney and J. Prendergast, *Study of Articulated Concrete Revetment Mattress: Test and Analysis–Results of FY 1974 Program,* U. S. Army Construction Engineering Research Laboratory Technical Report M-94/ADA021774, 1976).

by these authors

FOREWORD

This study was performed for the Memphis Engineering District, Lower Mississippi Valley Division (LMVD), U. S. Army Corps of Engineers under IAO LMMDC-FA-75-2, dated 30 July 1974. Mr. B. D. Gray is project coordinator. Personnel most closely associated with the project were Messrs. J. Graham and H. Harz (LMVD); Messrs. R. B. Deason, C. L. Curry, J. Creed (Memphis District); and Messrs. J. Harrison and R. Campbell (Vicksburg District). Professor V. J. McDonald of the Civil Engineering Department, University of Illinois at Urbana-Champaign, was Consultant to the U. S. Army Construction Engineering Research Laboratory (CERL) for this project.

The study was performed by the Metallurgy Branch and the Structural Mechanics Branch, Materials and Science Division, CERL. CERL personnel conducting this investigation included Dr. J. Prendergast and Messrs. F. Kearney, H. Stringfellow, R. Neu, and T. Kenney.

Dr. G. Williamson is Chief, Materials and Science Division; Dr. A. Kumar is Chief, Metallurgy Branch; and Dr. W. Fisher is Chief, Structural Mechanics Branch.

COL J. E. Hays is Commander and Director of CERL and Dr. L. R. Shaffer is Deputy Director.

CONTENTS

FIGURES

FIGURES (cont'd.)

TABLES

STUDY OF ARTICULATED CONCRETE REVETMENT MATTRESS: TEST AND ANALYSIS – RESULTS OF FY 1975 PROGRAM

1 INTRODUCTION

Background

For the past 45 years, the Corps of Engineers has used articulated concrete mattresses (mats) as revetments on the banks of the lower Mississippi River to prevent erosion and to aid in maintaining channel stability. Placement of these mats is a costly procedure; the average cost is $1 million/mi ($625,000/km), for a total annual cost of $35 to $40 million.

A mattress is composed of units called "squares," which are nominally 4 ft (1.2 m) wide and 25 ft (7.6 m) long. Each square is composed of uniform concrete blocks connected with a corrosion-resisting wire fabric unit made of either stainless steel wire or bimetallic copper-clad steel wire. Corrosion-resisting twist wires and parallel wire cables connect the squares to form a mattress. About 600,000 units or 125 million lin ft (38.1 million m) of wire are required annually at a cost of between $4 and $6 million. (See Appendix A for a detailed description of the mats.)

A value engineering study has indicated that substantial economic benefits could be achieved by changing the design of these mats. In March 1972, the U. S. Army Construction Engineering Research Laboratory (CERL) was asked to determine the magnitude and distribution of forces developed during launching of the mats. An analytical study was also requested to provide guidance for design changes in the mat structure.

CERL conducted field tests during the fiscal year 1973 (FY 73) launch season – August through December 1972. The analytical study and laboratory tests began at the same time and continued until June 1973. Appendix B summarizes the results of that program, which are fully reported in CERL Interim Report M-84.[1]

The major observations of the initial study were: (1) that the bracket wire and longitudinal wires had much more than adequate strength and (2) that the highest forces in the longitudinal wires were occurring on the launch plant as the mat went over the side. It was recommended that the possibility of using two (rather than the three currently used) 4000-lbf (17.8 kN) breaking strength longitudinal wires be investigated.

CERL performed additional field tests and expanded the analytical study during FY 74. The results of that program, which are reported in CERL Technical Report M-94[2] and summarized in Appendix C, verified that maximum longitudinal wire forces are produced as the mat traverses the launch plant edge. The work also indicated the structural feasibility of reducing the diameter of the longitudinal wires from 0.162 in. (4.1 mm) to 0.141 in. (3.6 mm).

As a result of these two studies, it was decided to launch approximately 10,000 squares cast with two 4000-lbf (17.8 kN) breaking strength longitudinal wires (0.162 in. [4.1 mm] diameter) during the FY 75 launch season (August through December 1974). This report presents the results of CERL's monitoring of some of these launches.

Objective

The objective of this study was to measure the performance of two-longitudinal-wire test mattresses subjected to different launch conditions. The data were to be used to confirm the results of previous CERL tests and analyses which indicated that such a mattress would be structurally feasible.

Approach

Effective demonstration of the structural adequacy of a two-longitudinal-wire mat required that the 10,000 test squares be launched under the most adverse loading conditions (as determined by previous testing and experience of Corps of Engineers Lower Mississippi Valley Division [LMVD] personnel); these conditions were:

1. deep water (more than 100 ft [30.5 m] deep)
2. turbulent flow
3. launching with "mat puller."

The squares were apportioned between the Memphis and Vicksburg Districts to permit evaluation of the sig-

[1] F. Kearney and F. Plummer, *Study of Articulated Concrete Revetment Mattress: Test and Analysis*, Interim Report M-84 (U. S. Army Construction Engineering Research Laboratory [CERL], 1974).

[2] F. Kearney and J. Prendergast, *Study of Articulated Concrete Revetment Mattress: Test and Analysis – Results of FY 1974 Program*, Technical Report M-94/ADA021774 (CERL, 1976).

nificance of mechanical differences in the two Districts' mat-sinking units.

The logistics of transporting the test squares from the casting fields to the launching plants were also considered in selecting launch site locations. The number of squares launched at the selected launch sites was as follows:

1. 5000 copperweld squares were launched by the Memphis District plant at Goldbottom, LA (deep water and turbulence).

2. 2500 stainless steel squares were launched by the Memphis District plant at Manchac, LA (deep water and turbulence).

3. 2500 stainless steel squares were launched by the Vicksburg District plant at Cross Bayou, LA (deep water and mat puller).

CERL monitored some of these launches using the mechanical and electromechanical gages previously developed for mattress measurements. Appendix D describes the gages. Appendix E contains the instrumentation location charts for each test. Since previous work[3] showed that the maximum force levels occur close to the mat's upstream edge, as many gages as possible were installed in square three. Gaging squares one and two was usually not possible because of double layering of mattress squares. When mat physical irregularities or launching exigencies precluded placing the gages in square three, the most practicable upstream position was selected.

Electrical signals from the electromechanical forces gages were recorded on Ampex Model ES-100 instrumentation tape recorders conforming to Inter-Range Instrumentation Group standards. The recording bandwidth was 0 to 6.75 kHz; the playbacks presented in this report were made on a chart recorder having a response of 0 to 150 Hz. The electrical signals do not contain some of the peak forces recorded by the mechanical gages because of the 150-Hz upper frequency response limit. However, that the peaks were recorded on the magnetic tape was verified by using voltage peak detectors during playback at CERL. A continuous narration (voice log) was made of the launch progress as the electrical data signals were recorded.

[3]F. Kearney and J. Prendergast, *Study of Articulated Concrete Revetment Mattress: Test and Analysis – Results of FY 1974 Program*, Technical Report M-94/ADA021774 (CERL, 1976).

Low force levels (less than 500 lbf [2.2 kN]) found during FY 73 and 74 field tests on bracket wires showed that the strength of the bracket wire connections to the launch cable was excessive (greater than 4000 lbf [17.8 kN]). Therefore, use of smaller wrapping, which would result in a material savings, was considered for these connections. Field and laboratory tests using smaller diameter bracket wrapping wire were conducted to resolve whether the slip resistance of the smaller wire would be adequate and whether the automatic wrapping tool would accommodate it.

The New Orleans District uses a redundant or auxiliary cable in the bank tie-off system in conjunction with the regular launch cable; this corrosion-resistant cable's three strands each measure 0.181 in. (4.6 mm) in diameter, which is 0.019 in. (0.5 mm) larger than the mating fabric wire (0.162 in. [4.1 mm] diameter). Tests comparing the failure strength of the auxiliary tie-off wire for 0.181 in. (4.6 mm) diameter, and 0.162 in. (4.1 mm) diameter were conducted at CERL to determine if the connection using the smaller wire would have acceptable strength.

2 FIELD AND LABORATORY TESTS

Mechanical Gage Tests

Appendix E presents the force levels in the two-longitudinal-wire* mat on the Memphis and Vicksburg sinking units measured by the brass mechanical gage targets** during the FY 75 launching season. Figure 1 is a histogram summarizing the mechanical force gage readings in 500-lbf (2.2 kN) intervals. The histograms for the FY 73 and FY 74 tests are included in Figures 2 and 3 for comparison.‡

As many gages as possible were installed in square three, since the maximum force levels occur in the upstream portion of the mat, as shown in Appendix D (Figure D2). Mat physical irregularities or launching exigencies sometimes precluded this location; in these instances, the alternate location was the most practicable upstream position.

*See Appendix A for explanation of the terminology and mattress array.

**See Appendix D for description of the force gages.

‡The FY 73 histogram shows a preponderance of bracket wire tests, since it was thought that these wires might be the weakest link in the mat array; since the tests and analysis showed this was not the case, bracket wire testing was discontinued during the FY 74 launch season.

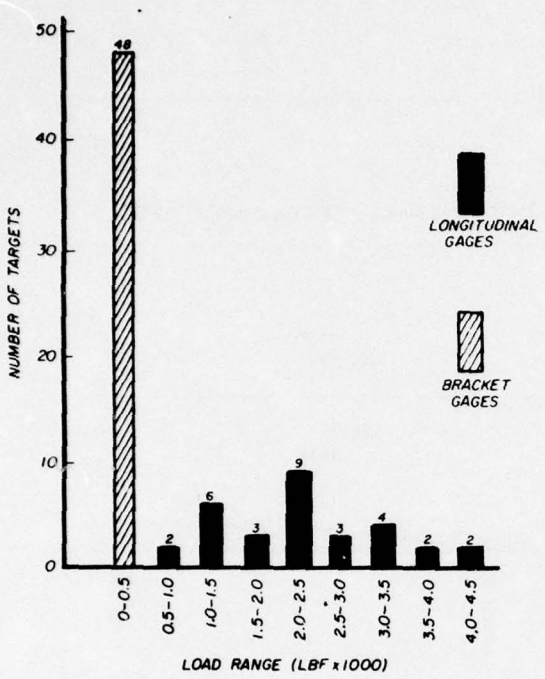

Figure 1. Summary of FY 75 tests – distribution of measured forces. SI conversion factor: 1 lbf = 4.448 N.

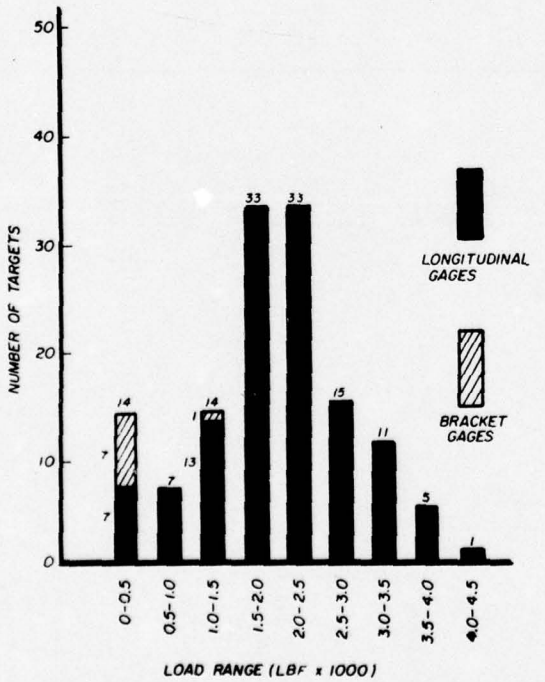

Figure 2. Summary of FY 74 tests – distribution of measured forces. SI conversion factor: 1 lbf = 4.448 N.

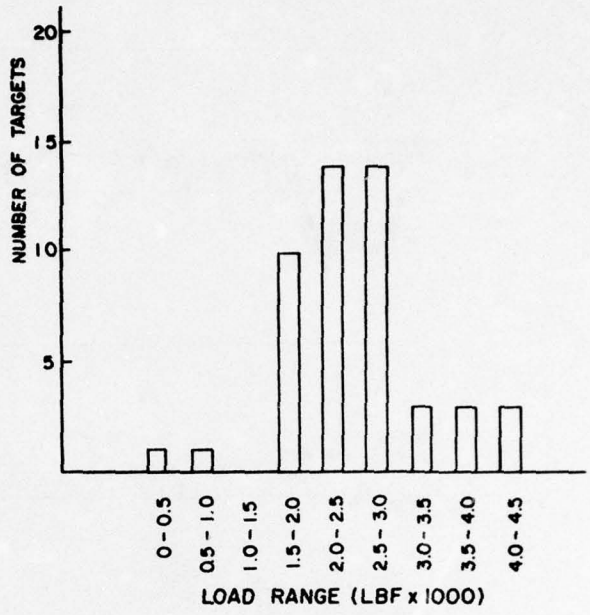

Figure 3. Summary of FY 73 tests – distribution of measured forces. SI conversion factor: 1 lbf = 4.448 N.

As indicated by the histograms (Figures 1 through 3) and the instrumentation data sheets in Appendix E, the mechanical gage data are very similar to those obtained in FY 73 and 74.

Electromechanical Gage Tests

Figures 4 and 5 are typical recordings of the electrical data obtained during the FY 75 testing. The data were recorded in fairly deep water at launches 13-14 and 20-21. Thus, the effect of the dead weight of several launches hanging over the side of the mat-sinking unit can be seen. The water velocities during the tests ranged from 4 to 6 ft/sec (1.2 to 1.8 m/sec) with stochastic loading due to turbulence.

As had been observed in previous testing, the longitudinal wires reached force levels of approximately 1000 lbf (4.4 kN) as soon as a launch began.

CERL Interim Report M-84 and Technical Report M-94 (summarized in Appendices B and C) discussed the effect of the launch finger apron. In the FY 75 tests, it was observed that high force levels were induced in the longitudinal wires as they passed over these "fingers"; this effect is most noticeable in Figure 6, which is a typical trace of electrical data signals from a three-wire mat. Trace A of Figure 6 shows an

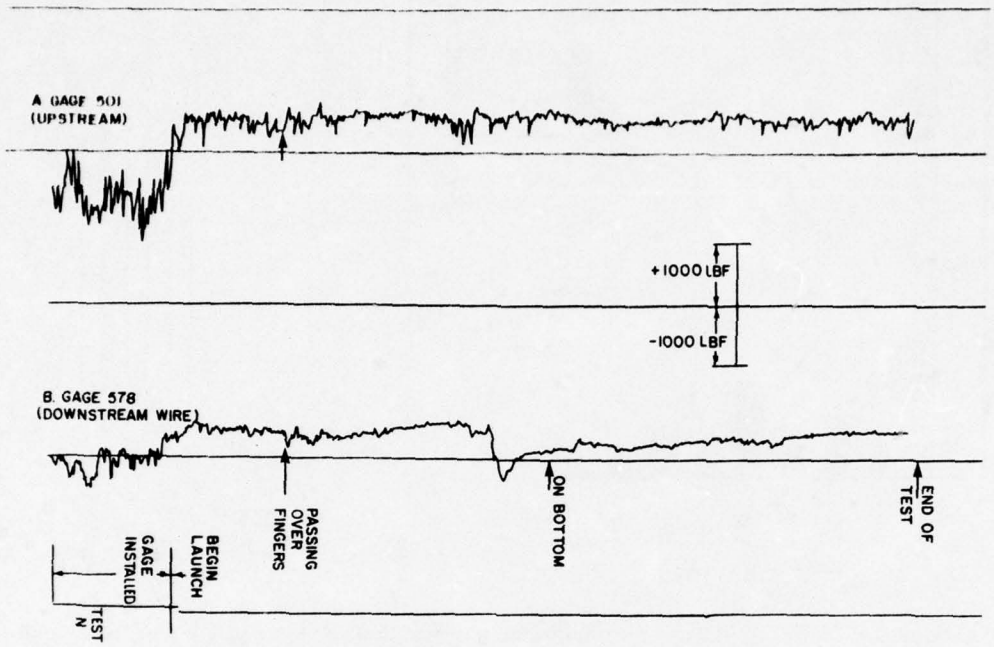

Figure 4. Tracing from electromechanical gage, two-wire system; 80-ft (24.4 m) water depth. SI conversion factor: 1 lbf = 4.448 N.

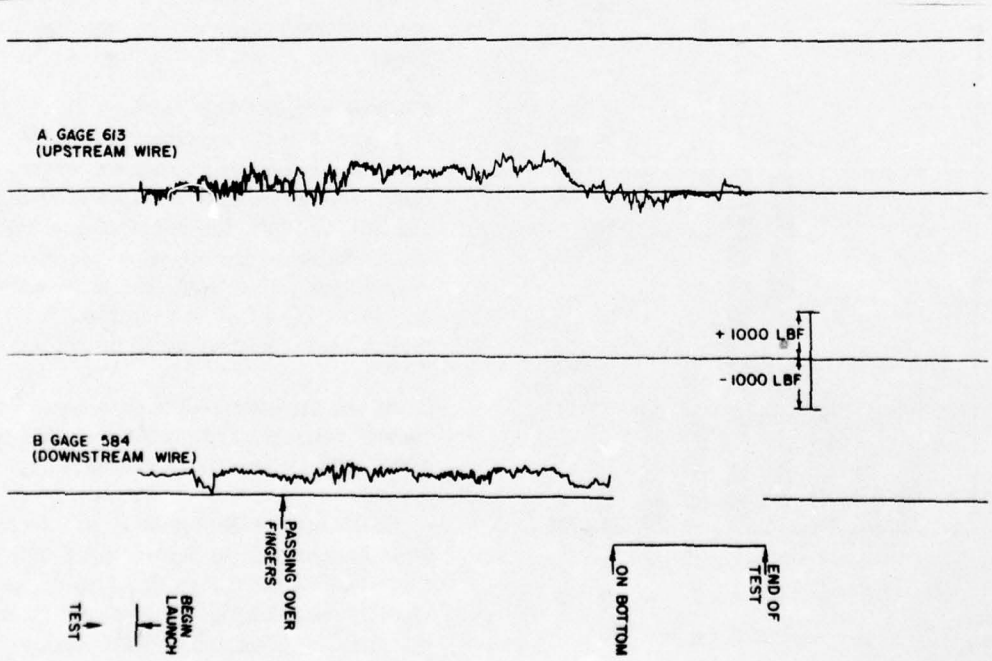

Figure 5. Tracing from electromechanical gage, two-wire system; 120 ft (36.6 m) water depth. SI conversion factor: 1 lbf = 4.448 N.

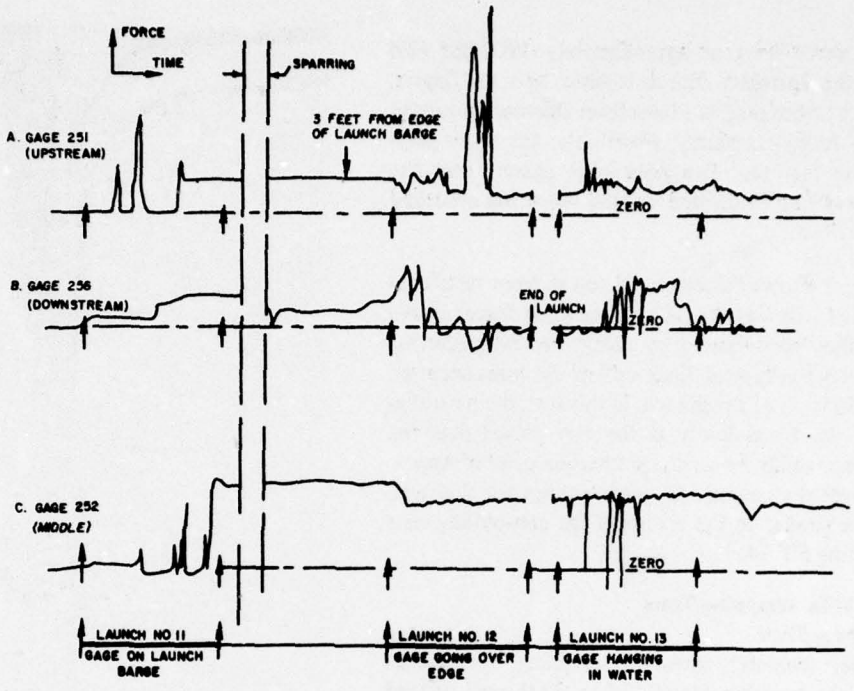

Figure 6. Tracing of electrical longitudinal wire gages – force vs time, three-wire system.

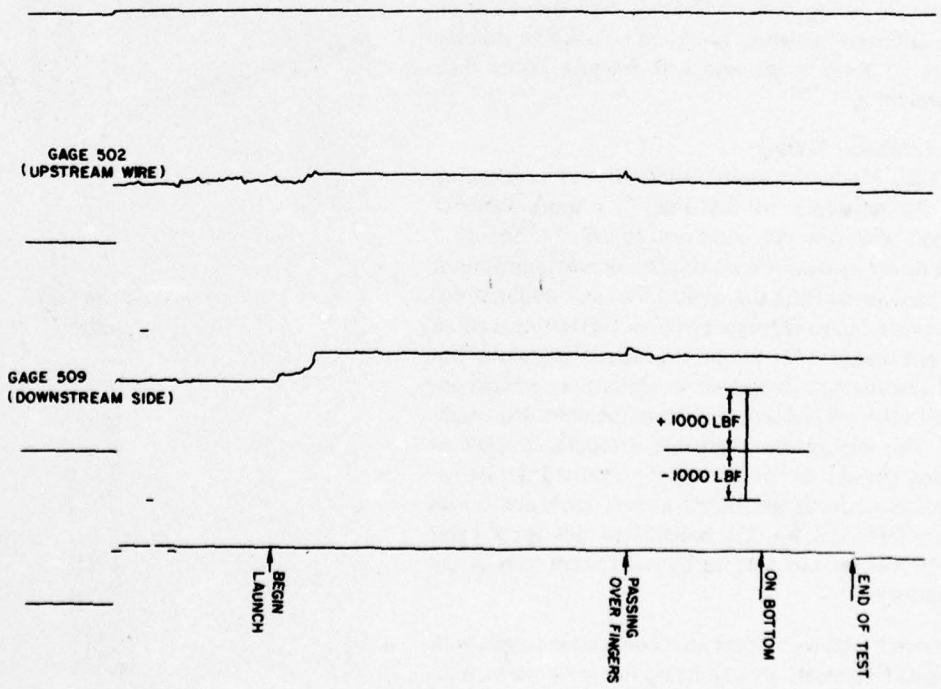

Figure 7. Tracing of electromechanical gages on mat placed using mat puller. SI conversion factor: 1 lbf = 4.448 N.

induced force level of approximately 1900 lbf (8.4 kN) for the upstream wire as it passes over the fingers. For the two-wire mat, the force level fluctuation caused by these fingers is hardly discernible; for some playbacks, the fact that the gages were passing over the fingers was only indicated by the voice log recorded during the test.

Figure 7 shows the electrical traces from tests conducted at Cross Bayou, LA to determine forces in the longitudinal wires caused by using the mat puller. As can be seen, the typical "load-up" of the wires occurred at the initiation of the launch. In this test, the perturbations in the force levels as the mat passed over the fingers can readily be seen. The chart on p. 63 of Appendix E gives the mechanical gage readings for this test, which are similar to the results of the mat-pulling tests done during FY 74.

Bracket Wire Wrapping Tests

Unwrapping Tests

Smaller diameter wires for wrapping the bracket wires to the launch cable (0.114 in. [2.9 mm] instead of 0.128 in. [3.3 mm] diameter wire) were tested on several mats during the FY 75 launch season. (Laboratory tests had previously been conducted at CERL in FY 74 and 75 using fixtures to apply forces that simulate the "unwrapping" forces the connection would experience during launch.) The field tests showed negligible difference between the two wire sizes. The ultimate failure of these wraps was wire fracture rather than "unwrapping."

Slip Resistance Testing

CERL conducted several laboratory tests comparing the slip resistance of 0.114-in. (2.9 mm) diameter bracket wire wrapping connections and 0.128-in. (3.3 mm) diameter connections. Electronic instrumentation was used to measure the applied load and resultant displacement due to slippage; however, this testing method was not practical for use on the mat-sinking units. The field test method devised used white spray enamel applied to the wrapped connection in the unloaded condition. This application resulted in a smooth, continuous coating (Figure 8). When slippage occurred during application of load, unpainted launch cable metal was exposed (Figure 9). The validity of this spray paint test procedure was verified by correlation tests in the laboratory.

Several tests on bracket wire connections made with the small diameter wire utilizing the spray paint technique were conducted at Manchac, LA and Goldbottom, LA. Slippage was not observed in any of these tests.

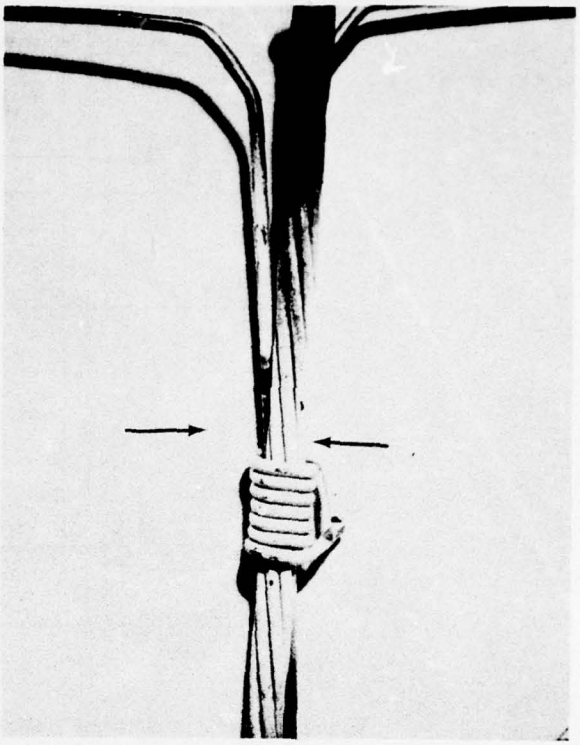

Figure 8. Painted connection before loading.

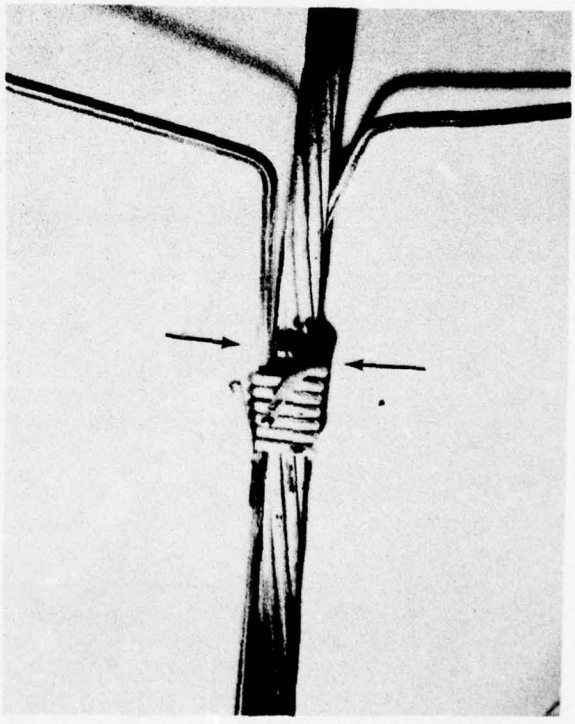

Figure 9. Painted connection after loading. Slippage shows by exposure of bare metal.

None of the tests on the mat-sinking units using small diameter wrapping wire resulted in untoward events due to slippage or unwrapping.

Auxiliary Shore Tie-Off Wire Tests

Twenty four connections were made between launch one longitudinal wire end loops and auxiliary copperweld shore tie-off wire as is done in the New Orleans District mat anchor system; 12 used the 0.181-in. (4.6 mm) diameter copperweld shore wire that is presently used, and 12 used 0.162-in. (4.1 mm) diameter wire (fabric wire diameter). Figures 10 and 11 give typical load-deflection curves for currently used shore tie-off wire and fabric wire, respectively. As the figures show, the conventional system has a load capacity about 500 lbf (2.2 kN) greater than the system using the fabric size wire.

3 SUMMARY AND DISCUSSION OF FY 73 THROUGH 75 PROGRAM

Bracket Wires

At the outset of the program, it was thought that the mat element subjected to the most loading was the bracket wires. However, the field testing and subsequent analysis indicated that the forces on the bracket wires were less than 500 lbf (2.2 kN). Even removing half of the bracket wire connections did not produce any discernible increase in the force measurements.

The belief that bracket wires had high force levels was engendered by the so-called "zipper effects," which were one of the revetment problems mentioned at the initial project briefings. Zipper effects involve a chain-type failure of bracket wire connections along the entire length of a launch cable. It was determined that this zipper effect has not occurred since the automatic pneumatic wrapping tool has been employed. Previously, the bracket wire attachment system consisted of three or four rigid cable clamp connections accompanied by loose twist connections. This resulted in high stress concentrations at the rigid cable clamp connections; these concentrations initiated failure, which propagated along the launch cable by breaking the loose twist connections.

Use of the wrapping tool has achieved more uniform stress distribution and has obviated stress concentrations. In addition, the bracket wire wrap formed by the pneumatic tool imparts a springiness or shock-absorbing mechanism to the mattress assembly. Therefore, when abnormally high forces occur, the load is not concentrated at three or four rigid connections; rather, it is distributed among the wrapped connections.

Presently, the bracket wires are most prone to failure during handling of the squares in the casting fields and the launch plant prior to placement. CERL Interim Report M-84 discusses this problem.

Fluidic Forces

Appendix D summarizes development of a model of the pressure forces caused by the river current; the analysis of the model assumed uniform forces such as would occur in laminar flow. In most instances, these conditions prevail and the analyses are valid. The difficulty often experienced by LMVD and CERL personnel in selecting test sites along the river that would provide rough, turbulent water to produce adverse and difficult launch conditions supports this assumption. Prior to CERL quantitative force measurements, visual observations by LMVD revetment personnel were the only source of descriptive effects of rough water on mat placement. These observations were grouped into the following categories:

1. Launch cable fracture. In this type of fracture, one or more of the 3/8 in. (9.5 mm) or 5/16 in. (7.9 mm) diameter launch cables fracture, causing a droop in the mat in the region of fracture. The severity and extent of this defect depend on the number of launch cables broken.

2. Automatic cut-off. In this case, all launch cables break, causing the entire mat to sink in an uncontrolled condition. In nearly all cases, the failure initiates at the upstream cable and propagates along the width of the mat; this automatic cut-off usually occurs as the last launch is hanging over the side of the sinking unit.

Normal cut-off of the mat is controlled by moving the sinking unit into the river channel until the entire mat is on the bottom; the launch cables are then manually cut.

If the mat sinks properly after an automatic cut-off, the failure is inconsequential; however, if it folds or collapses either longitudinally or laterally, another mat must be placed.

3. Zipper failure. In this case, all bracket wire connections fail; the failure propagates from the mat squares in the river along the launch cable up to the sinking unit deck. However, as mentioned previously, this failure has not occurred since the automatic wrapping tool has been used.

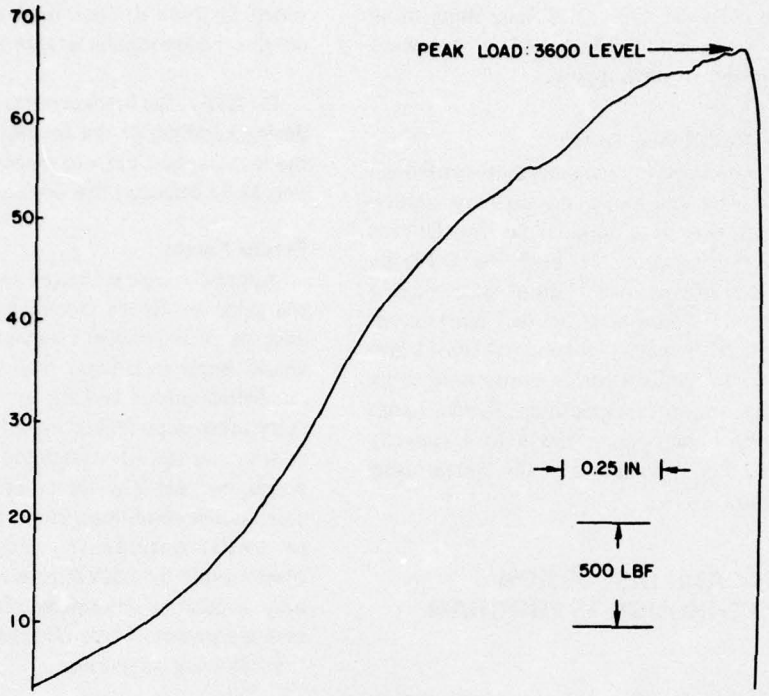

Figure 10. Auxiliary shore tie-off load vs deflection test; 0-181-in. (4.6 mm) diameter shore wire. SI conversion factor: 1 lbf = 4.448 N.

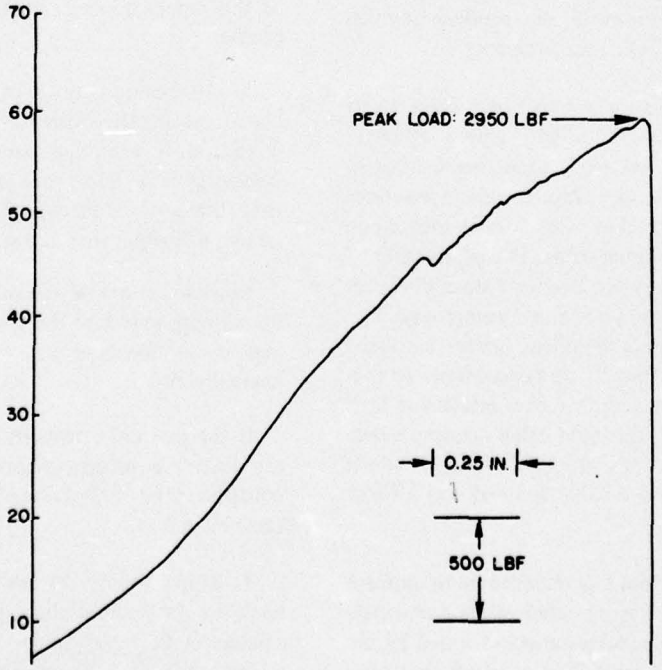

Figure 11. Auxiliary shore tie-off load vs deflection test; 0.162-in. diameter (4.1 mm) shore wire. SI conversion factor: 1 lbf = 4.448 N.

4. Floating mattress. The floating mattress phenomenon involves several launches or, in some cases, almost the entire mat actually floating on the river surface and then gradually sinking–usually with no deleterious results. This curious anomaly was thought to induce severe forces.

In each of these abnormal situations (except the zipper failure), CERL had gages installed and obtained definitive data. These field data, which are discussed in detail in CERL Technical Report M-94, indicate that fluidic forces are not as large as previously believed and validate the models developed.

4 CONCLUSIONS

Based on a review of the field data from the FY 74 and 75 test programs and the analysis conducted with the multi-square force distribution model discussed in Appendix C, it was concluded that:

1. The results of the FY 75 test program are in good agreement with the results of the FY 74 test program, and the conclusions and recommendations developed for the FY 74 study remain valid.

2. The FY 74 and 75 field data collected and the analysis conducted with the multi-square force distribution model still suggest that the peak forces are induced in the longitudinal connection wires (end-twist-tie connections) as the mat passes over the launch finger apron.

3. Based on the conditions assumed in the analysis, the field test data, and the expected ultimate capacities of the 0.162 in. (4.1 mm) diameter wires, a two-wire 0.162 in. (4.1 mm) diameter end-twist-tie and longitudinal wire system appears to have adequate "average" strength.

4. Based on the average value of the individual end-twist-tie connection force of 2.49 kips (11.1 kN) and the expected ultimate capacities of the individual end-twist-tie system made from either stainless steel or copper clad 0.141 in. (3.6 mm) diameter wire, it appears that a two-wire 0.141 in. (3.6 mm) diameter end-twist-tie and longitudinal wire system will have adequate "average" strength. However, due to the distribution of the measured end-twist-tie forces and the estimated ultimate capacities of the end-twist-ties, some connections can be expected to undergo distress and perhaps failure when the more severe loadings are experienced.

5 RECOMMENDATIONS

Based on the results of the entire program (FY 72 through 75), the following recommendations are made:

1. A two-longitudinal wire, 4,000-lb tensile strength square (0.161 in. [4.1 mm] diameter) should be used.

2. The handling system at casting fields and launch plants should be modified to allow use of 3,000-lb bracket wires.*

3. The number of bracket wire wraps per square should be reduced from 20 to 10.

4. Auxiliary corrosion-resistant shore tie-off wire strength should be reduced to the same wire strength as fabric.

5. Based on the forces developed in this study and the shore pull-out tests previously determined,[4] the entire launch cable system should be evaluated to reduce overdesign of shore tie-off methods.

6. Field tests should be conducted to determine the adequacy of a two-wire 0.141 in. (3.6 mm) diameter longitudinal wire mat.

---

*In view of the small bracket wire forces measured during launch, bracket wire tensile strength could be reduced to 1000 to 1500 pounds if handling techniques could be appropriately modified.

[4] *Shore Anchor Pull-Out Tests; Force Study BPP No. 8* (Revetment Operations Improvement Board, Memphis Engineer District, February 1966).

APPENDIX A: MATTRESS GEOMETRY AND TERMINOLOGY

Figures A1 and A2 show the mattress configuration used in the field tests.

The term "square" refers to a basic assembly of twenty 46-1/4 in. x 14 in. (1.2 m x 0.4 m) concrete blocks cast with corrosion-resistant wire fabric which runs laterally and longitudinally and forms a structure with overall dimensions of 25 ft x 4 ft x 3 in. (7.6 m x 1.2 m x 76.2 mm). The lateral wires are referred to as "bracket" wires.

These squares are assembled into an articulated array by connecting the longitudinal end loops (detail B, Figure A2) and the bracket wires (detail S, Figure A1). A pneumatic wrapping tool is used to make the mechanical ties.

The articulated system is assembled on the matsinking unit to form a mattress which is an array of L x S; L = number of launches (length) and S = number of squares. The term "launch" refers to a row of as many as 35 squares.

Figure A3 is an overview of the launch operation showing the squares connected in the horizontal direction. The water depth and river bottom grade determine the number of launches (length) of a particular mattress.

Launch numbers start at the shore and increase as placement proceeds out into the channel. Square numbers start at the mooring barge (upstream edge – extreme left, Figure A3) and increase downstream; square one is always farthest upstream.

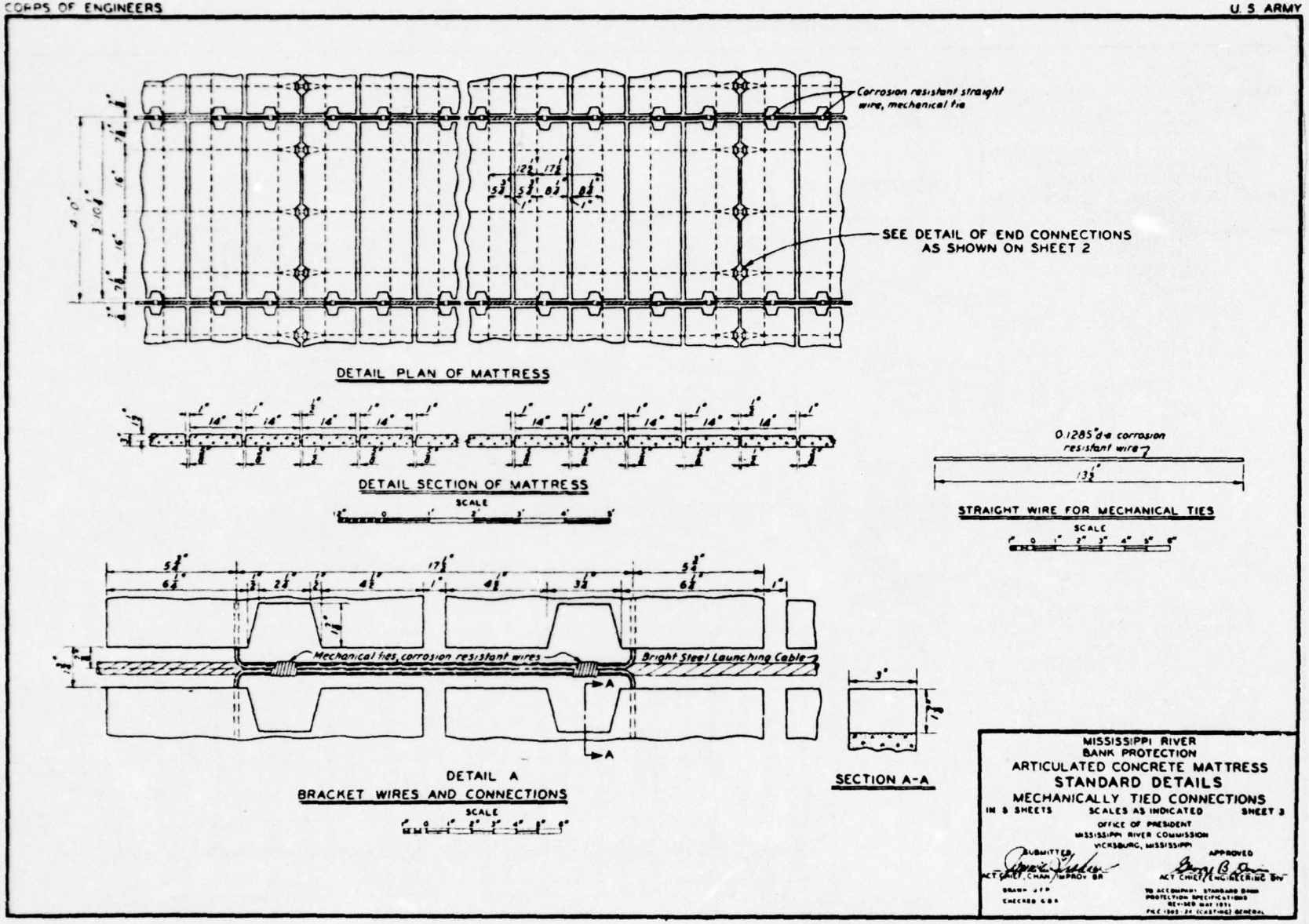

Figure A1. Test mattress and mechanical-manual tie wraps for 20-block square.

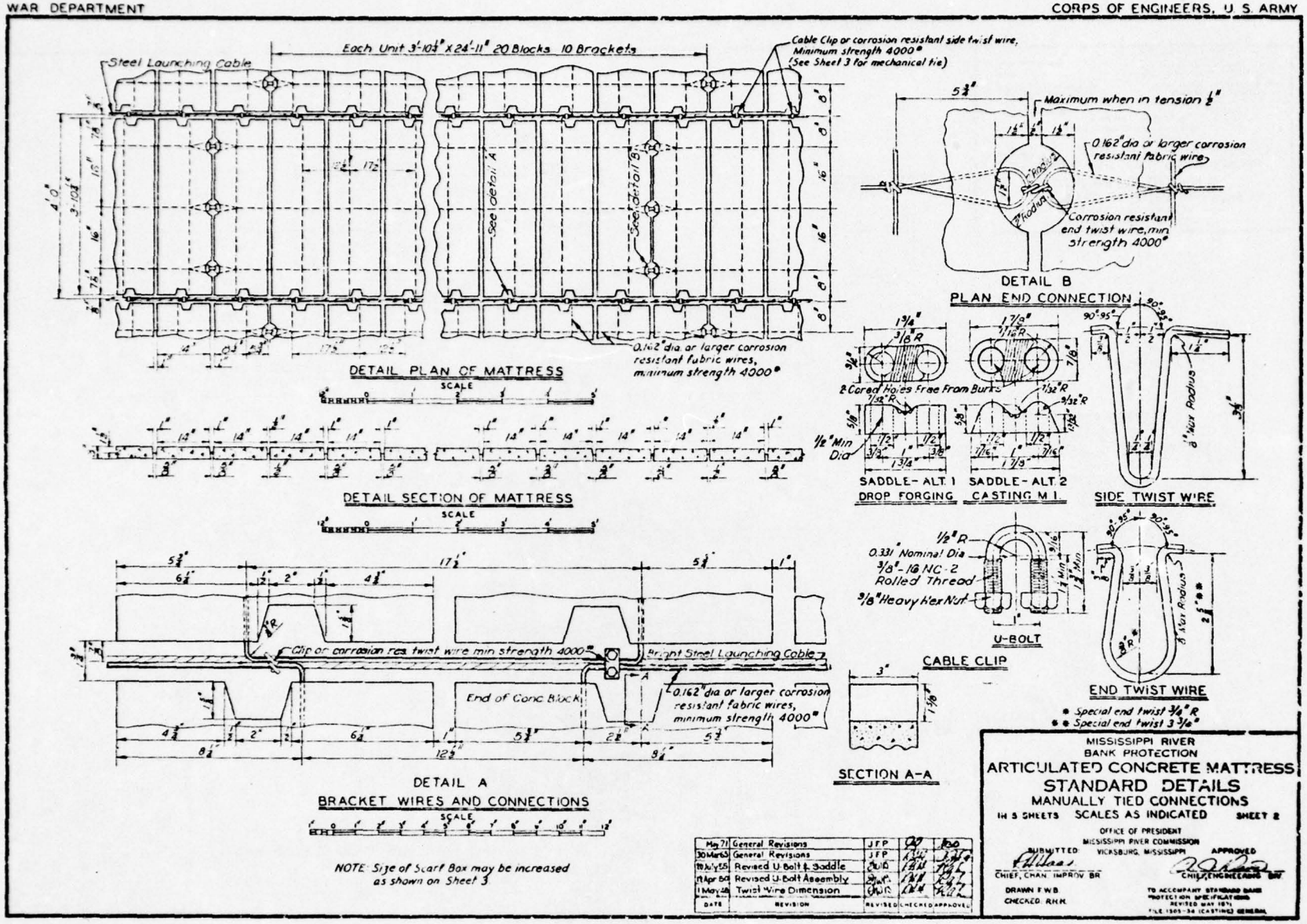

Figure A2. End twist connections for three longitudinal wires.

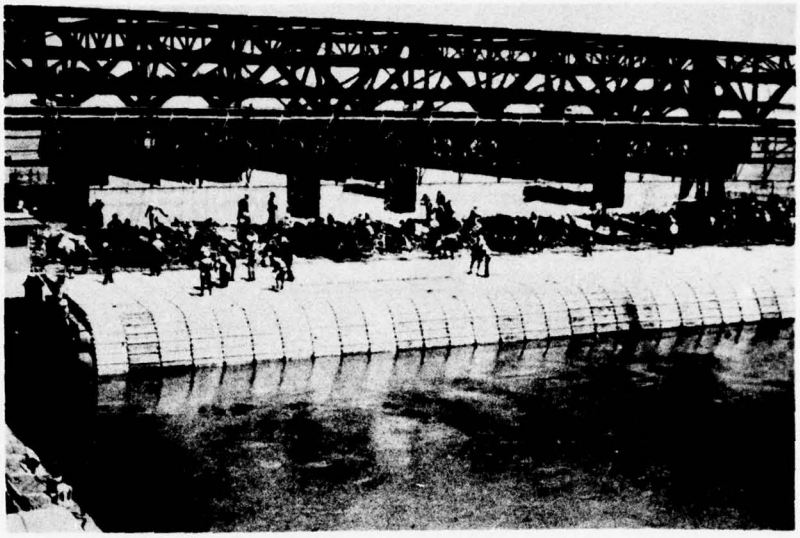

Figure A3. Overview of launch operation.

APPENDIX B: HYDRODYNAMIC FORCE MODEL

Scope of Evaluation

This appendix summarizes the results of the FY 73 work, which is fully reported in CERL Interim Report M-84.[5] The major mat components considered in this study were the longitudinal wires, the bracket wires, and their associated connecting ties and wraps. The launch cable system was considered in a previous report,[6] and was not evaluated in this investigation.

The primary tasks undertaken in the evaluation were as follows:

1. Investigation of the nature and magnitude of the fluid forces exerted on the mat during launch.

2. Determination of the forces and deformations exerted on the mat by the launch barge during launch.

3. Determination of the ultimate strength and load-deformation resistance of the longitudinal wires, bracket wires, and their connecting ties.

4. Comparison of present force levels in longitudinal wires, bracket wires, and their connecting ties with their estimated ultimate loads.

A large-scale computer simulation of the mat structure was considered beyond the scope of the investigation.

Forces Exerted on the Mat Components

The components of the mattress system must be capable of sustaining the forces and deformations applied to them during all phases of their life from the casting yard through service on the river bottom. Scouring, corrosion, and other effects generated once the mat is on the river bottom were not considered. The detailed field evaluation of these various activities reveals that the maximum forces are probably generated during three distinct operations: (1) lifting the mat over the edge of the launch plant, (2) motion of the mat over the edge of the launch plant, and (3) passage of the mattress through the water and settlement on the bottom.

Analysis of Fluid Forces

Basic Model

A preliminary model for estimating the magnitude of the fluid forces on the mattress was suggested by Murtha.[7] The mat was assumed to be a flat plate ori-

[5] F. Kearney and F. Plummer, *Study of Articulated Concrete Revetment Mattress: Test and Analysis,* Interim Report M-84 (U. S. Army Construction Engineering Research Laboratory [CERL], 1974).

[6] *Shore Anchor Pull-Out Tests; Force Study BPP No. 8,* (Revetment Operations Improvement Board, Memphis Engineer District, February 1966).

[7] J. P. Murtha, *Hydrodynamic Force Model for the Articulated Concrete Mattress,* Letter Report (University of Illinois, 22 September 1972).

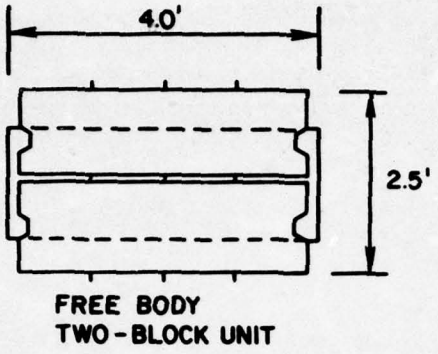

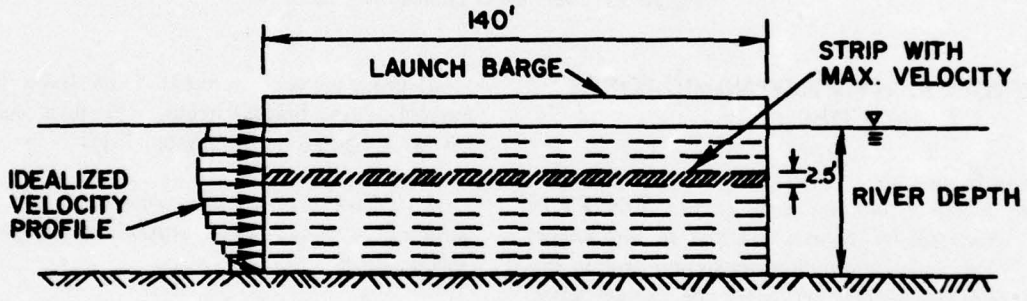

Figure B1. "Strip Theory" model for calculating fluid forces. SI conversion factor: 1 ft = 0.3048 m.

ented vertically in a steady flow and inclined at some angle of attack to the direction of flow. The unit section of the mat was taken as two blocks interconnected by longitudinal and bracket wires (Figure B1). The flow is idealized as illustrated in Figure B1, and the velocity is assumed uniform over a strip 2.5 ft (0.8 m) wide and 140 ft (42.7 m) long. Pressure distributions on two-dimensional plates at various angles of attack were obtained from Fage and Johansen's report.[8] A computer program was written integrating the pressure forces over a 2.5-ft (0.8 m) strip of mattress to give the resultant pressure forces perpendicular to each two-block unit. The boundary friction forces (parallel to the mat) were calculated from the expression:[9]

$$F_F = \frac{C_D A \rho V o_2}{2} \qquad \text{[Eq B1]}$$

where C_D = the drag coefficient =

$$\frac{1}{(1.89 + 1.62 \log_{10}\frac{L}{\epsilon}) 2.5}$$

L = length of a strip ρ = mass density of the fluid

ϵ = roughness factor Vo = velocity over the strip

A = area F_F = fluid friction factor

These friction factors were assumed to act on both sides of the mat.

[8] A. Fage and F. C. Johansen, *The Connection Between Lift and Circulation of an Inclined Flat Plate*, Reports and Memoranda No. 1104 (England: Aeronautical Research Committee, 1927).

[9] H. Schlicting, *Boundary Layer Theory* (McGraw-Hill, 1960), Chapters 20-21.

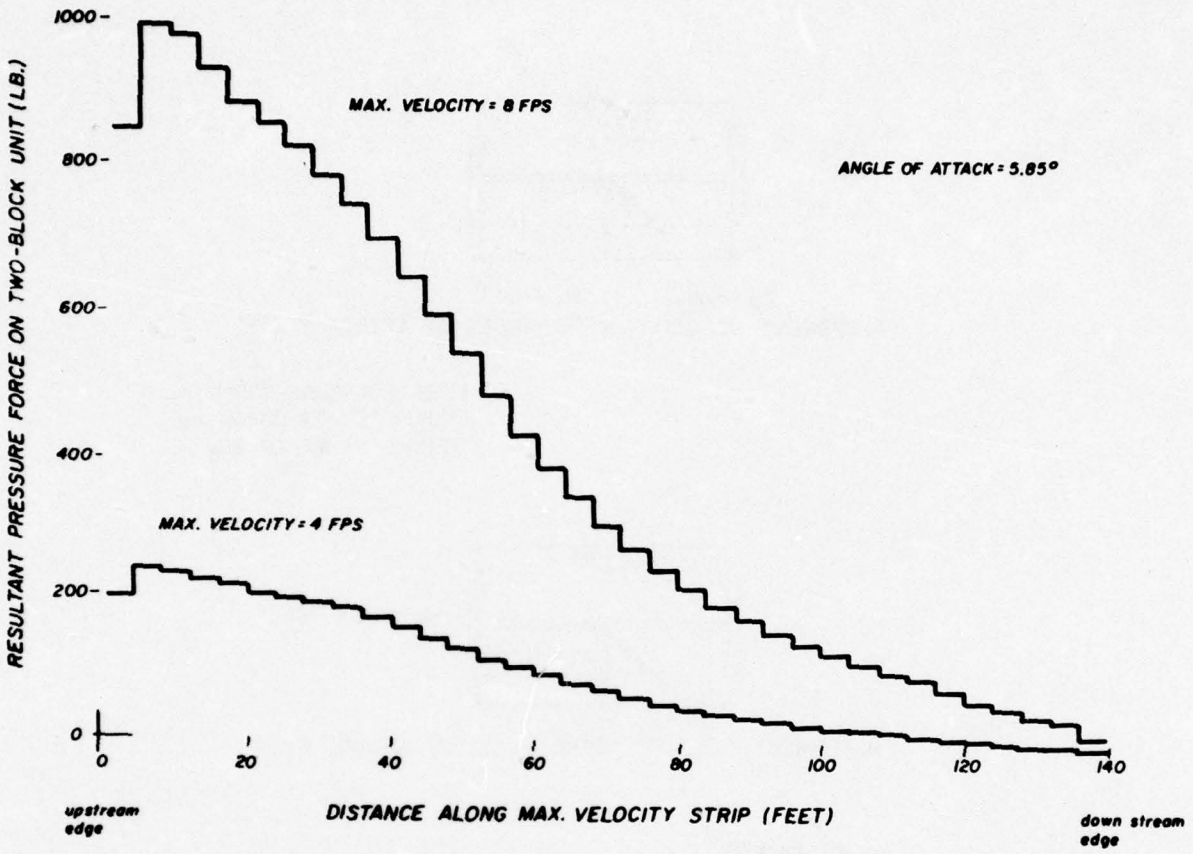

Figure B2. Resultant pressure forces on two-block units along the strip of maximum velocity. SI conversion factor: 1 ft = 0.3048 m; 1 lbf = 4.448 N.

The porosity of the mat was neglected, and the inertial fluid forces generated during launching were neglected for this preliminary model.

The resultant pressure forces acting on each two-block unit along the strip of maximum velocity were plotted in Figure B2 for an angle of attack of 5.85° and maximum current velocities of 4 and 8 ft/sec (1.2 and 2.4 m/sec). It is seen that for this small angle of attack the maximum pressure force occurs close to the upstream edge of the mat. For large angles of attack the peak pressure displaces toward the center of the mat.

Figure B3 shows the fluid pressure force (F_p), fluid friction force (F_F), and the weight in water (W_W) which act on the most highly stressed two-block unit. For a maximum velocity of 4 ft/sec (1.2 m/sec) the pressure force and effective weight are of approximately the same magnitude, while at higher current velocities the pressure force dominates. In both cases the fluid friction force (F_F) is insignificant.

Fluid Forces – During Launch Operations

From the preliminary model it is seen that for small angles of attack there is a sharp pressure gradient across a horizontal strip of mat. Under normal conditions the mat forms an angle of attack of from 0° to 15° relative to the flow. The current impinges on what will ultimately be the top of the mat, and the pressure forces hold the mat in a stable position against the launch barge and the river bottom.

Under abnormal conditions the current may impinge on the back or underside of the mat, causing the mat to become unstable. For small angles of attack against the backside of the mat, the pressure gradient would most likely tend to peel the upstream edge of the mattress downstream and toward the shore. (This phenomenon is also often observed during the launch of the

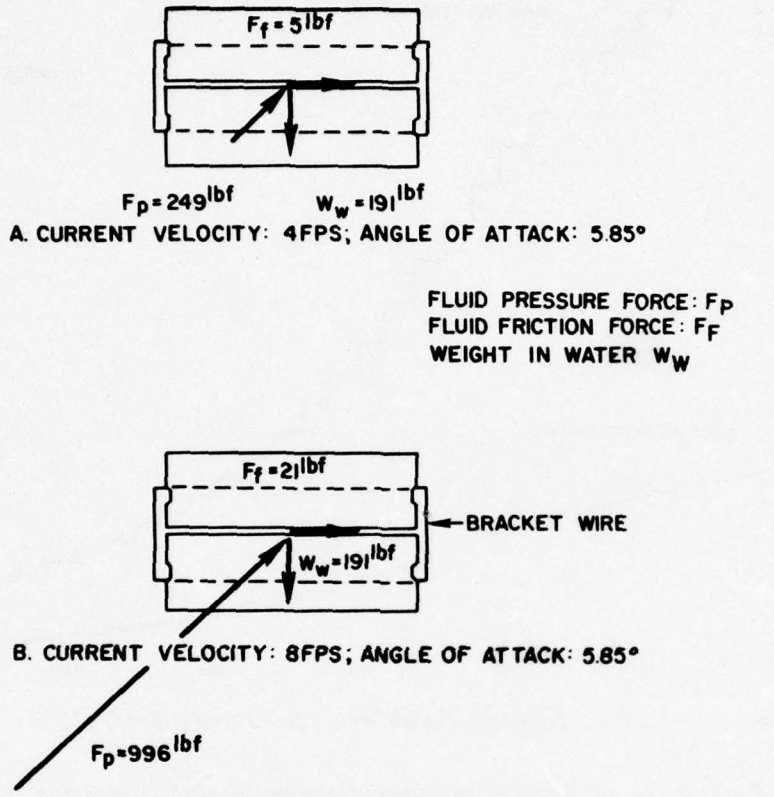

Figure B3. Forces applied to two-block unit. SI conversion factor: 1 lbf = 4.448 N.

mat. Once the final launch leaves the mat plant, it loses its upper edge support against the barge and tends to execute large deformations. This is shown in Figure B4 by the launch cables which are displaced downstream.) For large angles of attack against the backside of the mat, one would expect a more uniform and general billowing of the mattress away from the bottom and toward the river surface.

The launch process itself can cause a tendency for the mat to become unstable. Figure B5 shows the path that the mattress would take while settling to the bottom. Measurement of the velocity of the launch barge and the velocity of the mat relative to the launch barge indicates that mat velocities of approximately 0.5 ft/sec (0.2 m/sec) can be developed during normal launching operations. A relative component of current velocity is generated against the mat which could neutralize the pressure forces on the front of the mat for small angles of attack. Fluid inertial effects might also contribute to an unstable condition.

The most effective method of controlling unstable behavior during launching is to maintain current on the top of the mattress and to restrain the upstream edge of the mat from any appreciable movement. The weight of the mattress also contributes to maintaining a stable mat configuration. Although the present toggle beam system will restrain the upstream edge, it is time consuming to attach toggle cables at less than 25-ft (7.6 m) intervals (i.e., more than one per launch). Under these conditions, a 25-ft (7.6 m) section of mat becomes free when the toggle cable is released from the bottom of the toggle beam, and the mat can then execute large deformations.

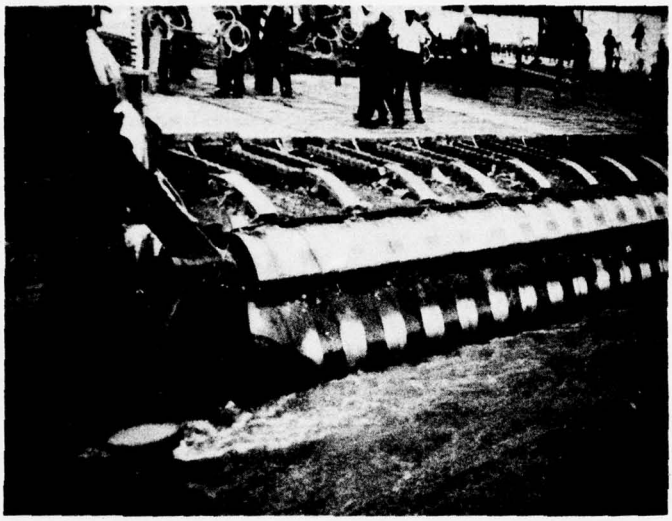

Figure B4. Last launch – launch cables pulled downstream.

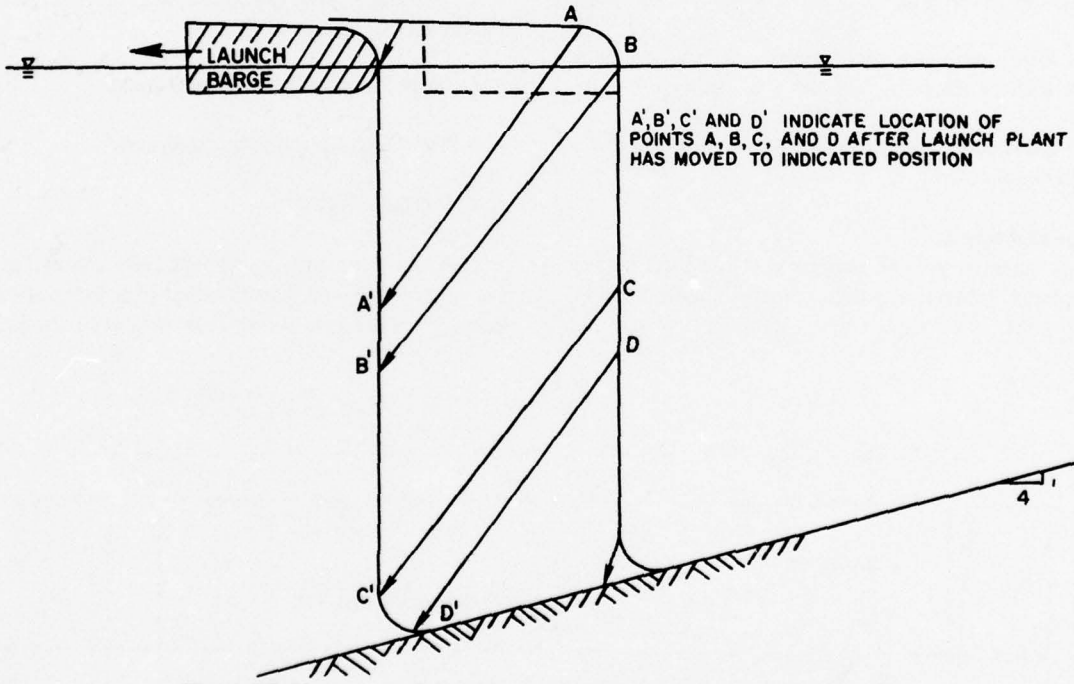

Figure B5. Movement of the articulated concrete mattress during launch.

Longitudinal Wire Analysis

Longitudinal wires are defined as the three wires which run along the long axis of a square (Figure A1). The longitudinal wires of adjacent squares are connected with end-twist-tie connections. Various types of links are used to compensate for different intersquare spacing. All field measurements of longitudinal wire force were accomplished by inserting either a mechanical or an electromechanical gage in place of an end-twist-tie connection. No longitudinal forces were measured between the concrete blocks within a square. The mean ultimate tensile strength of the standard end-twist link was determined to be 3587 lbf (16.0 kN) by slow monotonic extension tests. The wire fabric has a tensile strength exceeding 4000 lbf (17.8 kN); thus, the end twist is the weakest link in the longitudinal wire system.

APPENDIX C: STRUCTURAL ANALYSIS OF ARTICULATED MATTRESS

Basis for Analyses

The first phase of the test program was conducted September-December 1973. Electrical/mechanical gages were used to determine the location and nature of the maximum longitudinal wire force. The time history recorded from these gages revealed that: (1) the gages were not loaded simultaneously nor to the same level, and the loading was very erratic; (2) the maximum forces occurred as the mat began its descent over the edge of the launch barge; and (3) by the time the gages entered the water and left the influence of the launch barge, the forces had diminished significantly and appeared to be redistributed among the longitudinal wires. To explain these phenomena, the second phase of the test program in October-December 1973 was structured to include special tests to:

1. Determine why the forces in the longitudinal wires decrease when the mat enters the water

2. Investigate force distribution among the three longitudinal wires.

Scope of Analyses

An elaborate simulation model of the behavior of an articulated concrete mattress was not undertaken, because a mat is a complicated structural assemblage and is subjected to a series of dynamic forces of undetermined magnitude during the launching process. Instead, the analyses were restricted to simple static calculations and analytical models which could provide insight into the general behavior of the mattress and could be correlated with the field data.

Analyses

During the launch process several factors induce forces in the longitudinal wires. Included among these are:

1. Static friction between the mat and the rollers

2. Rolling friction between the mat and the rollers

3. Sliding friction between the mat and the launching barge edge

4. The sharp curvature occurring as the mat traverses the launch finger apron

5. Fluid forces on the submerged mat

6. The weight of the submerged mat

7. Inertial effects.

However, time-history records from the electrical/mechanical gages used in the field tests indicated that the peak longitudinal forces were, in general, associated

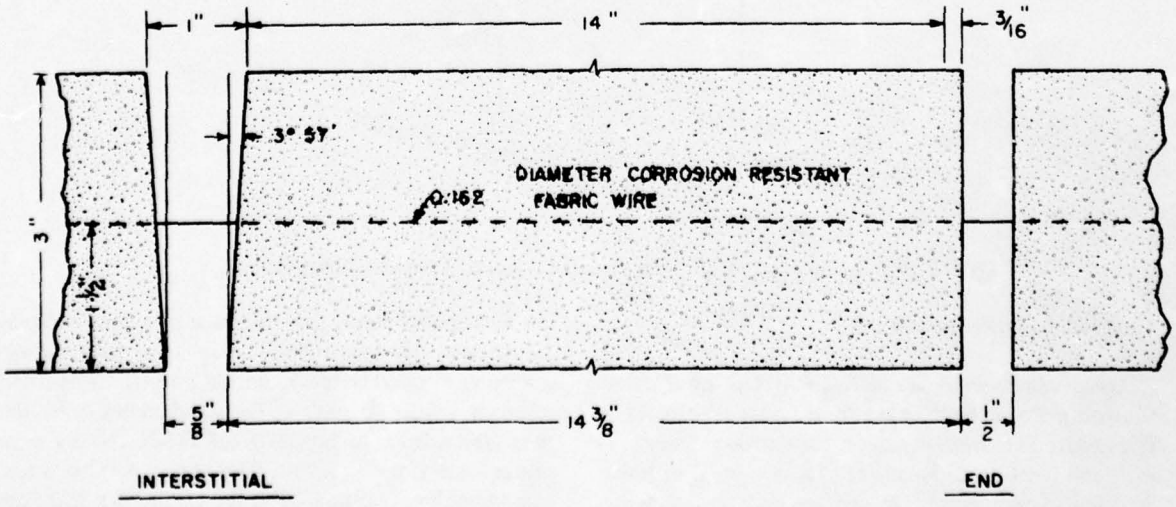

Figure C1. Block dimensions and spacings. SI conversion factor: 1 in. = 25.4 mm.

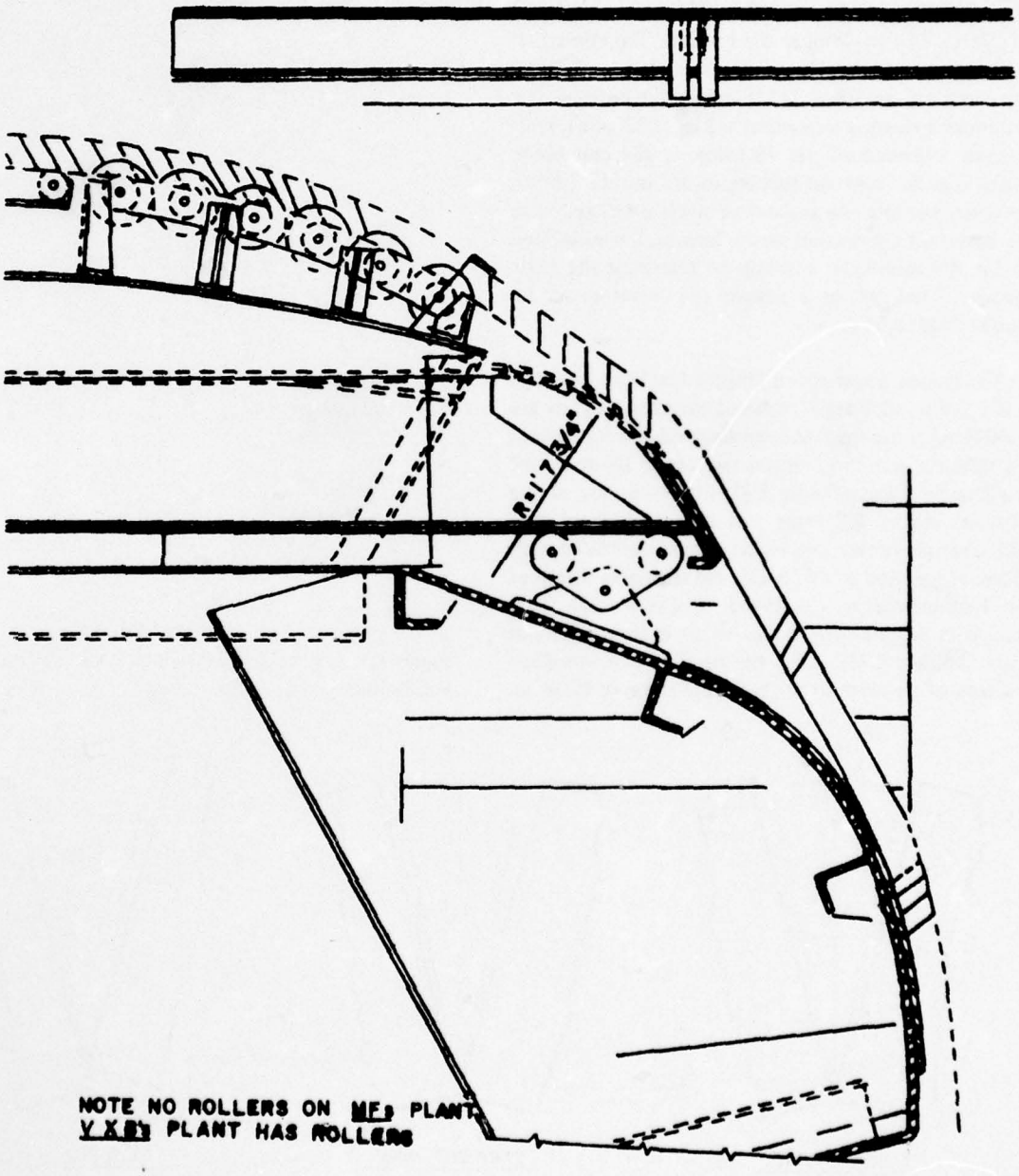

Figure C2. Section of launch plant showing launch fingers and curved bearing surfaces.

with the mat's progress over the edge of the launch plant. At this stage in the launch operation, forces produced by the angle change associated with the mat traversing the launch finger apron would be most likely to cause the peak forces.

The basic cross-sectional dimensions and spacings of a typical concrete end block of a square are shown in Figure C1. A typical block is 3 in. (76.2 mm) thick and 14 3/8 in. (4.4 m) long at the bottom. The interstitial spacing between the blocks is 1 in. (25.4 mm) at the top and tapers to 5/8 in. (15.9 mm) at the bottom. The end block spacing is a constant 1/2 in. (12.7 mm). End-twist-tie connections are installed at the end block which has the constant spacing of 1/2 in. (12.7 mm); however, because the amount of slack associated with the end-twist connection was unknown, it was decided to use the interstitial spacings to determine the angle change of the mat as it follows the curvature of the launch finger apron.

The launch finger apron (Figure C2) has a radius of 1 ft 7 3/4 in. (0.5 m). If adjacent blocks in a square are considered to be rigid and are assumed to adopt a configuration where they remain tangent to the radius of the launch finger (Figure C3), lower corners of the adjacent blocks will meet and the longitudinal wire will undergo strain. The angle change associated with this configuration is 39° 59'43" and change in length of the longitudinal wire is 0.465 in. (11.8 mm). That change in length corresponds to an average strain of approximately 0.437 in./in. (m/m). This would produce fracture of the wire since the failure strain of the wire, determined by laboratory testing, was about 0.015 in./in. (m/m).

Results of this simple calculation prompted further examination of the possible angle change which adjacent blocks could assume without inducing fracture strain in the longitudinal wires. For these calculations, the three configurations shown in Figure C4 were assumed

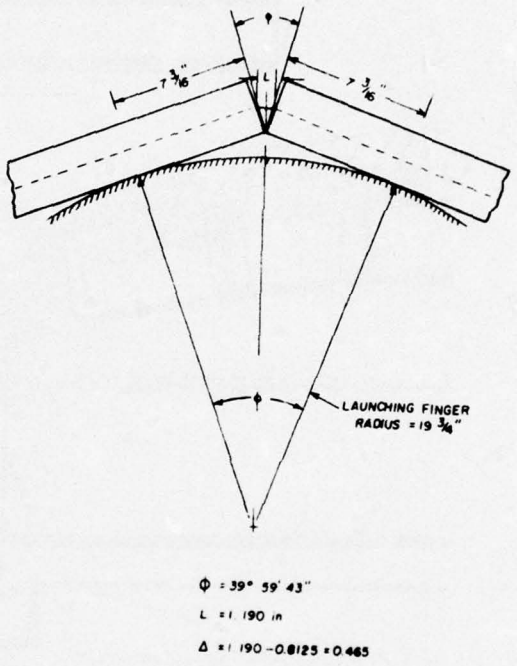

Figure C3. Angle change at launch finger apron. SI conversion factor: 1 in. = 25.4 mm.

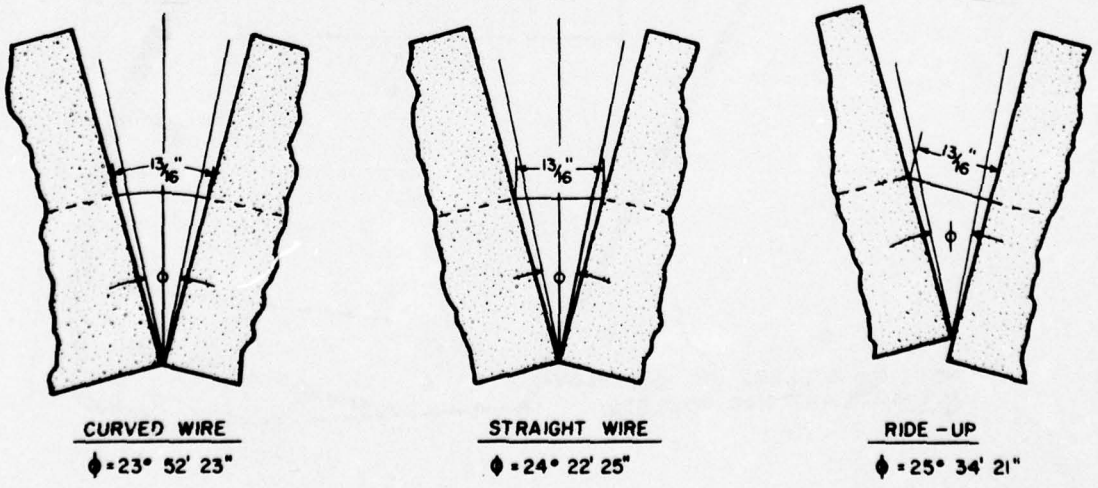

Figure C4. Potential angle change configurations SI conversion factor: 1 in. = 25.4 mm.

to represent conditions that might exist in the field. In the first and second configurations the blocks were assumed to lock at their lower corners, while in the third configuration one block was allowed to ride up on the other. In the first configuration the longitudinal wire was assumed to adopt a curvature that produced an angle change of 23° 52' 28". For the second configuration, the longitudinal wire was assumed to remain straight and the angle change was computed to be 24°33'25". In the third configuration the angle change was 25°34'21".

The angle change that can occur in the blocks without causing failure strain was computed to be only about 60 percent of the maximum angle change the blocks might experience while traversing the launch finger apron. It was anticipated that any force in the longitudinal wires induced by the weight of the mat suspended below the launch finger apron might result in sufficient force for the mat to experience an angle change larger than 23° to 25°—and thus produce the peak force in the longitudinal wires.

It was also recognized that several potential effects could be responsible for the 40 percent difference between (1) the angle change the blocks could undergo without breaking the longitudinal wires, and (2) the angle change associated with the launch finger apron. These effects are:

1. Crushing of the concrete at the lower corners of the blocks when the blocks lock up

2. Different spacings between the blocks

3. Different radii for the launch finger aprons

4. The effective angle in the launch finger apron being less than 39° 59' 43".

5. Crushing of the concrete around the points where the longitudinal wires enter and exit the block, caused by high bearing stress imposed by deformation of the longitudinal wires as the blocks traverse the launch finger apron.

6. Placement of the longitudinal wires at other than mid-height of the block.

Of all these effects, the most logical explanation appeared to be that the effective angle change experienced at the launch finger apron is less than 39°59'43". If the launch finger were retracted more than is shown in Figure C2, the angle change experienced by the blocks would decrease. Likewise, if the blocks did not fully conform to the launch finger apron radius—i.e., if the lead block were restrained from conforming to the launch finger apron radius by the force in the longitudinal wires—an effective angle change less than 39° 59' 43" would also result.

The field data were analyzed to determine if they supported the theory that the maximum forces were occurring as the mat traversed the launch finger apron and that these forces were being induced in the longitudinal wires as a result of an angle or curvature change other than that caused by actual forces being applied to the mat and then transmitted to the longitudinal wires. Special field tests were conducted to confirm this theory.

Since the results from the special field tests tended to support the theory that the forces induced in the longitudinal wires were produced by the angle changes associated with the launch finger apron, it was decided to analyze the end connection force data recorded by the mechanical gages in the two- and three-gage configurations. Theoretically, if the peak forces induced in the longitudinal wires were attributable to the angle change at the launch finger apron, the total connection force would be proportional to the number of longitudinal wires; i.e. the total force for the two-gage configuration would be two-thirds of the total force for the three-gage configuration. (Note that for the two-gage configuration the center end-twist-tie connection was not installed; consequently the two mechanical gages installed on the outer longitudinal wires carried all the force transmitted between squares. In the case of the three-gage configuration, however, the three wires do not carry equal loads because of dimensional variations in assembling the mat on the launch plant. One of the gages is likely to carry only a percentage of the average of the force being carried by the two gages which initially define a straight line.

Table C1 summarizes the two-gage connection force measurements and indicates that the average total force for the two-gage configuration was 4.79 kips, with a standard deviation of 1.76 kips (21.3 kN). Table C2 summarizes the three-gage connection force measurements and indicates that the average total force for this configuration was 6.55 kips (29.3 kN), with a standard deviation of 2.43 kips (10.8 kN). Based on these average values, the ratio of the total two-gage connection force to the total three-gage connection force is 0.74 which is about 10 percent higher than the theoretical

Table C1

Summary of Two-Gage Connection Force Measurements

Location	Date	Mat Number	Launch Barge	Individual Gage Forces (kips)* 1	3	Total Force (kips)*
Marchant, LA	22 Oct 73	15	Vicksburg	1.65	1.6	3.25
Marchant, LA	22 Oct 73	15	Vicksburg	2.2	1.9	4.10
Marchant, LA	22 Oct 73	15	Vicksburg	2.4	1.3	3.70
Marchant, LA	22 Oct 73	16	Vicksburg	2.5	1.7	4.20
Marchant, LA	22 Oct 73	16	Vicksburg	2.3	2.0	4.30
Allendale, LA	26 Oct 73	7	Vicksburg	3.15	3.75	6.90
Coochie, LA	12 Nov 73	12	Vicksburg	2.4	2.3	4.70
Coochie, LA	13 Nov 73	19	Vicksburg	2.85	3.2	6.05
Pt. Breeze, LA	15 Nov 73	19	Vicksburg	2.7	2.5	5.20
Pt. Breeze, LA	15 Nov 73	20	Vicksburg	2.9	2.15	5.05
Pt. Breeze, LA	15 Nov 73	21	Vicksburg	2.5	1.4	3.90
Pt. Pleasant, LA	4 Dec 73	4	Memphis	5+	5	10.0
Pt. Pleasant, LA	4 Dec 73	4	Memphis	2.75	1.1	3.85
Pt. Pleasant, LA	4 Dec 73	5	Memphis	2.5	2.7	5.20
Pt. Pleasant, LA	5 Dec 73	11	Memphis	0.9	0.95	1.85
Pt. Pleasant, LA	5 Dec 73	12	Memphis	3.3	2.25	5.55
Pt. Pleasant, LA	5 Dec 73	12	Memphis	3.9	1.4	5.30
Pt. Pleasant, LA	5 Dec 73	13	Memphis	2.05	1.8	3.85
Pt. Pleasant, LA	6 Dec 73	17	Memphis	3.5	2.95	6.45
Pt. Pleasant, LA	6 Dec 73	17	Memphis	1.6	0.75	2.35
					Average:	4.79
					Standard Deviation:	1.76

* SI conversion factor: 1 kip = 4.448 kN.

Table C2

Summary of Three-Gage Connection Force Measurements

Location	Date	Mat Number	Launch Barge	Individual Gage Forces (kips)* 1	2	3	Total Force (kips)*	Smallest Force ½ ϵ large forces
Burnside, LA	19 Oct 73	23	Vicksburg	1.25 K	1.4 K	1.6 K	4.25	0.83
Marchant, LA	22 Oct 73	14	Vicksburg	3.1	2.0	2.15	7.25	0.75
Allendale, LA	25 Oct 73	1	Vicksburg	2.8	1.8	2.0	6.60	0.75
Allendale, LA	26 Oct 73	7	Vicksburg	2.15	1.65	1.9	5.70	0.81
Baleshed, MS	7 Nov 73	6	Memphis	2.9	2.1	2.2	7.20	0.82
Coochie, LA	12 Nov 73	12	Vicksburg	1.8	1.75	1.65	5.20	0.93
Coochie, LA	13 Nov 73	19	Vicksburg	2.5	2.15	2.5	7.15	0.86
Pt. Breeze, LA	15 Nov 73	18	Vicksburg	1.65	0.5	2.05	4.20	0.27
Pt. Breeze, LA	15 Nov 73	19	Vicksburg	1.9	2.0	1.8	5.70	1.00
Pt. Pleasant, LA	4 Dec 73	4	Memphis	1.3	3.7	0.5	5.50	0.20
Pt. Pleasant, LA	4 Dec 73	4	Memphis	2.95	5+	5	12.95	0.59
Pt. Pleasant, LA	4 Dec 73	5	Memphis	1.9	1.7	2.3	5.90	0.81
Pt. Pleasant, LA	5 Dec 73	11	Memphis	3.6	1.8	4	9.40	0.47
Pt. Pleasant, LA	5 Dec 73	12	Memphis	1.65	0.5	0.75	2.90	0.42
Pt. Pleasant, LA	5 Dec 73	13	Memphis	2.4	2.1	1.3	5.80	0.20
Pt. Pleasant, LA	5 Dec 73	13	Memphis	4.3	1.1	0.55	5.95	0.58
Pt. Pleasant, LA	5 Dec 73	14	Memphis	3.5	5+	3	11.50	0.71
Pt. Pleasant, LA	5 Dec 73	14	Memphis	2.0	.95	2.4	5.35	0.43
Pt. Pleasant, LA	6 Dec 73	17	Memphis	3.2	1.65	1.9	6.75	0.65
Pt. Pleasant, LA	6 Dec 73	17	Memphis	2.25	2.1	1.3	5.65	0.60
						Average:	6.55	0.63
						Standard Deviation:	2.43	0.24

* SI conversion factor: 1 kip = 4.448 kN.

value of 0.67. This, however, does not include a correction for the fact that one gage of the three-gage configuration is not 100 percent effective. To estimate the effectiveness of that gage for each set of three-gage data, the smallest gage force was divided by the average of the two larger gages; the results of this calculation appear in Table C2. Based on the 20 sets of data, the smallest gage force was an average of 63 percent of the average of the two larger gage forces—i.e., one end-twist-tie connection is only 63 percent effective. Consequently, the average force of 6.55 kips (29.3 kN) for the three-gage configuration must be corrected by the factor

$$\frac{3.0}{2.63} = 1.14$$

to compensate for the fact that on the average only 2.63 gages were fully effective. Applying this correction factor results in an average three-gage force of 7.47 kips (33.2 kN). If the mat assembly tolerances were such that the three gages were fully effective, 7.47 kips (33.2 kN) would be the average total force for the three-gage configuration. The ratio of the average values of the total two-gage connection force to the corrected total three-gage connection force now becomes 0.64. This ratio compares extremely favorably (within 1/2 percent) with the theoretical value of 0.67.

Although the results of this analysis were encouraging, it was necessary to determine the force induced in the longitudinal wire by the submerged mat hanging vertically in the water, to ascertain that the forces recorded by the mechanical gages were not attributable solely to the weight of the hanging mat. To estimate the total force at the connection for the case of one square submerged in water, the simple calculation illustrated in Figure C5 was performed, with the following assumptions:

1. A fixed support is representative of the constraint conditions at the river surface

2. A free support is representative of the constraint conditions at the river bottom

3. Fluid pressure and frictional forces are negligible

4. Inertial forces are negligible

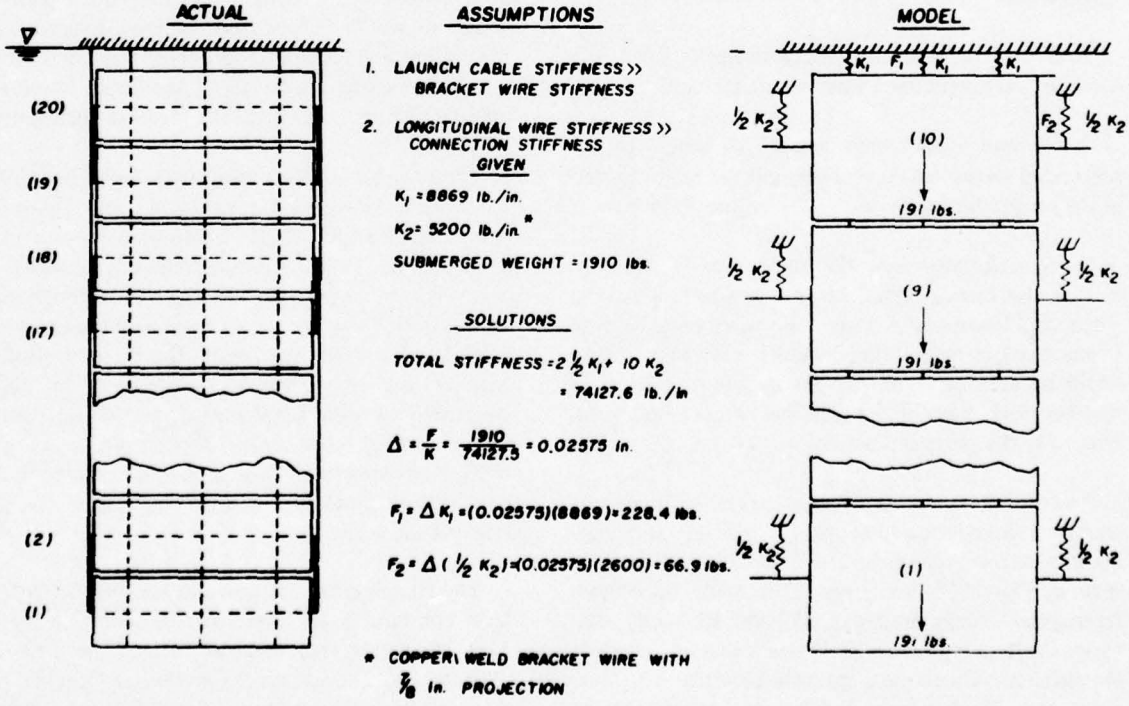

Figure C5. Simple force distribution model. SI conversion factor: 1 lbf = 4.448 N; 1 in. = 25.4 mm.

5. The launch cable stiffness is many times greater than the bracket wire stiffness

6. The blocks of the square are rigid.

On the basis of these assumptions the solution to the problem was simplified to one equation with one unknown. Laboratory tests indicated that the longitudinal stiffness of an individual end-twist-tie connection was approximately 8869 lbf/in. (1.6 kN/mm) and the longitudinal bracket wire stiffness was about 5200 lbf/in. (0.9 kN/mm). Also, field data from the initial phase of the test program indicated that when all three longitudinal wires were connected by mechanical gages at the connection between squares, the third gage recorded only about 50 percent of the average force recorded by the other gages. It was consequently assumed that the total longitudinal wire connection stiffness was about 2 1/2 times the individual stiffness. Using these numerical values, solving the single equation, and back-substituting the result to calculate the forces, it was determined that the total end-twist-tie connection force would be about 571.0 lbf (2.5 kN) and the total bracket wire force would be about 133.8 lbf (0.6 kN). While both these values appeared reasonable because they did not contradict the observed field data, it was realized that:

1. If the launch cable stiffness were included, the forces in the longitudinal wires would increase

2. If more squares were added, the weight of the suspended model would increase and the forces carried in the longitudinal wires would consequently increase

3. To determine how the forces were distributed among the launch cable, bracket wires, longitudinal wires, and longitudinal connection wires (end-twist-tie connection), a more refined model was required that could be used to investigate the impact of changes in number and size of longitudinal wires. Figure C6 illustrates the more refined model that was developed.

The model, consisting of 40 block systems, represents the force distribution in four squares of mattress hanging in water at a depth of 100 ft (30.5 m) or more. As seen in Figure C6, each system is made up of two rectangular blocks weighing 95.5 lbf (0.4 kN). The various springs represent the different wires throughout the mattress. The vertical spring with stiffness K_1 connects each block system and is representative of the launch cable stiffness. The bracket wires, which pass through the concrete blocks latitudinally and are connected to the launch cable longitudinally, are represented by the vertical springs with stiffnesses of K_2 equal to one-half the bracket wire longitudinal stiffness. These springs are mutually connected within each block system, and have the launch cable spring, K_1, as a common point.

After every tenth block system, which represents a square, the following block system is connected by a spring with a stiffness, K_3, equal to the total connection wire stiffness in the actual mattress. The other systems are all connected by a vertical spring, K_4, which joins the center of the upper block of each system to the lower block of the system above it. K_4 represents the total stiffness of the longitudinal wires embedded in the concrete blocks.

The assumptions for this analysis are similar to those for the simple force distribution analysis, except that in this multi-square force distribution model, the launch cable stiffness and the longitudinal wire stiffness are included, and the forces in these wires are determined. In the multi-square force distribution model the submerged weight of the concrete blocks causes each spring to displace, creating a force which is representative of the actual forces induced in the wires of the mattress. A series of simultaneous equilibrium equations was developed based on the displacements of the springs. A computer program was then written which solved the equations by the Gauss Elimination method and then calculated the forces in each spring.

The analysis of the multi-square force distribution model can be divided into three cases. Each case calculated the total forces which would occur in the launch cable, bracket wires, longitudinal wires, and end-twist-tie connections for (1) a three-longitudinal-wire system, (2) a two-longitudinal-wire system, and (3) a one-longitudinal-wire system. The three-longitudinal-wire system represents the mattress in its original configuration with three longitudinal wires; the two-longitudinal-wire system represents the deletion of one of the three longitudinal wires; and the one-longitudinal-wire system represents deletion of two of the three longitudinal wires.

The launch cable stiffness and bracket wire stiffness were constant in all three cases. However, in the first case, stiffnesses representative of 0.162-in. (4.1 mm) diameter wire were used for the longitudinal wire springs, and stiffnesses representative of the end-twist-tie wire were used for the end-twist-tie connection springs. In case two, stiffnesses representative of 0.141-

in. (3.6 mm) diameter wire were used for the longitudinal wire springs and the stiffnesses of the end-twist-tie connection springs remained the same. The final case also used stiffnesses representative of the 0.141-in. (3.6 mm) diameter wire; however, the stiffnesses of the end-twist-tie connection spring were reduced by 21 percent to simulate the use of smaller diameter end-twist-tie connection wires. The values of the different spring constants for these three cases are presented in Table C3.

The spring constant K_1 is representative of the stiffness of a 30-in. (0.7 m) length of 3/8 in. (9.5 mm) diameter launch cable and was determined from actual test data. K_2 represents the values determined from the longitudinal bracket wire tests on copperclad wire. The values for K_3 are integer multiples of the number of longitudinal wires used in the system—except for the three-wire system, in which K_3 was taken to be 2.63 times the individual end-twist-tie connection wire stiffness, as discussed earlier. The stiffness values of K_4, the longitudinal wire stiffness, were multiples of the number of longitudinal wires in the system times the average stiffness of a 15-in. (0.4 m) length of longitudinal wire.

Results from the refined force distribution model are presented in Figures C7 through C12. Figures C7 through C9 are plots of the launch cable forces and the longitudinal wire forces for cases 1, 2, and 3, respectively. These plots show that the forces in the launch cable and longitudinal wires increase approximately linearly with depth. The slight cusping effect is due to the transfer of forces between the launch cable and the longitudinal wire through the bracket wires. (For clarity, the data points between the cusps were deleted.)

Table C3

Spring Constants for Force Distribution Model

Case	Longitudinal Wires	Spring Constants K_1	K_2	K_3	(lb/in.)* K_4
	3	61261.1	2600.0	22172.0	105000.0
1	2	61261.1	2600.0	17737.0	70000.0
	1	61261.1	2600.0	8868.8	35000.0
	3	61261.1	2600.0	22172.0	82960.5
2	2	61261.1	2600.0	17737.0	55307.0
	1	61261.1	2600.0	8868.8	27653.5
	3	61261.1	2600.0	17518.1	82960.5
3	2	61261.1	2600.0	14014.0	55307.0
	1	61261.1	2600.0	7007.2	27653.5

* SI conversion factor: 1 lb/in. = 17.9 kg/m.

It should be noted that as the number of longitudinal wires is decreased within a given case, the launch cable takes up more of the load.

Figures C10 through C12 are plots of the forces in the bracket wires for cases 1, 2, and 3, respectively. The forces in the bracket wires are seen to fluctuate within each square of the 10-block system. It can also be seen that the bracket wires interact with the launch cable; as the launch cable forces increase and decrease, so do the bracket wire forces.

The total forces in the end-twist-tie connection wire and the bracket wires of the simple free distribution model are slightly less than those in the multi-square force distribution model, although the two models are in reasonable agreement. For the multi-square force distribution model at the tenth block system of case 1 for three wires, the total bracket wire force was 157.76 lbf (0.70 kN) and the total connection wire force was 725.78 lbf (3.25 kN). This compares to 133.8 lbf (0.60 kN) in the bracket wires and 571.0 lbf (2.54 kN) in the connection wires for the simple force distribution model.

The plot presented in Figure C13 was developed to check the results of the multi-square distribution model against the observed field data. The water depth at the time of launching of the various two- and three-mechanical-gage configurations used to acquire the data for the initial portion of this analysis was estimated from notes taken during the launching operations in FY 73 and some interpolation. The various data points in Figure C13 were plotted from the sum of the two- and three-wire forces recorded by the mechanical gages, and the estimated water depth. For comparison, Figure C13 also contains the estimated total end-twist-tie connection force predicted by the multi-square force distribution model of the original mat design. A comparison of the average total connection force for the two- and three-gage configuration and the result of the multi-square force distribution model indicates the weight of the hanging mattress should not influence the peak connection forces recorded by the mechanical gages, since all the observed field data plot above the force levels predicted by the model. Furthermore, the mats have to have been launched in 156 to 230 ft (47.5 to 70.1 m) of water for the weight of the hanging mat to exceed the peak forces induced when the mat traverses the curvature of the launch finger apron.

To evaluate results of the multi-square force distribution model, the maximum forces in the launch cable

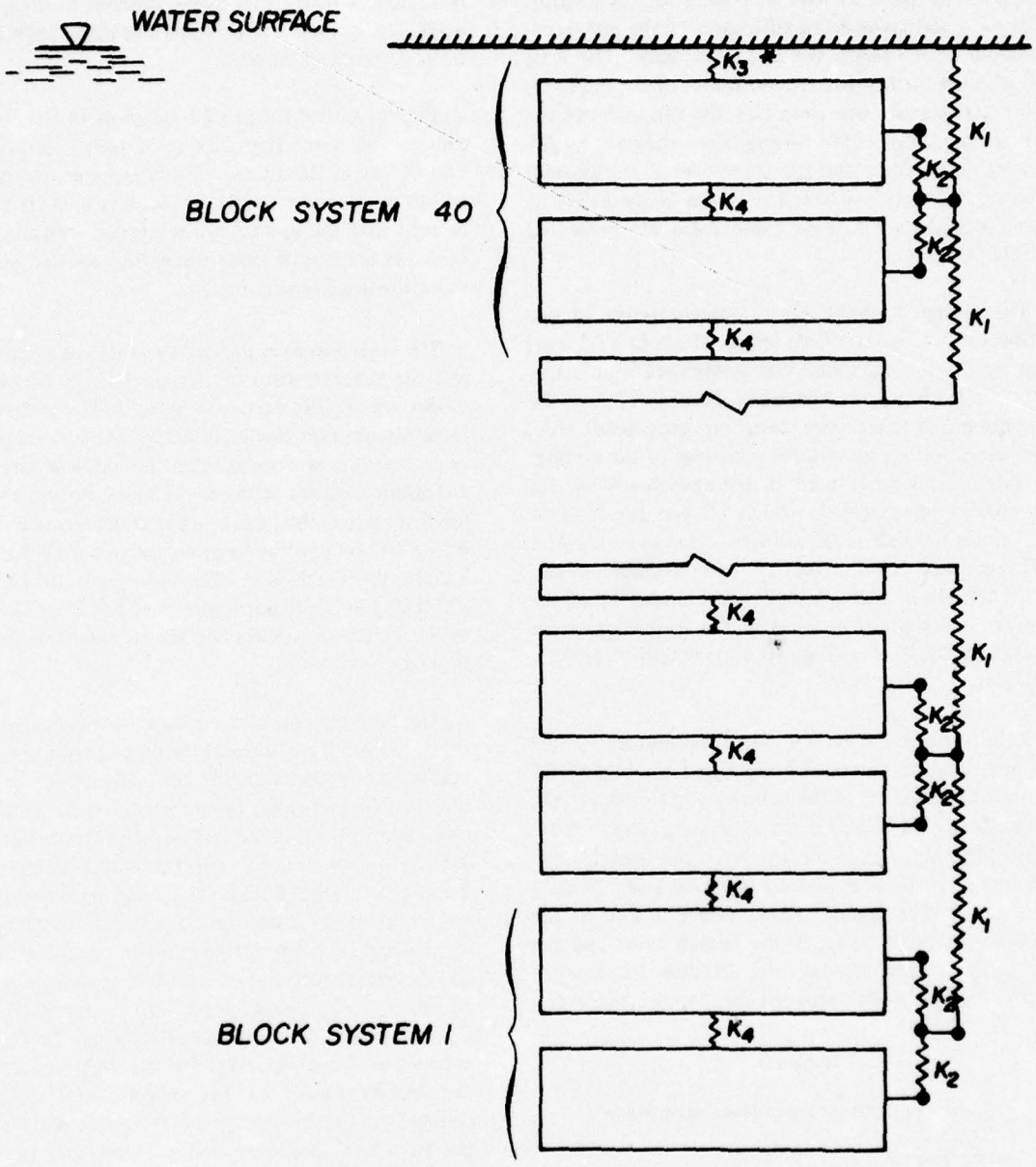

Figure C6. Multi-square force distribution model.

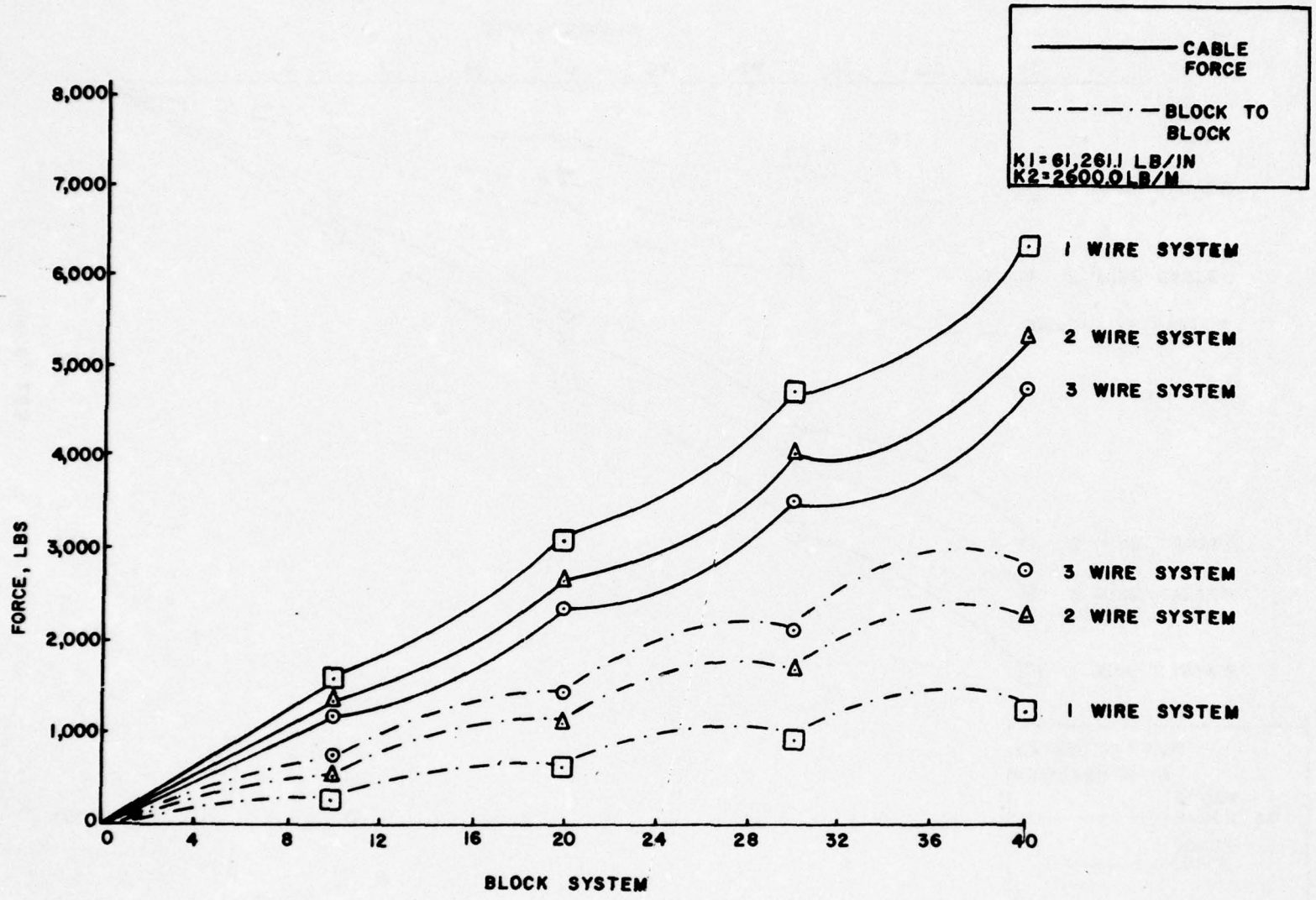

Figure C7. Launch cable, longitudinal wire and end-twist-tie forces for case 1. SI conversion factor: 1 lbf = 4.448 N.

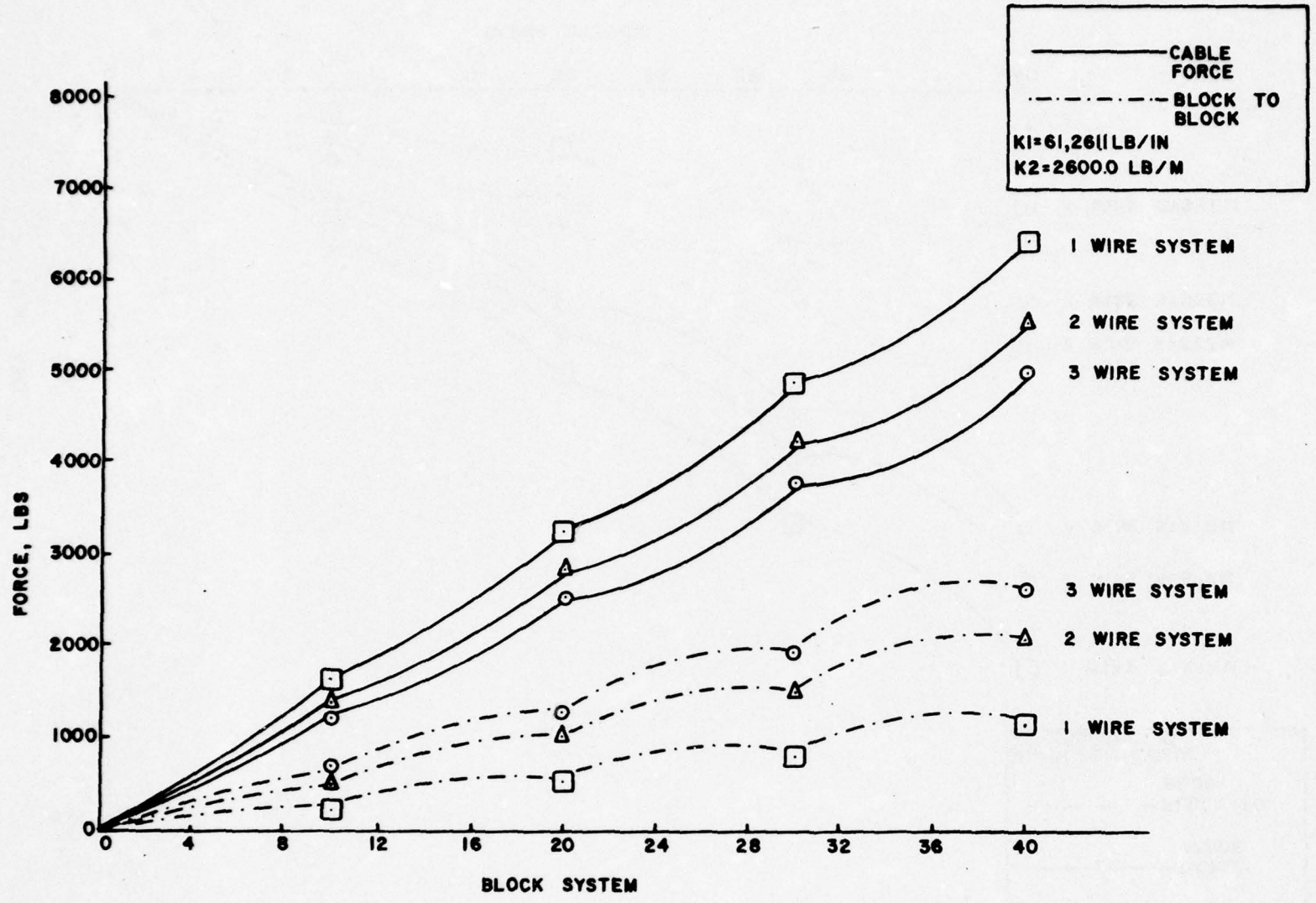

Figure C8. Launch cable, longitudinal wire and end-twist-tie forces for case 2. SI conversion factor: 1 lbf = 4.448 N.

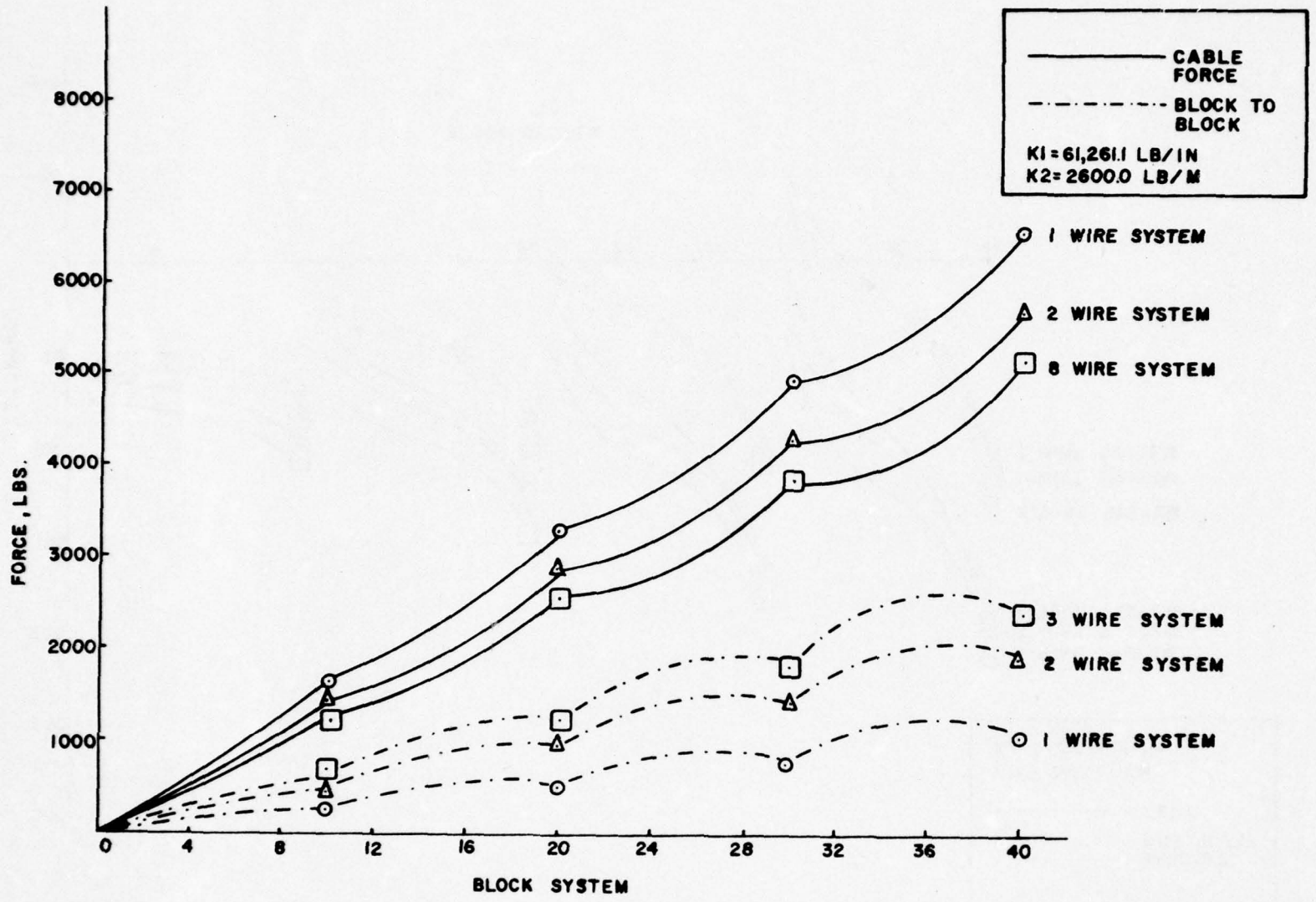

Figure C9. Launch cable, longitudinal wire and end-twist-tie forces for case 3. SI conversion factor: 1 lbf = 4.448 N.

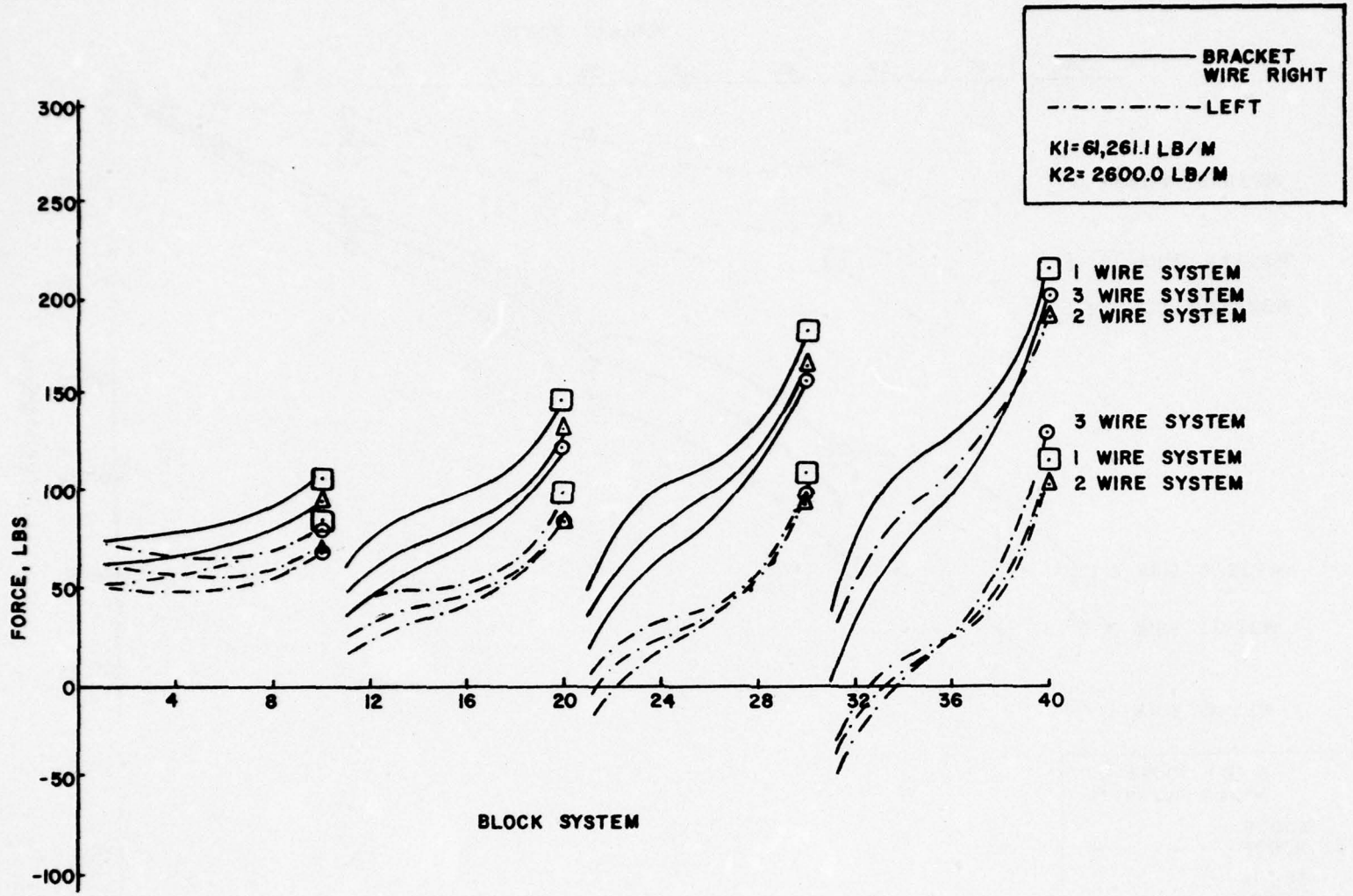

Figure C10. Bracket wire forces for case 1. SI conversion factor: 1 lbf = 4.448 N.

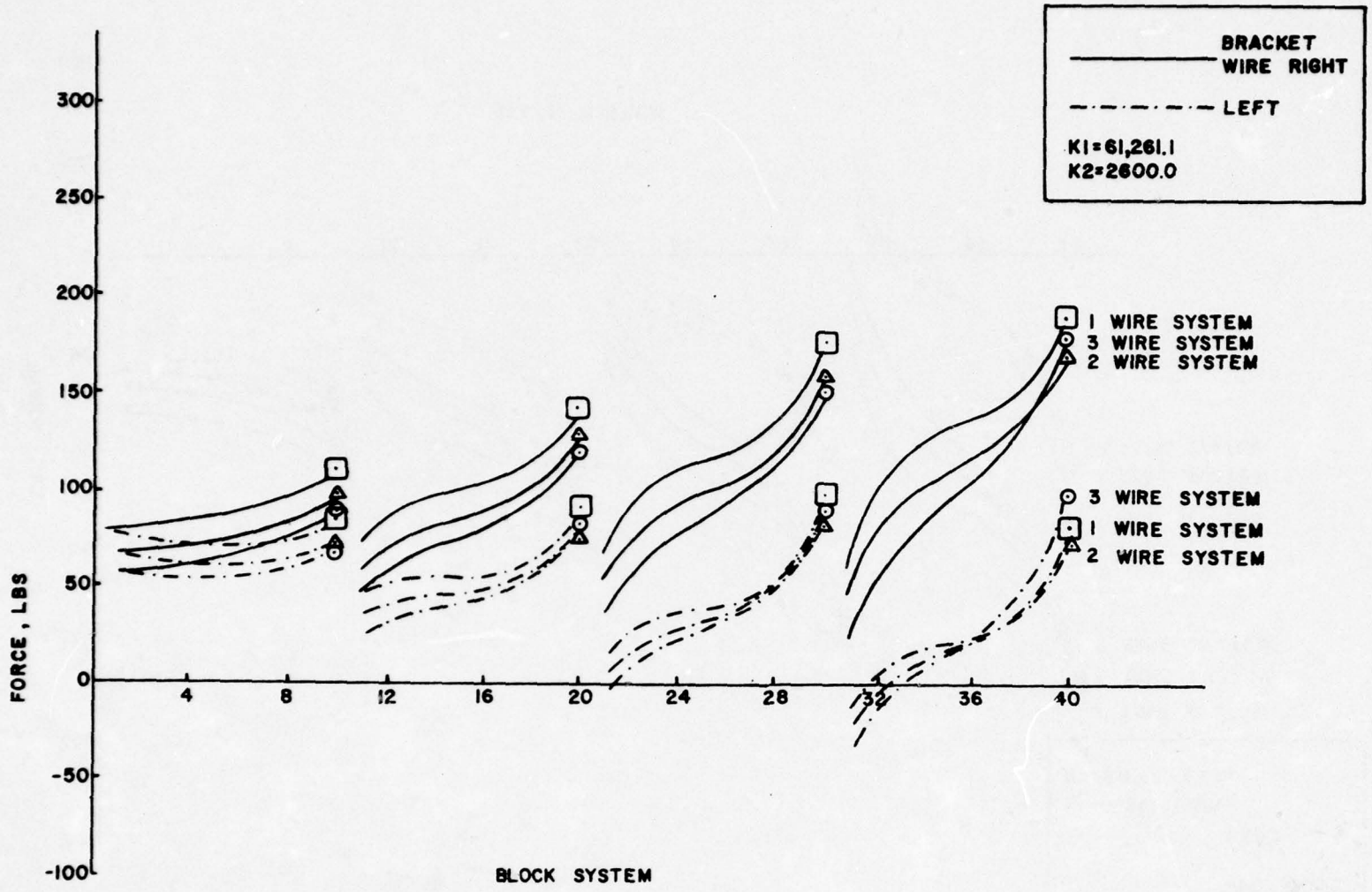

Figure C11. Bracket wire forces for case 2. SI conversion factor: 1 lbf = 4.448 N.

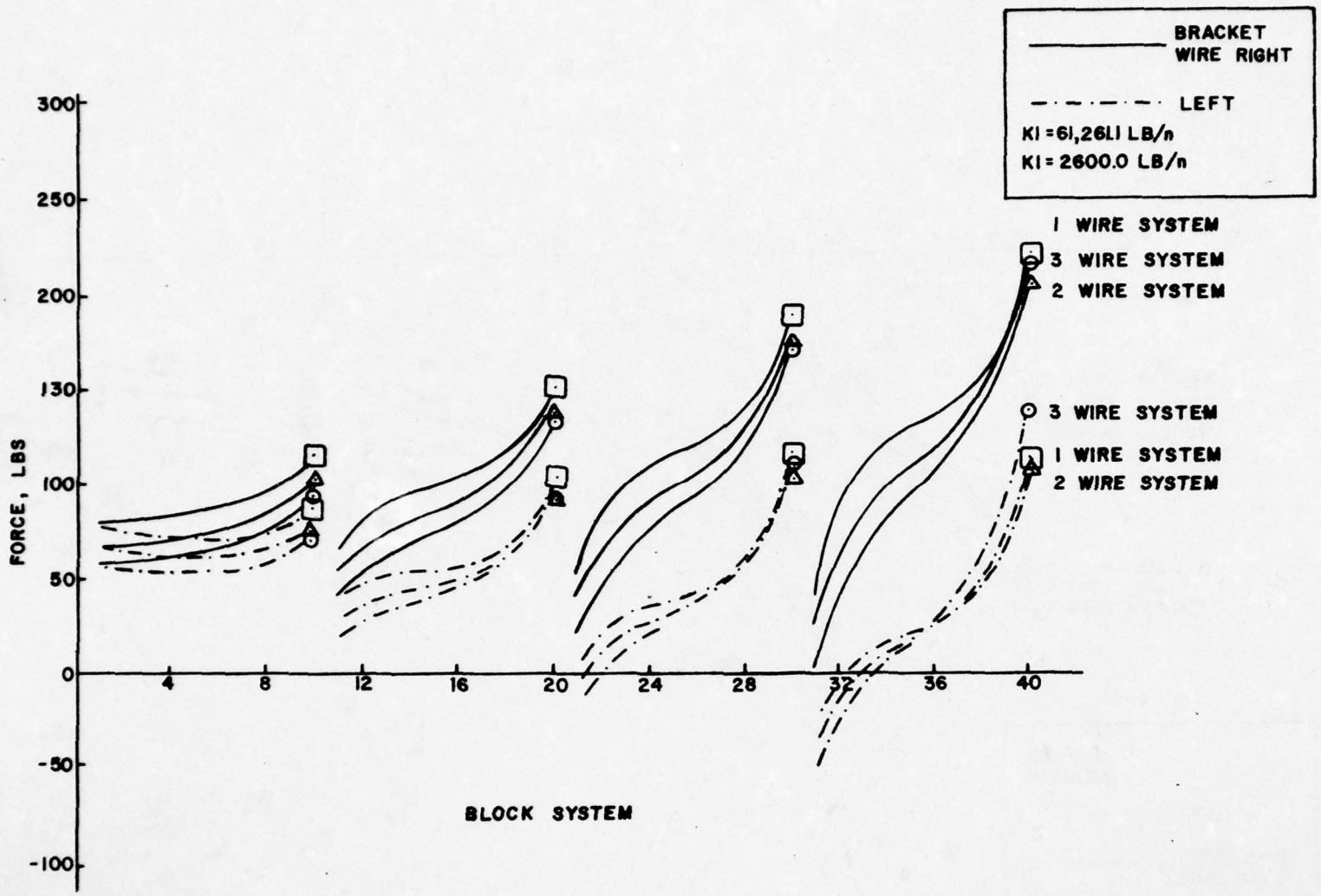

Figure C12. Bracket wire forces for case 3. SI conversion factor: 1 lbf = 4.448 N.

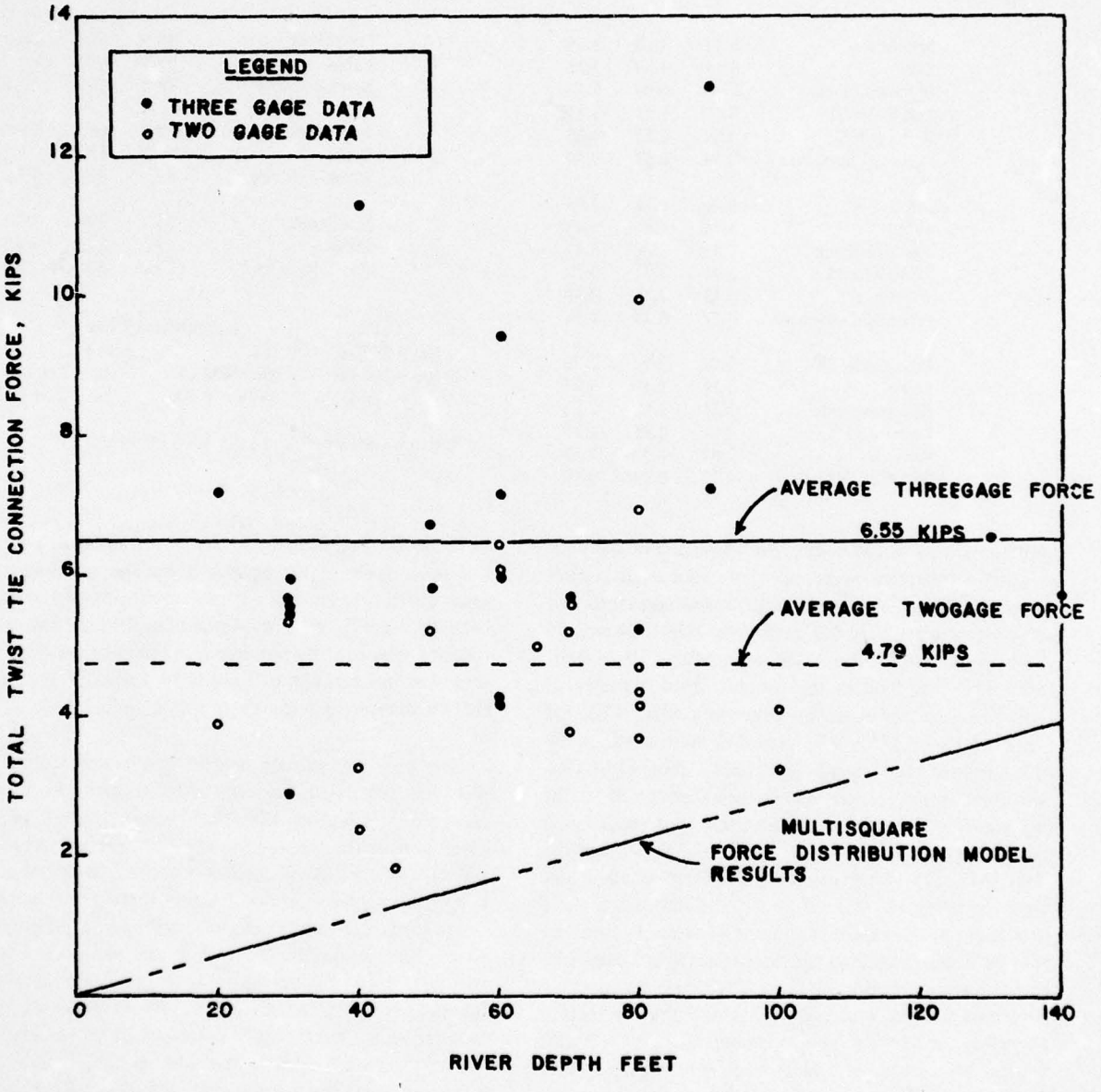

Figure C13. Total end-twist-tie connection vs river depth. SI conversion factors: 1 kip = 4.448 KN; 1 ft = 0.3048 m.

Table C4

Factors of Safety

Number of Longitudinal Wires	Wires	Case 1	Case 2	Case 3
	Interblock	3.47	3.10	3.18
	Cable	4.17	4.00	3.83
	Block-to-Block	3.43	3.04	3.13
3	End-Twist-Tie	3.67	3.97	3.83
	Average F.S.	3.69	3.53	3.49
	Standard Deviation	0.34	0.53	0.39
	Interblock	3.48	3.16	3.25
	Cable	3.74	3.61	3.49
	Block-to-Block	3.41	3.08	3.17
2	End-Twist-Tie	3.09	3.37	3.28
	Average F.S.	3.43	3.31	3.30
	Standard Deviation	0.27	0.24	0.14
	Interblock	2.86	2.70	2.76
	Cable	3.16	3.10	3.04
	Block-to-Block	2.75	2.57	2.62
1	End-Twist-Tie	2.70	2.96	2.96
	Average F.S.	2.87	2.83	2.85
	Standard Deviation	0.21	0.24	0.19

Table C5

Maximum Stress (ksi)*

Number of Longitudinal Wires	Wire	Case 1	Case 2	Case 3
	Interblock	48.9	57.7	56.2
1	Cable	59.8	62.5	65.2
	Block-to-Block	49.5	58.8	57.2
	Interblock	58.5	67.8	65.9
2	Cable	66.7	69.2	71.4
	Block-to-Block	59.5	69.5	67.5
	Interblock	71.1	79.4	77.7
3	Cable	79.1	80.5	82.2
	Block-to-Block	74.0	83.4	81.7

Cable	Longitudinal Wires	
fpu = 250 ksi	0.162	0.141
.8 fpu = 200 ksi	fpu = 204 ksi	fpu = 215 ksi
pu = 20 k	pu = 4.2 k	pu = 3.35 k

* SI conversion factor: 1 ksi = 6900 kN/m^2.

spring, the two longitudinal wire springs, and the end-twist-tie connection were selected from each system for the three different cases, and stresses and factors of safety were calculated for each wire. Tables C4 and C5 show these results. For these calculations, 20,000 lbf (89.0 kN) was used as the ultimate load capacity of the cable as determined by laboratory tests, 4200 lbf (18.7 kN) and 3350 lbf (14.9 kN) were used as the ultimate load capacity of the 0.162- and 0.141-in. (4.1 and 3.6 mm) diameter wires, respectively; 3550 lbf (15.8 kN) was used for the ultimate load capacity of end-twist-tie connection wire. Table C4 shows that for each case, the factor of safety is greater than 2 and tends to decrease as the number of longitudinal wires decreases. A more balanced factor of safety is observed for case 3 with two longitudinal wires; for this combination the average factor of safety is 3.30 and the standard deviation is 0.14. However, in considering the factors of safety, it should be remembered that fluid and inertial forces were considered negligible in the model and that the factor of safety is based on an average launch depth of 100 ft (30.5 m).

Table C5 presents the stress levels associated with the peak force levels predicted by the multi-square force distribution model with the exception of the end-twist-tie wires. Stresses were not calculated for the end-twist-tie wire because the area to be used in the calculation was indeterminate. Results in Table C5 indicate that all stresses are within acceptable levels.

The bending stresses within the concrete blocks were also calculated. For each of the three wire systems analyzed, the highest differential between the longitudinal wires at the top and bottom of the concrete block model was chosen. The block was then idealized as a simply supported beam with either three-, two- or one-point loads depending on the number of longitudinal wires. The maximum moment at the center line was then obtained for the given load condition and the bending stress was calculated. The values for the bending stress were very low (less than 15 psi [103.5 kN/m^2]) in each system and were not considered to have much influence on the overall analysis. Therefore, they can be disregarded.

APPENDIX D: DISCUSSION OF GAGES

CERL began development of the mechanical gage in April 1972, using a nine-square test mat assembled at the laboratory. The prototype gage was tested at Kentucky Point, KY, on 12 September 1972 and was then modified to facilitate field installation.

In operation, the gage is installed in place of the usual mechanical connection at the location on the mat where a force measurement is desired. For bracket wire measurements the wire wrap is replaced with the bracket wire gage; for longitudinal wire measurements the longitudinal gage is installed instead of the longitudinal end-twist-tie link. The wires press against the soft brass beveled-edge "target" as the mat is launched; the depth that the wires penetrate the target is a measure of the maximum force that occurred at that location in the mattress during the launching operation.

Figure D1 shows the gage configuration for longitudinal wire measurements and Figure D2 shows the configuration for bracket wire measurements (the semicircular notch is to accommodate the launch cable).

The target remains in place until it is retrieved, either while the mat is on the river bottom or at an earlier time. The retrieval mechanism is shown in Figure D3. The assembled gages (Figures D1 and D5) are held together by the "T" link; when this is pulled off by the retrieval line, the gage sides swing aside and release the target, which is recovered with the retrieval line.

Gages are calibrated by application of a known force through a wire configuration which reproduces the load geometry occurring on the fabric wire in the mat. The resultant target indentation is optically measured to provide a calibration curve of target indentation versus applied load. The loads are carefully applied to the calibration specimens so that a clear target indentation is obtained.

Indented targets obtained from field tests are measured in the same manner to establish the applied load. The penetration depth is taken as the perpendicular distance of penetration from the undisturbed gage profile line (Figure B4). In the case of light loads, the indentation mark obtained in the field is usually quite clean and appears to be identical to the calibration specimens. Where loads are 3000 lbf (13.3 kN) or more, however, the targets often have other deformation which results from gage frame distortions as described below.

Accurate measurement with this gage requires a solid supporting frame beneath the target so that the applied forces produce indentation in the knife edges of the target rather than distortion and bending of the target material.

The original gage frame (Figure D5) has a measured load-carrying capability in excess of 3600 lbf (16.0 kN) for sustained loads. Because of problems installing this gage in the restricted space between squares in the field, the frame was modified in 1972 to permit easier installation. The modification essentially involved changing a bolt hole into a slot so that one side member could be installed after the balance of the frame was in the proper position (Figure D6). This modification weakened the gage frame and consequently reduced the gage capacity for sustained loads. Failure of the gage frame occurred in the slotted section (Figure D7). The results obtained in 1972 and 1973 with both the modified and unmodified gages indicated, however, that the strength of the modified gage was adequate for most of the measurements taken.

It should be stressed, however, that despite the modified gage's reduced load capacity, it provided other valuable information relative to mat behavior. It has been observed in testing under laboratory calibration conditions that there is a finite time of failure of the gage frame at loads which may be as low as 1500 lbf (6.7 kN). The slotted hole section deforms relatively slowly; thus, this gage configuration has a certain time-dependency of life and load. If the loads are applied quickly and relieved quickly, the gage is capable of measurements significantly in excess of 1500 lbf (6.7 kN). The gage frame capacity under relatively rapid loads has been measured to at least 2400 lbf (10.7 kN) without frame failure or severe distortion. The maximum load measured with frame failure under particular testing conditions was 2700 lbf (12.0 kN). This value, however, should not be taken as a meaningful upper bound, in that the load application rate was neither rigorously controlled nor excessively high. Under sustained loads, the gage can be observed to fail quite slowly, in the order of a few seconds. Finally, it should be noted that these effects are not perfectly reproducible. The capacity of the gage is critically dependent on the frame geometry and manufacturing tolerances, because the effective lever system of the gage puts approximately 90 percent of the applied force on the slotted hole. Force on the target is not geometry-dependent.

Gage measurement tabulations have shown that some units indicated loads in excess of the 1500-lbf (6.7 kN) value—which, if sustained, would have produced gage failure. To better evaluate these readings, the target indentations were read and each target was inspected for deformation of the general shape. Such deformation was observed, primarily in the extremities of the target legs. If the frame fails or is in the process of failing, separation of the target tips or leg ends must occur. As the target tip deforms, the indentations lose their precise calibration because of sheering action and rotational effects of the wire and the change in geometry of the effective target area for the wire.

Since the indentations obtained in field testing were larger than desirable for precise calibration, all targets were inspected for gross deformation of one or both target tip ends. All targets in the 1973 series were also inspected for gross physical distortion of the target, and to determine if one or both tips were deformed. If a single side of the target was deformed and the second side retained its original geometry (Figure D8), it was assumed that the gage at least partially failed, but that during this time the load was still being carried properly by the tip which did not show distortion or bending. The straight tip retained its proper back support and, therefore, the load values determined from it should be valid. If gross gage failure occurred, due either to extremely high or sustained loads, then both tips would be significantly distorted upon total failure of the frame, since both would lose their back support. These effects have been verified in the laboratory. As described earlier, the target condition after recovery indicated the validity of the load values.

In summary, one can reasonably accept those values shown where at least one leg of the target remained straight or was deformed minimally. When both legs were severely bent and/or the target was badly deformed, the results are questionable.

In cases where only one leg was deformed while the other remained straight, one can conclude that the indicated loads did, indeed, exist long enough to cause frame failure.

There are also cases where loads of significant magnitude (3 to 4 kips [13.3 to 17.8 kN]) were measured, but gage frame failure did not occur. It must be assumed that these were short-duration loads.

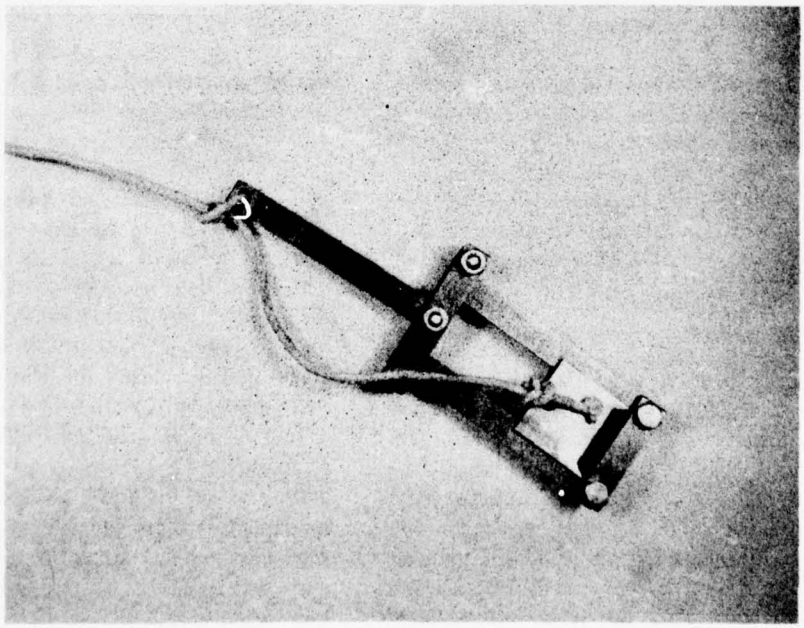

Figure D1. Longitudinal wire gage.

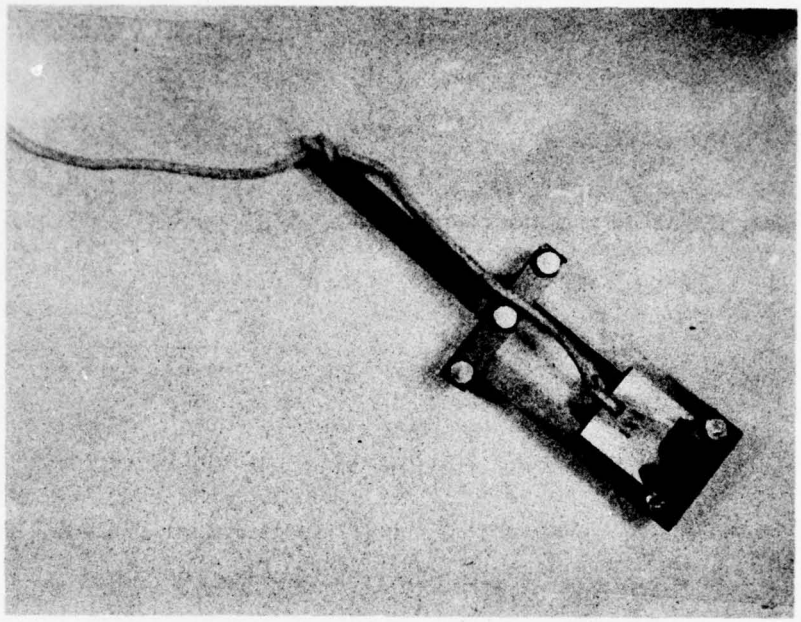

Figure D2. Bracket wire gage.

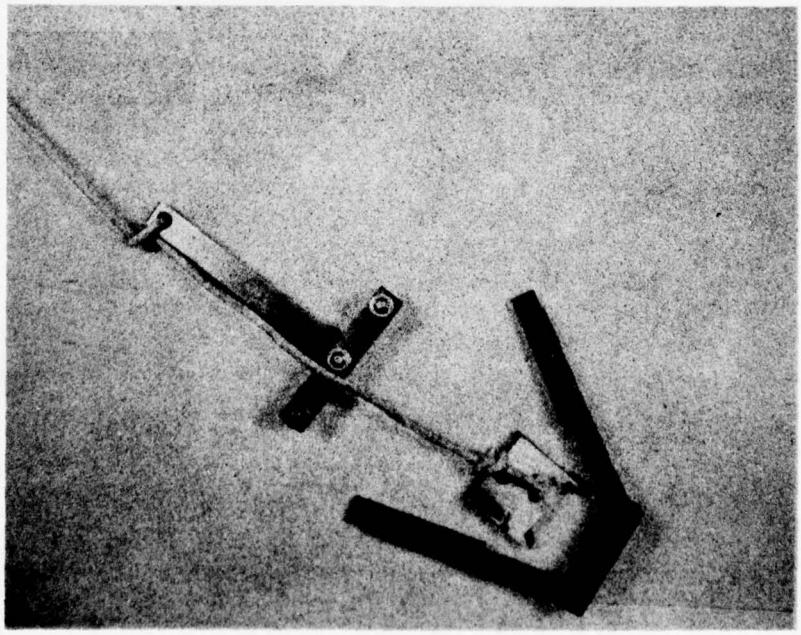

Figure D3. Gage in retrieval mode.

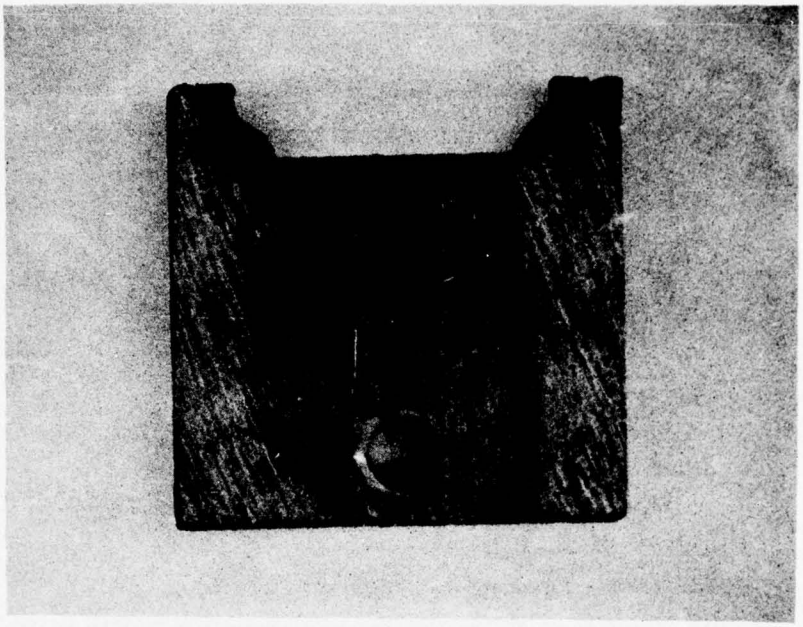

Figure D4. Typical target showing indentations corresponding to a 2200-lb (9.7 kN) force.

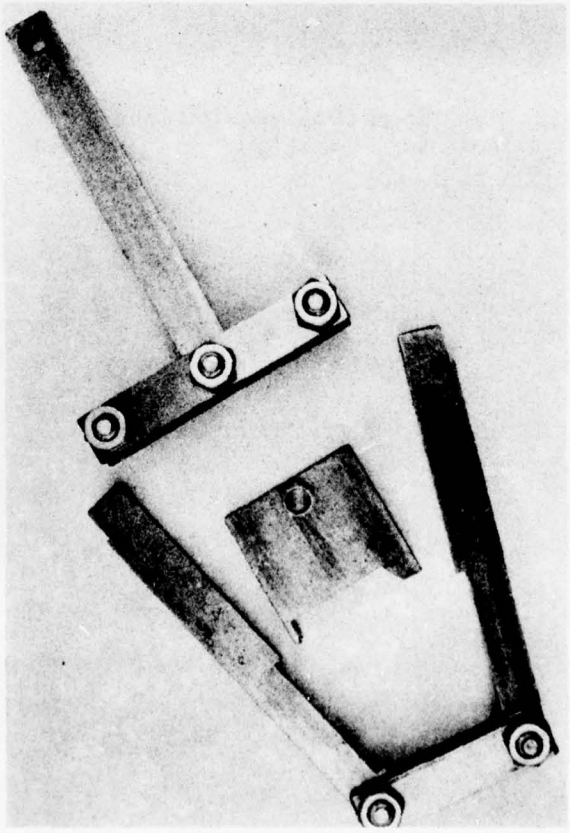

Figure D5. Original gage frame.

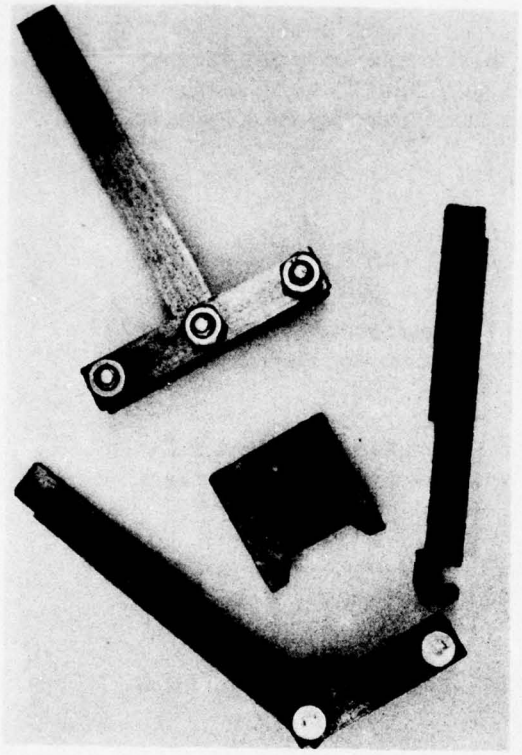

Figure D6. Modified gage frame—slotted frame member.

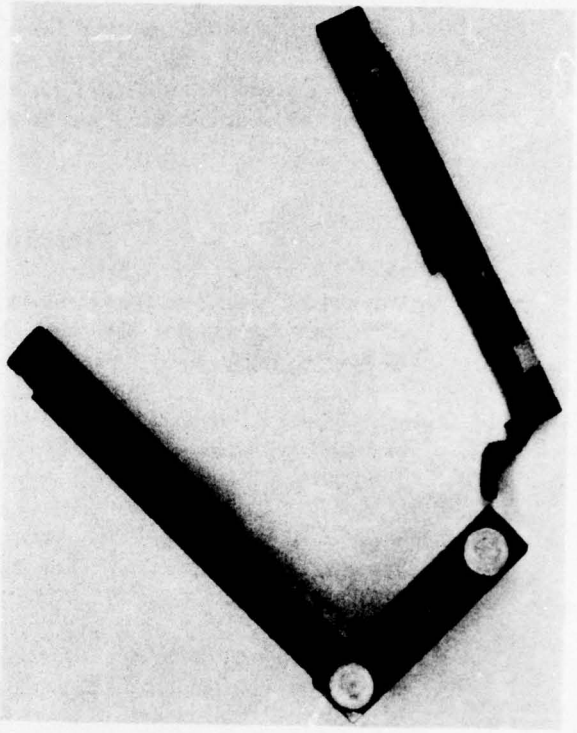

Figure D7. Gage frame failure at slotted section.

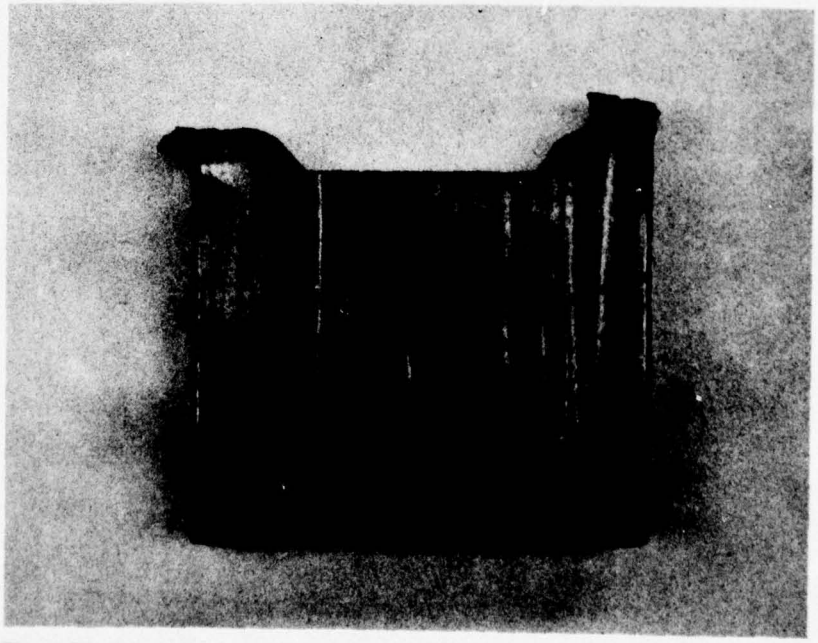

Figure D8. Target from failed gage frame—indentation on the right side acceptable.

APPENDIX E: SUMMARY OF FY75 FORCE MEASUREMENTS

An instrumentation location chart for recording the field data was devised. The chart grid corresponds to the mattress array so that each chart shows the spatial location of gages on the mat and the force level recorded for that mat. Terminology and designations conform with those described in Appendix A.

REFERENCES

Fage, A. and F.C. Johansen, *The Connection Between Lift and Circulation of an Inclined Flat Plate,* Reports and Memoranda No. 1104 (England: Aeronautical Research Committee, 1927).

Kearney, F. and F. Plummer, *Study of Articulated Concrete Revetment Mattress: Test and Analysis,* Interim Report M-84 (U.S. Army Construction Engineering Research Laboratory [CERL], 1974).

Kearney, F. and J. Prendergast, *Study of Articulated Concrete Revetment Mattress: Test and Analysis–Results of FY 1974 Program,* Technical Report M-94/ADA021774 (CERL, 1976).

Murtha, J.P., *Hydrodynamic Force Model for the Articulated Concrete Mattress,* Letter Report (University of Illinois, 22 September 1972).

Schlicting, H., *Boundary Layer Theory* (McGraw-Hill, 1960).

Shore Anchor Pull-Out Tests; Force Study BPP No. 8 (Revetment Operations Improvement Board, Memphis Engineer District, February 1966).

MATTRESS INSTRUMENT LOCATION CHART

Location: GOLDBOTTOM, LA Date: 31 OCT 74

Remarks: TWO LONGITUDINAL WIRE MAT #38
COPPERWELD

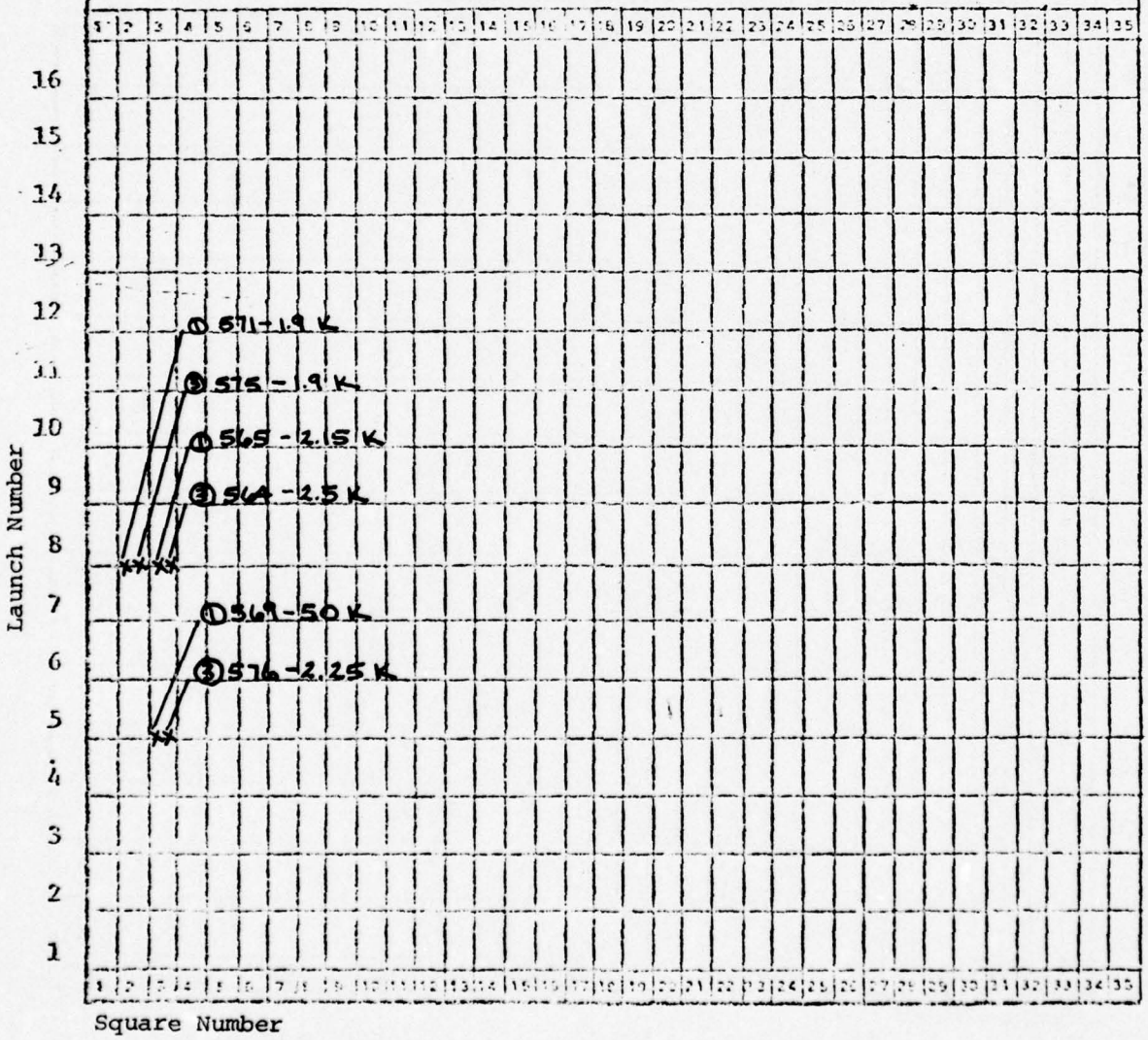

MATTRESS INSTRUMENT LOCATION CHART

Location: GOLDBOTTOM, LA Date: 31 OCT 74

Remarks: TWO LONGITUDINAL WIRE MAT #39
COPPERWELD

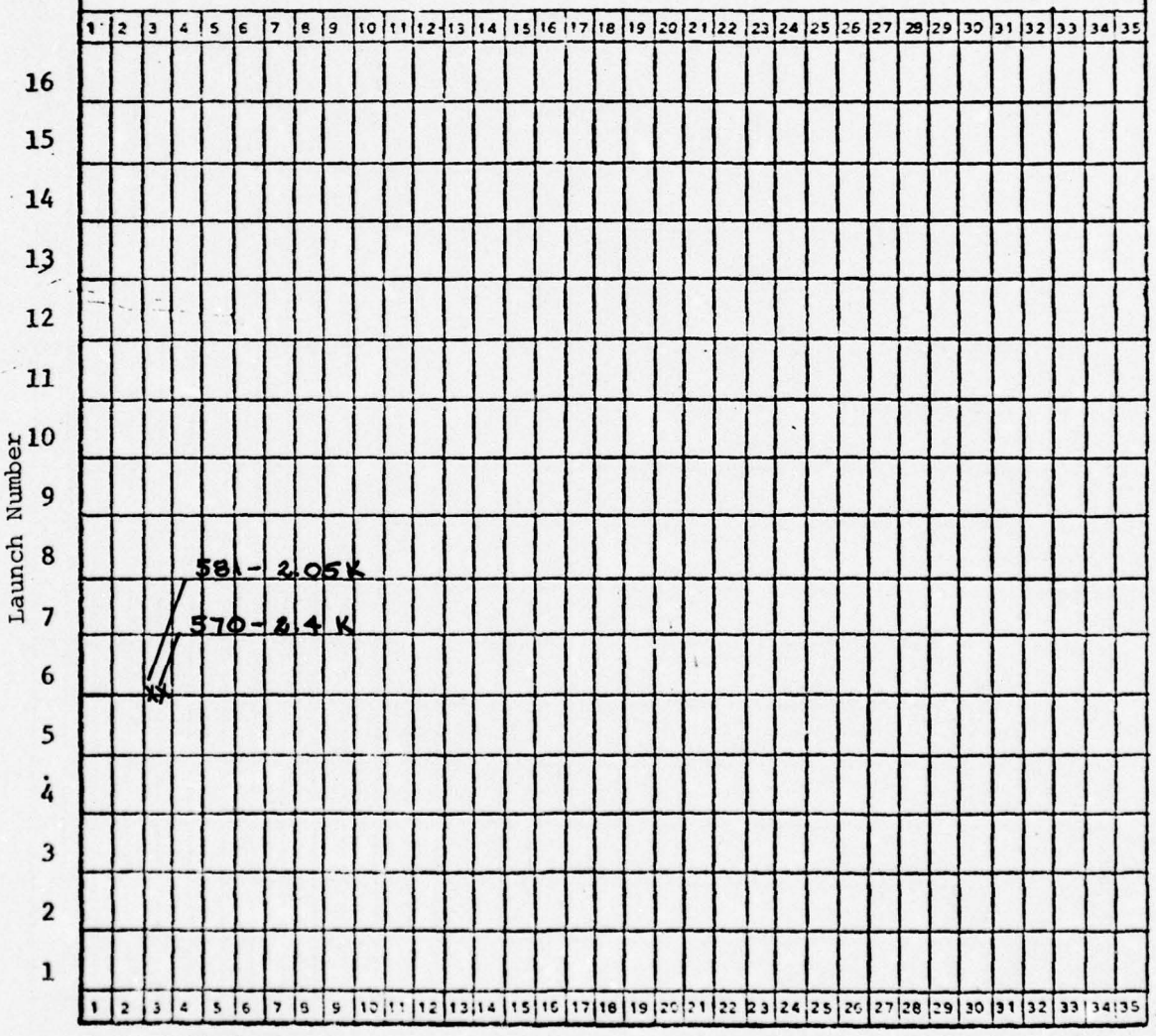

MATTRESS INSTRUMENT LOCATION CHART

Location: GOLDBOTTOM, LA Date: 31 OCT 74

Remarks: TWO LONGITUDINAL WIRE MAT #40
COPPERWELD

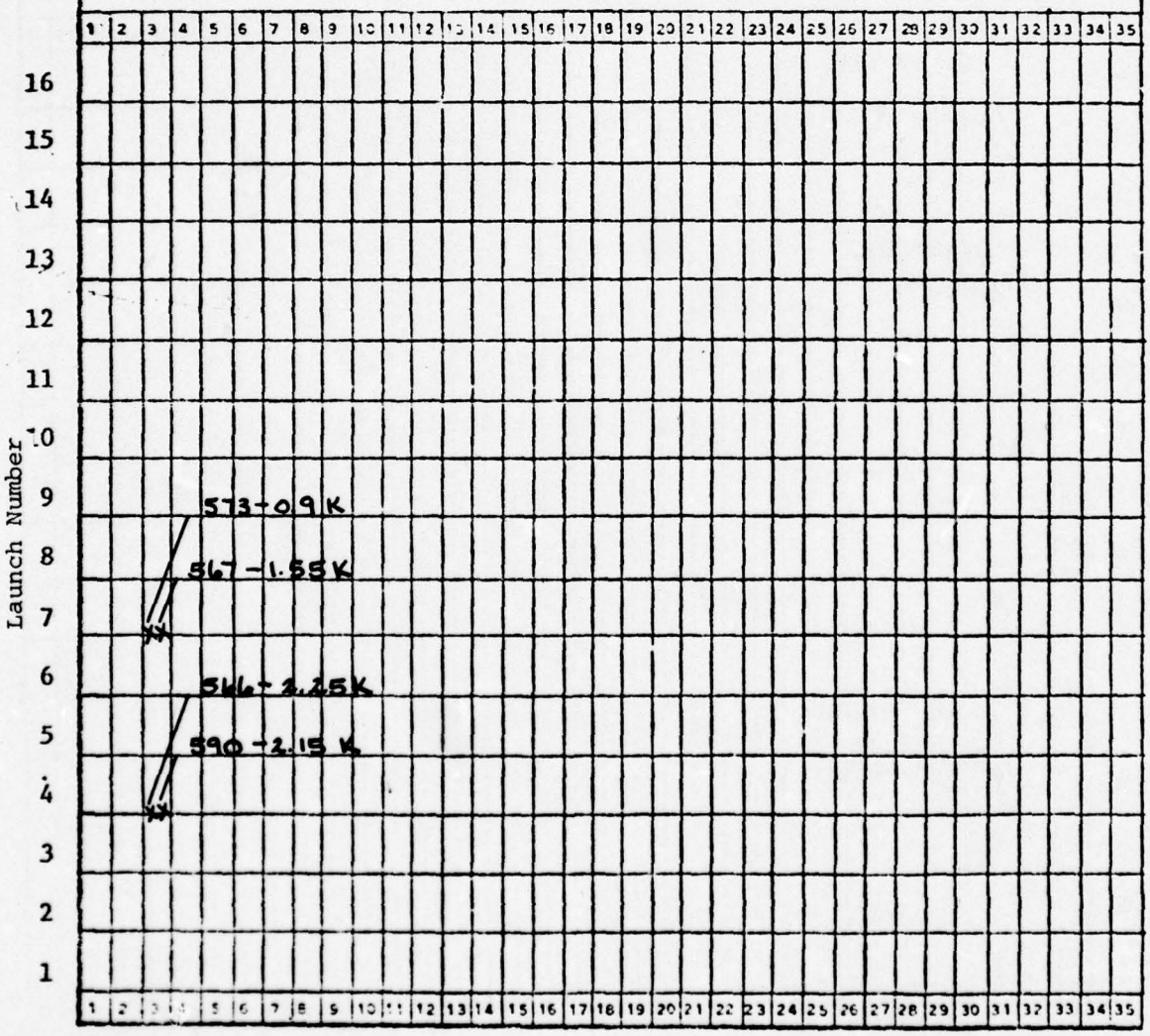

MATTRESS INSTRUMENT LOCATION CHART

Location: GOLDBOTTOM, LA Date: 1 NOV 74

Remarks: TWO LONGITUDINAL WIRE MAT #48
COPPERWELD

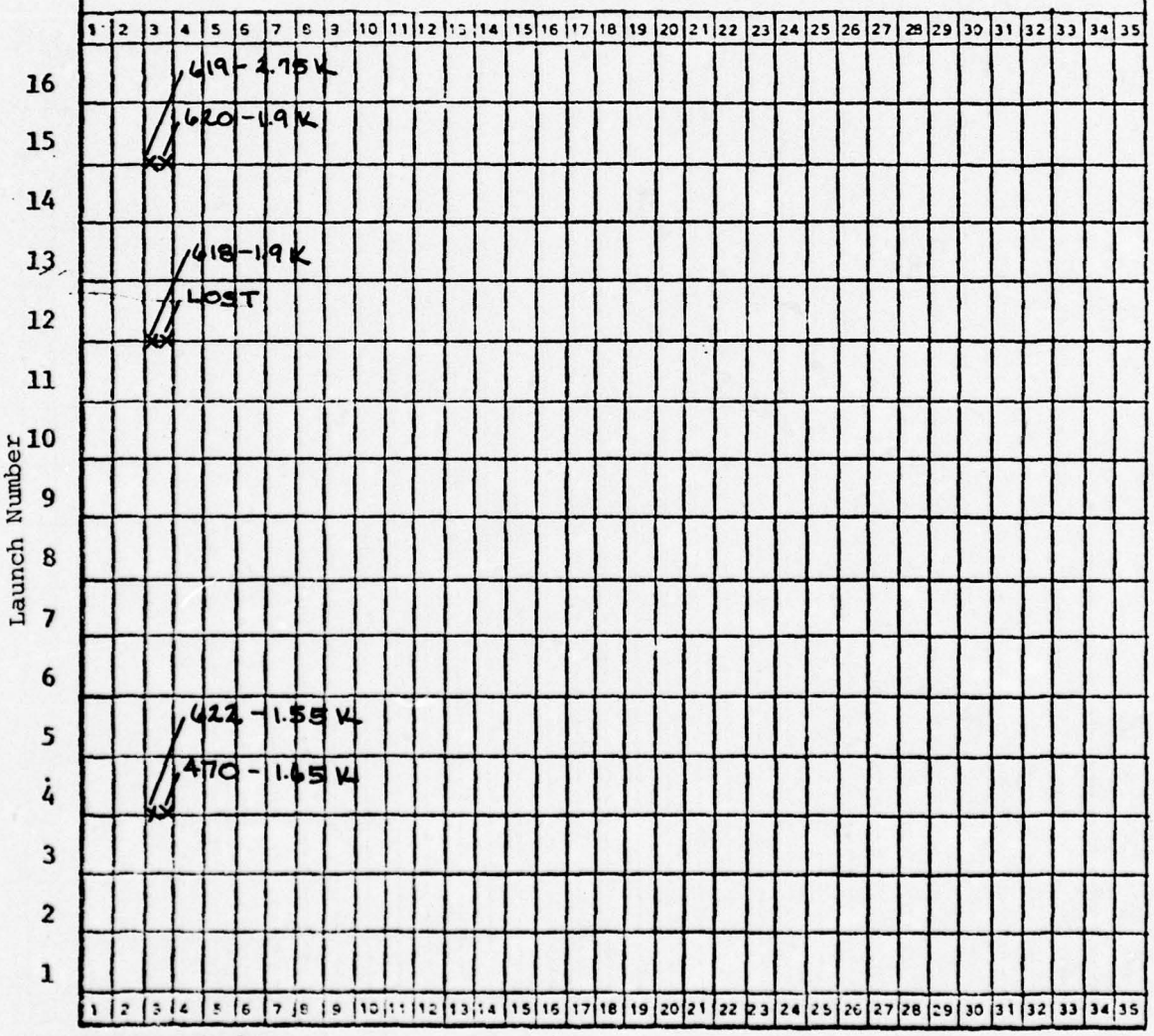

MATTRESS INSTRUMENT LOCATION CHART

Location: MANCHAC, LA Date: 3 DEC 74

Remarks: THREE LONGITUDINAL WIRE MAT #85

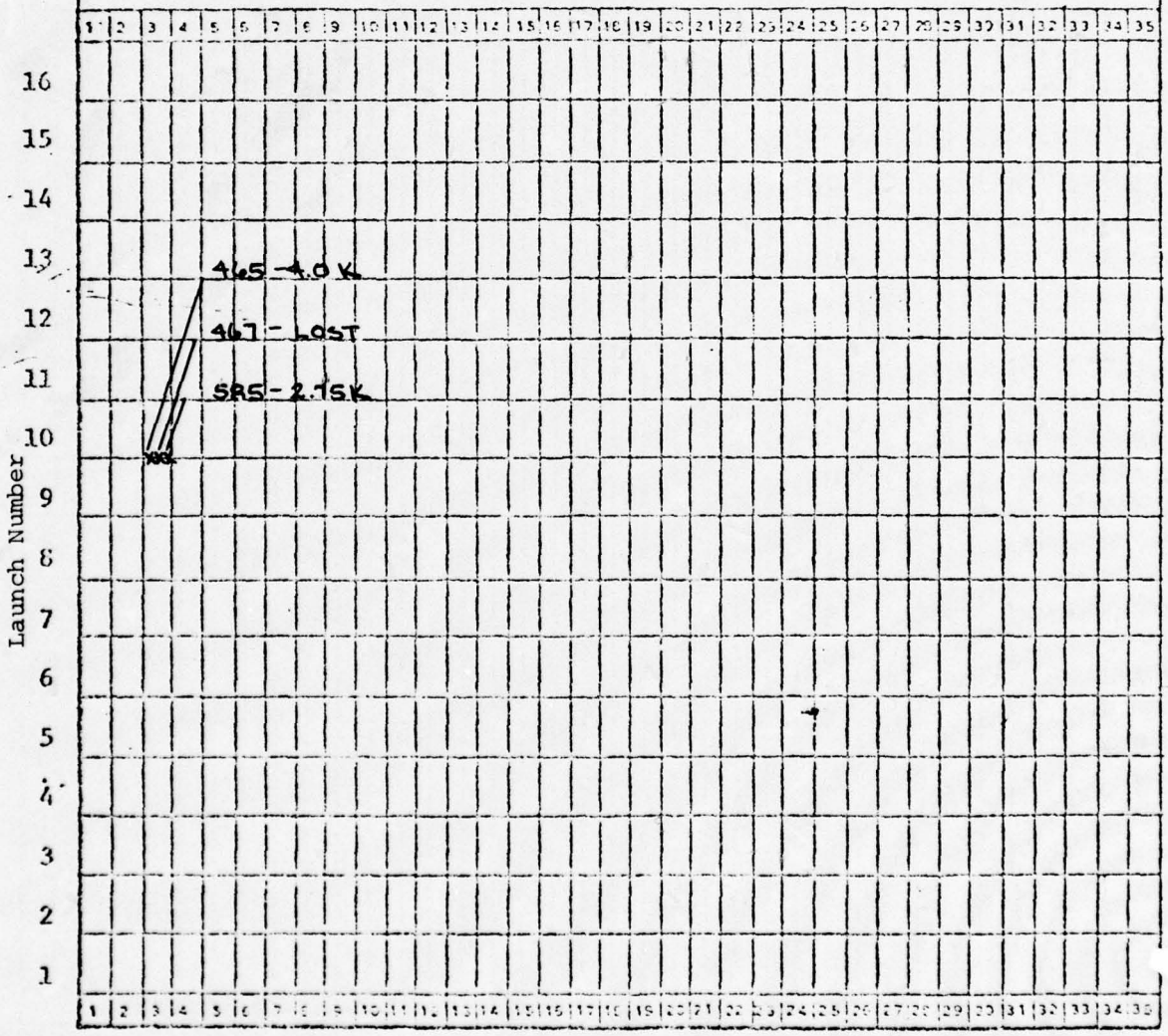

MATTRESS INSTRUMENT LOCATION CHART

Location: MANCHAC, LA Date: 3 DEC 74

Remarks: THREE LONGITUDINAL WIRE MAT #85

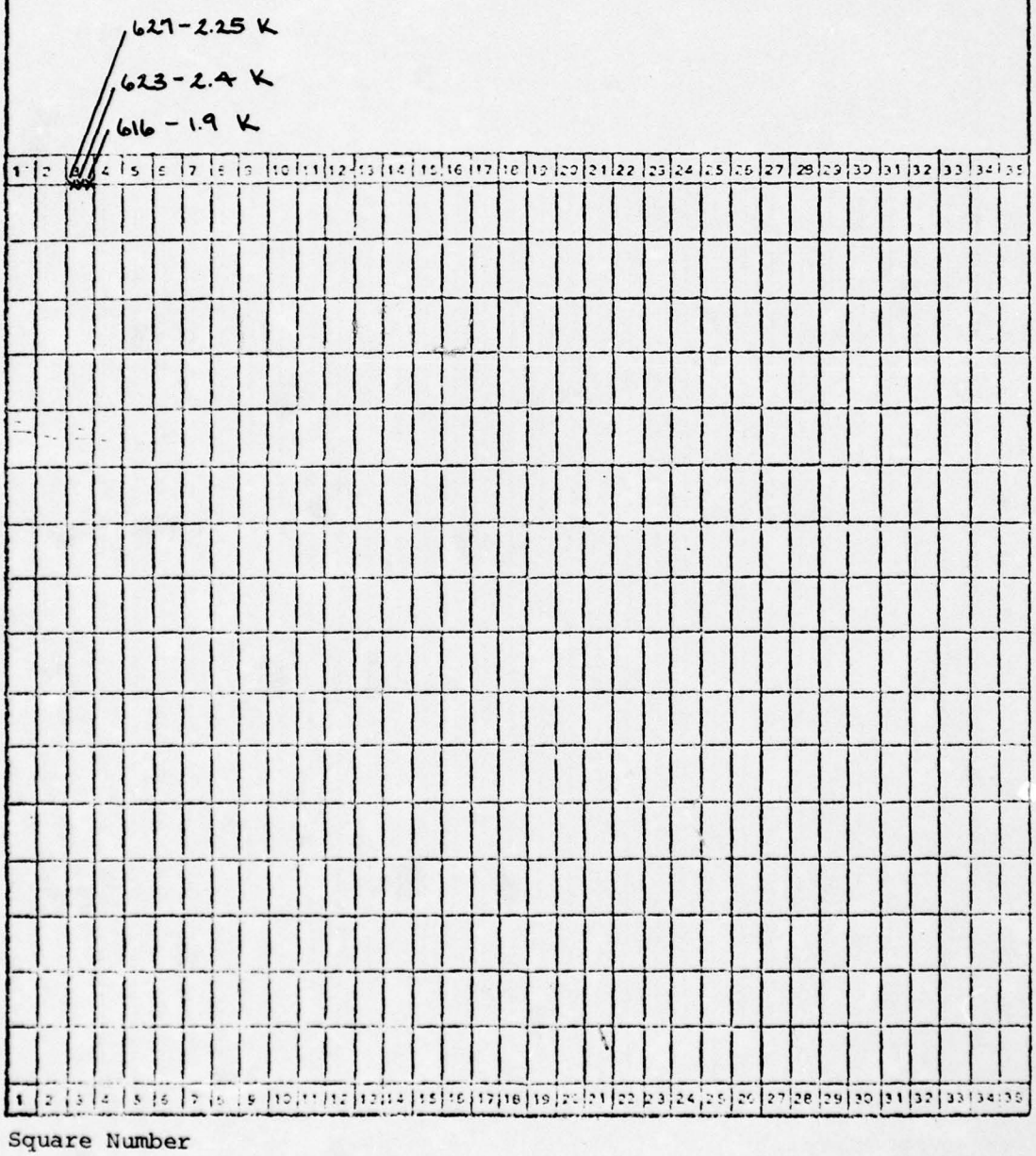

MATTRESS INSTRUMENT LOCATION CHART

Location: MANCHAC, LA Date: 3 DEC 74

Remarks: THREE LONGITUDINAL WIRE MAT #87

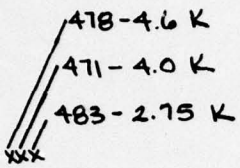

Launch Number

19
18
16
15
14
13
12
11
10
9
8
7
6
5
4
3
2
1

1 2 3 4 5 6 7 8 9 10 11 12 13 14 15 16 17 18 19 20 21 22 23 24 25 26 27 28 29 30 31 32 33 34 35

Square Number

MATTRESS INSTRUMENT LOCATION CHART

Location: MANCHAC, LA Date: 4 DEC 74

Remarks: THREE LONGITUDINAL WIRE MAT #92
GAGES INSTALLED ON UPSTREAM & DOWNSTREAM WIRES-
CENTER WIRES NOT TIED

476 - 3.0K
597 - 2.9 K
XX

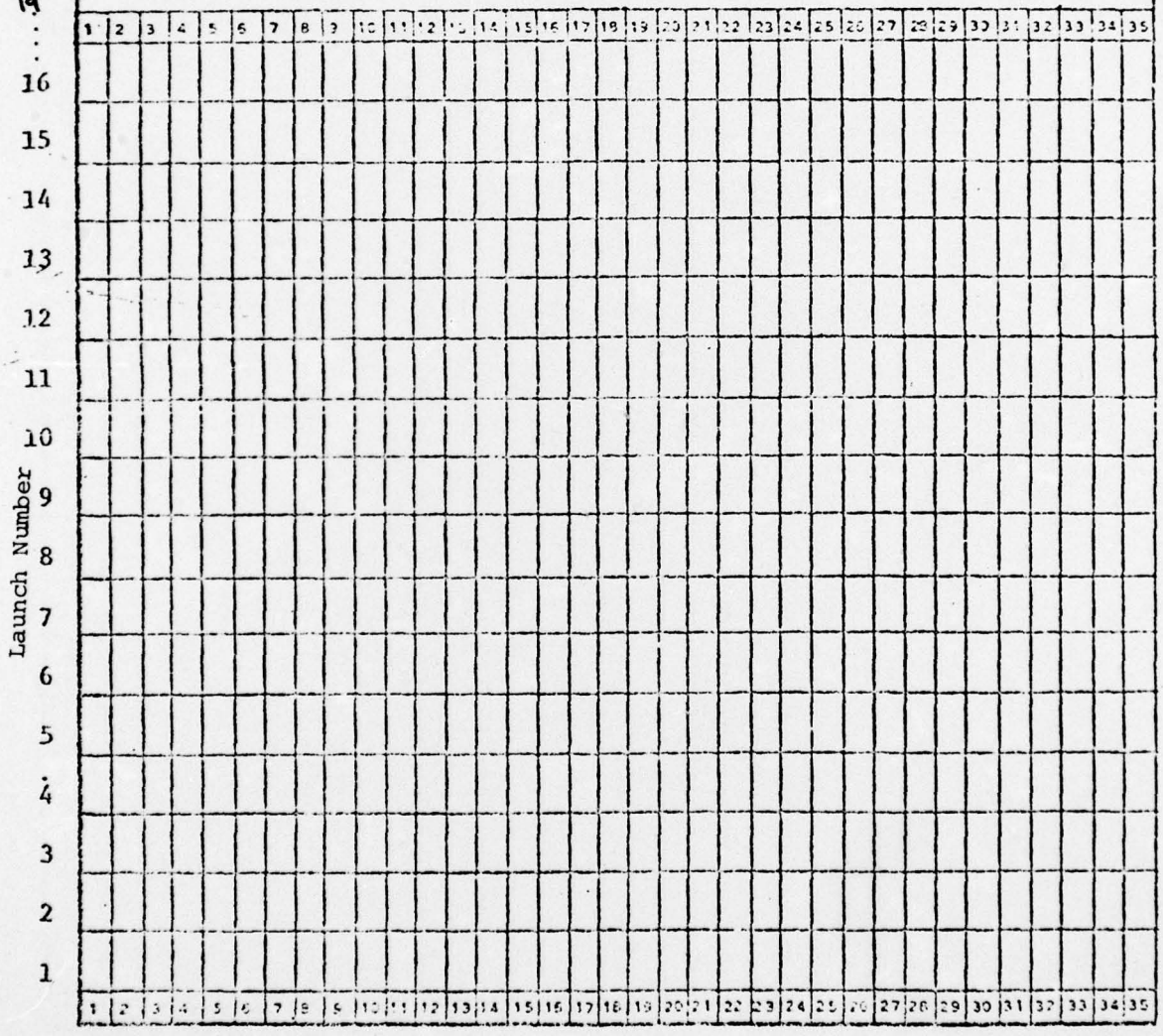

MATTRESS INSTRUMENT LOCATION CHART

Location: MANCHAC, LA Date: 4 DEC 74

Remarks: THREE LONGITUDINAL WIRE MAT #93
GAGES INSTALLED ON UPSTREAM & DOWNSTREAM
WIRES - CENTER WIRES NOT TIED

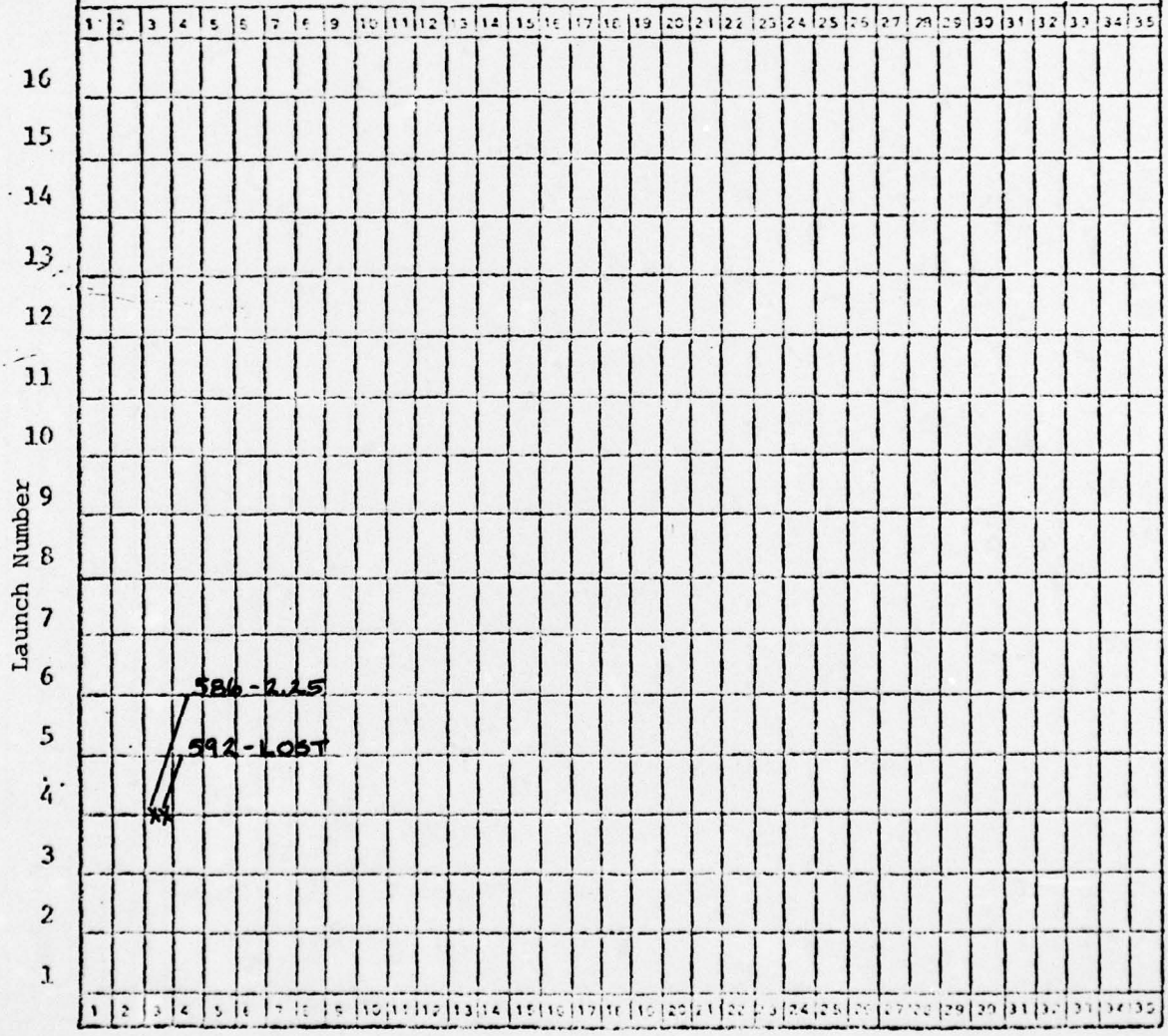

MATTRESS INSTRUMENT LOCATION CHART

Location: MANCHAC, LA Date: 4 DEC 74

Remarks: THREE LONGITUDINAL WIRE MAT #94

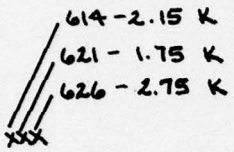

Launch Number

22
21
16
15
14
13
12
11
10
9
8
7
6
5
4
3
2
1

1 2 3 4 5 6 7 8 9 10 11 12 13 14 15 16 17 18 19 20 21 22 23 24 25 26 27 28 29 30 31 32 33 34 35

Square Number

MATTRESS INSTRUMENT LOCATION CHART

Location: MANCHAC, LA Date: 5 DEC 74

Remarks: TWO WIRE LONGITUDINAL WIRE MAT #99
STAINLESS STEEL

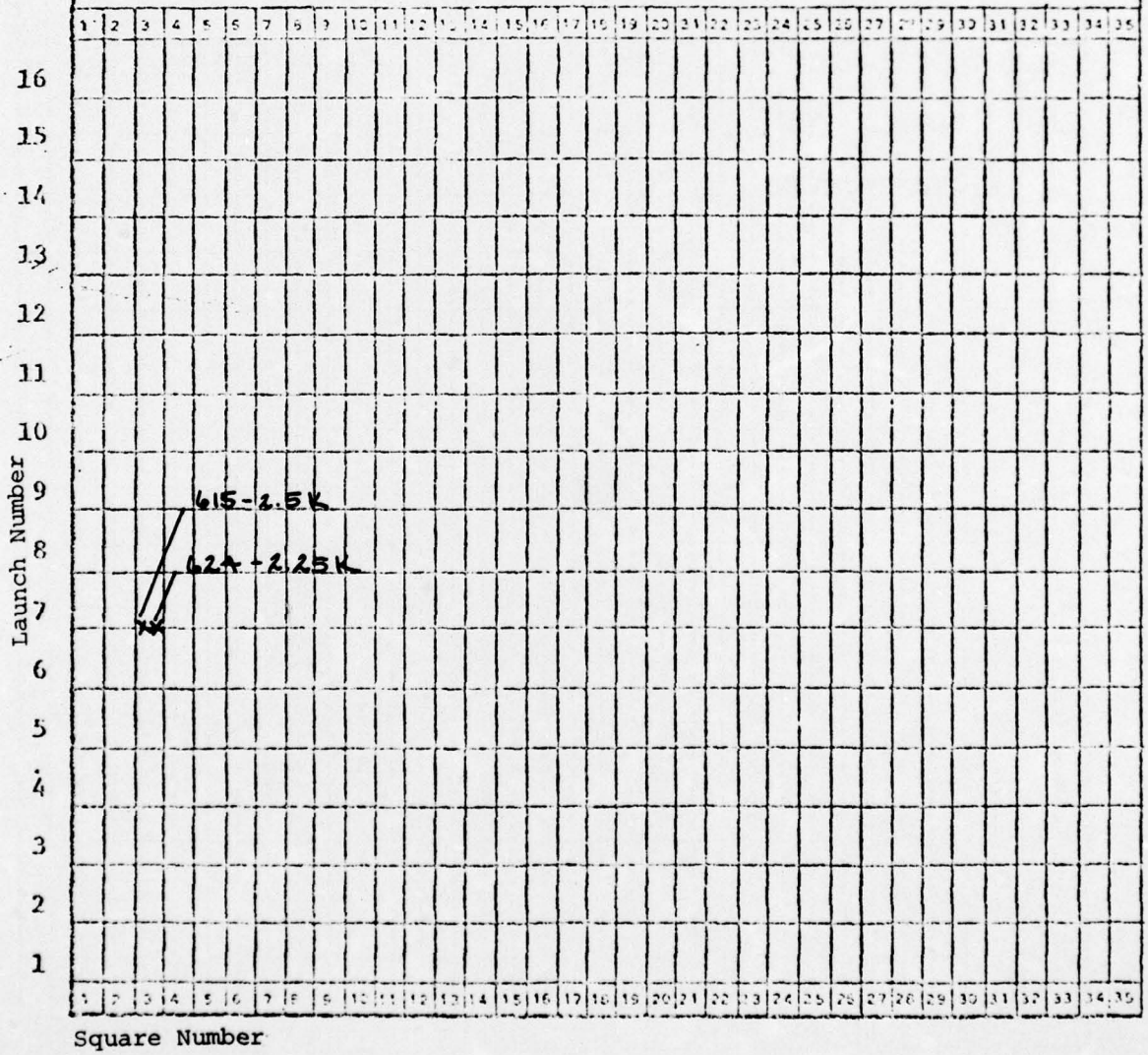

MATTRESS INSTRUMENT LOCATION CHART

Location: MANCHAC, LA Date: 5 DEC 74

Remarks: TWO WIRE LONGITUDINAL WIRE MAT #99
STAINLESS STEEL

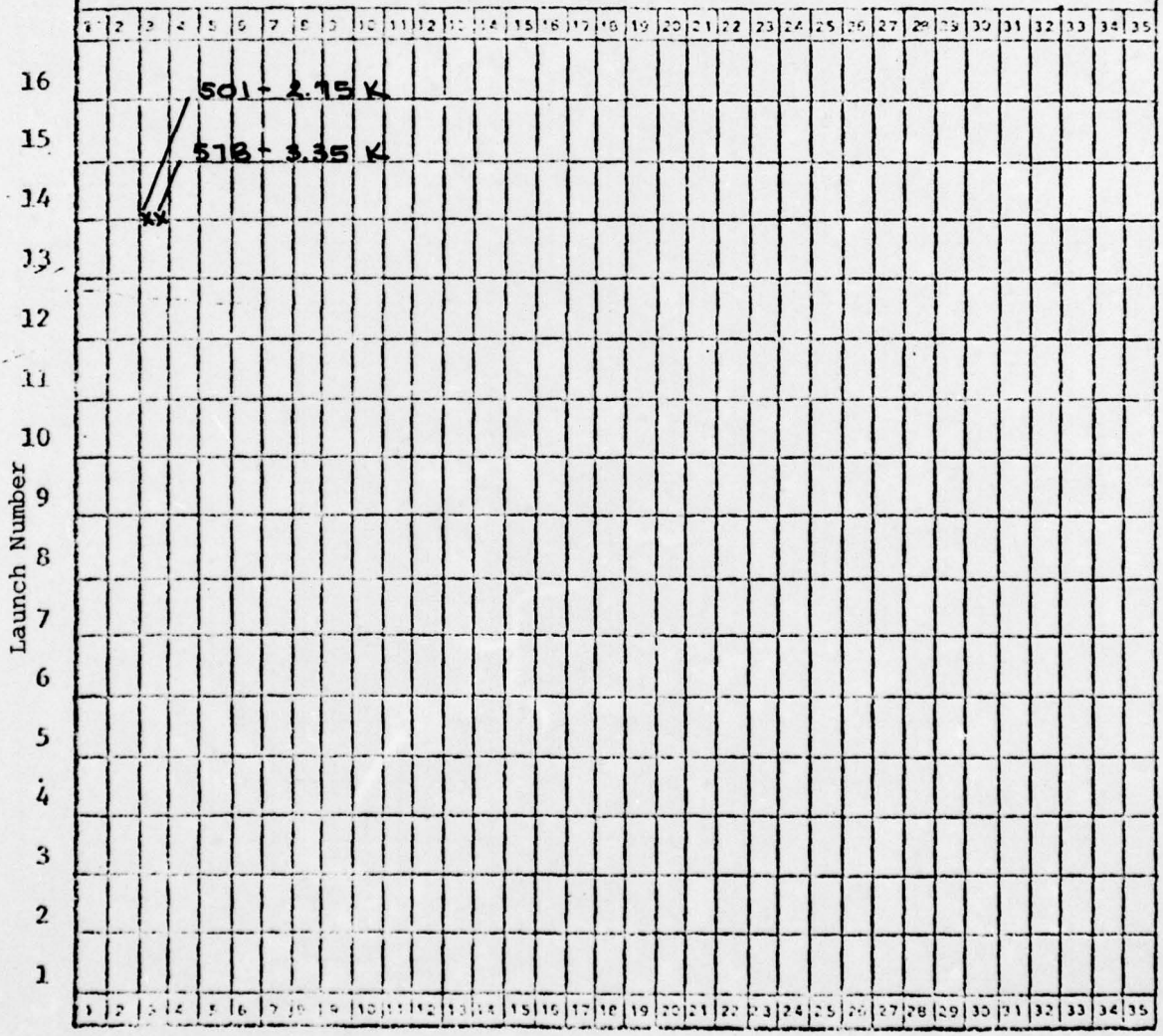

MATTRESS INSTRUMENT LOCATION CHART

Location: MANCHAC, LA Date: 5 DEC 74

Remarks: TWO WIRE LONGITUDINAL WIRE MAT # 99
STAINLESS STEEL

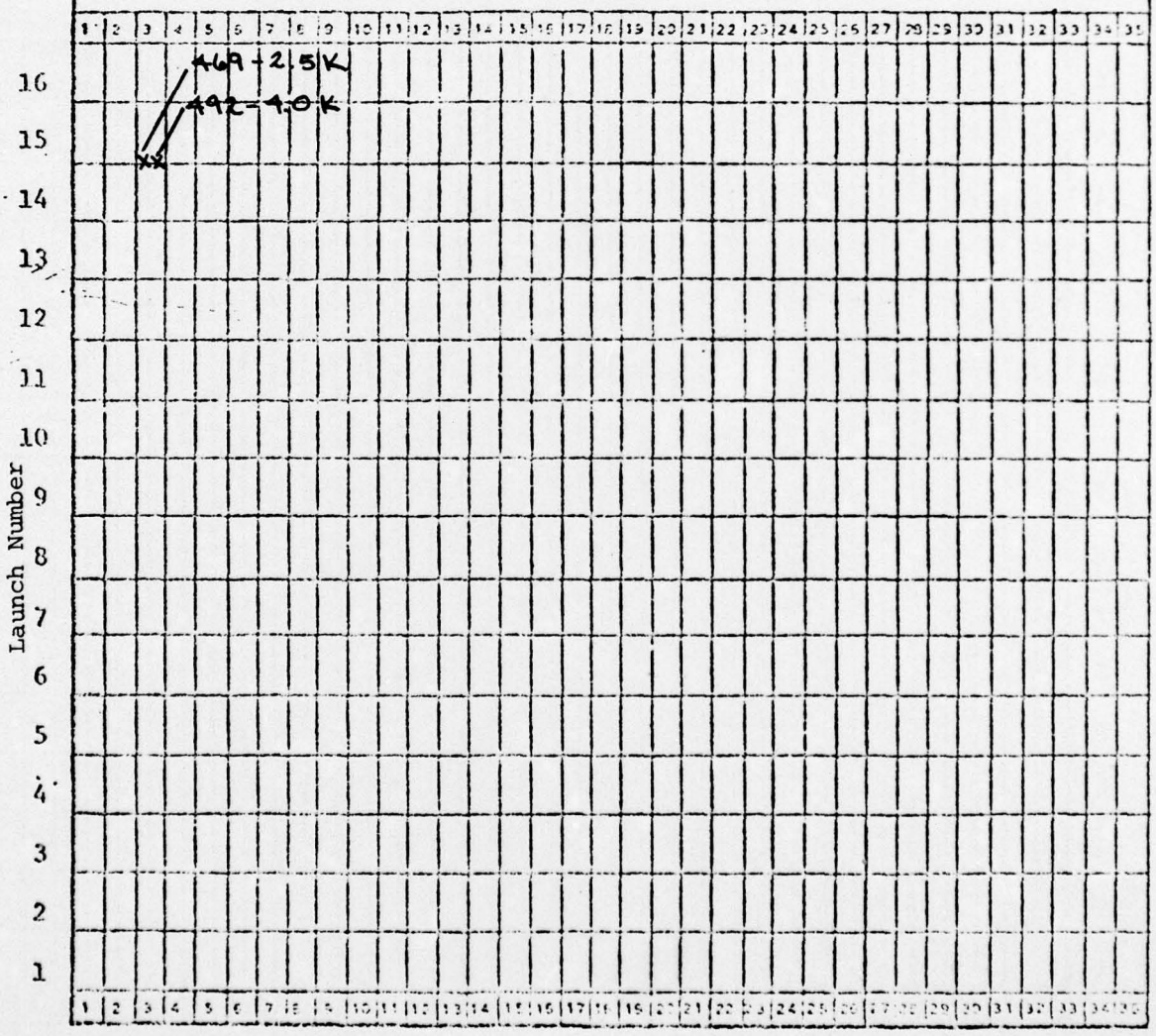

Square Number

MATTRESS INSTRUMENT LOCATION CHART

Location: MANCHAC, LA Date: 5 DEC 74

Remarks: TWO LONGITUDINAL WIRE MAT #99
STAINLESS STEEL

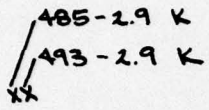

Launch Number

Square Number

MATTRESS INSTRUMENT LOCATION CHART

Location: MANCHAC, LA Date: 5 DEC 74

Remarks: TWO LONGITUDINAL WIRE MAT #99
STAINLESS STEEL

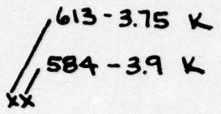

Launch Number

Square Number

MATTRESS INSTRUMENT LOCATION CHART

Location: CROSS BAYOU, LA Date: 5 DEC 74

Remarks: THREE LONGITUDINAL WIRE MAT #7

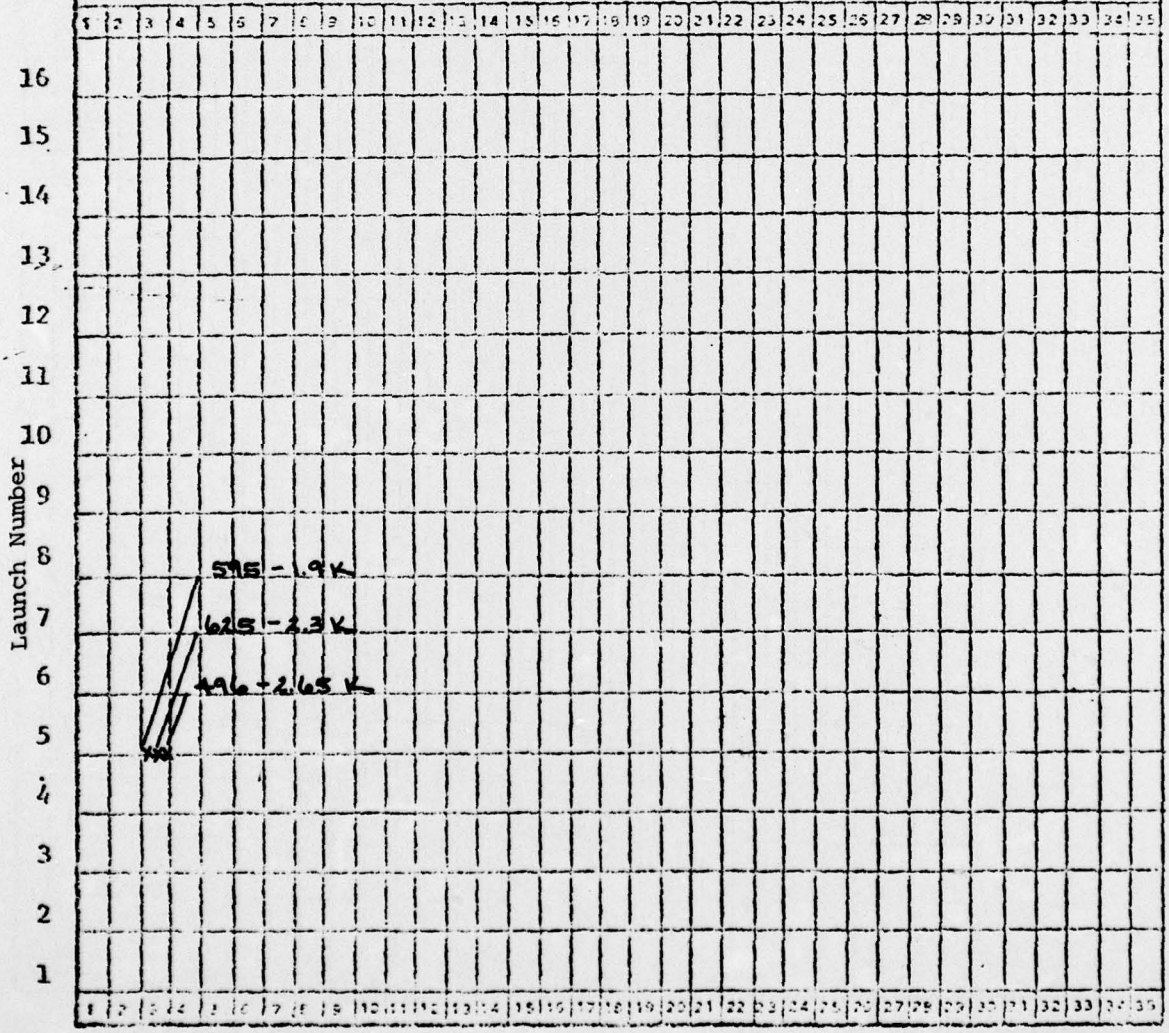

MATTRESS INSTRUMENT LOCATION CHART

Location: CROSS BAYOU, LA Date: 6 DEC 74

Remarks: THREE LONGITUDINAL WIRE MAT #11
MAT PULLER USED ON THIS TEST
MIDDLE WIRE NOT CONNECTED

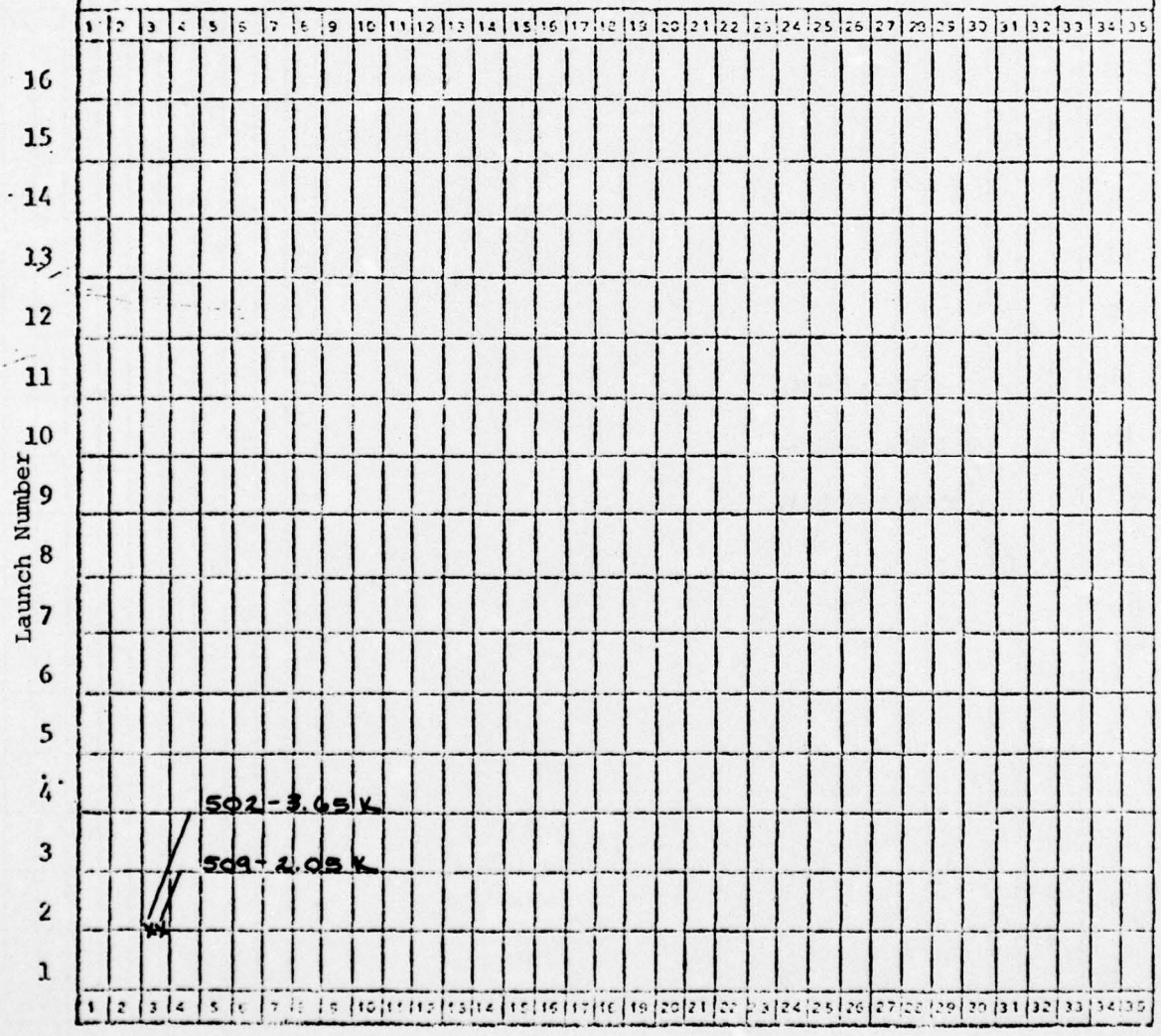

MATTRESS INSTRUMENT LOCATION CHART

Location: CROSS BAYOU, LA Date: 6 DEC 74

Remarks: THREE LONGITUDINAL WIRE MAT #11

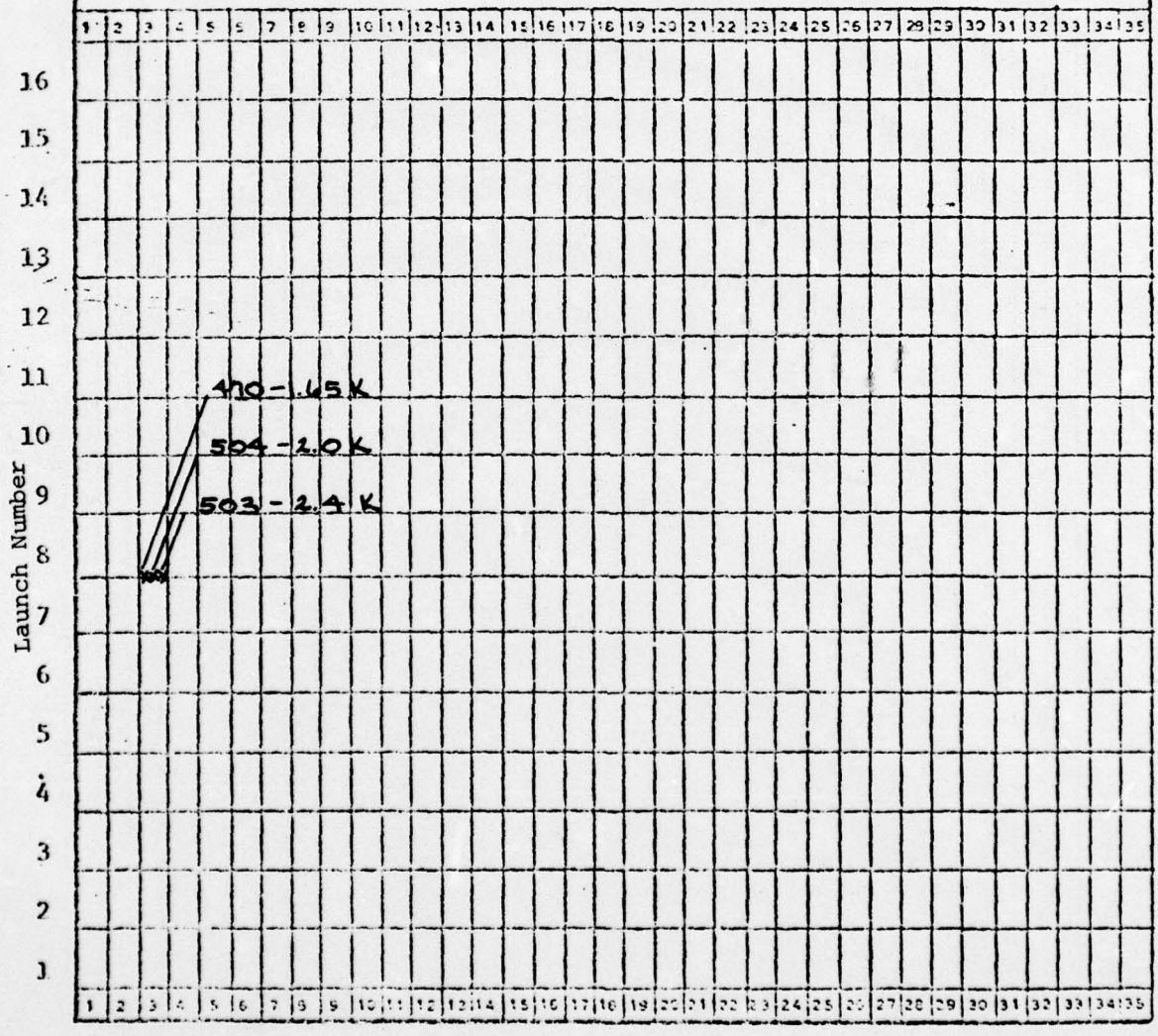

MATTRESS INSTRUMENT LOCATION CHART

Location: CROSS BAYOU, LA Date: 6 DEC 74

Remarks: THREE LONGITUDINAL WIRE MAT #11

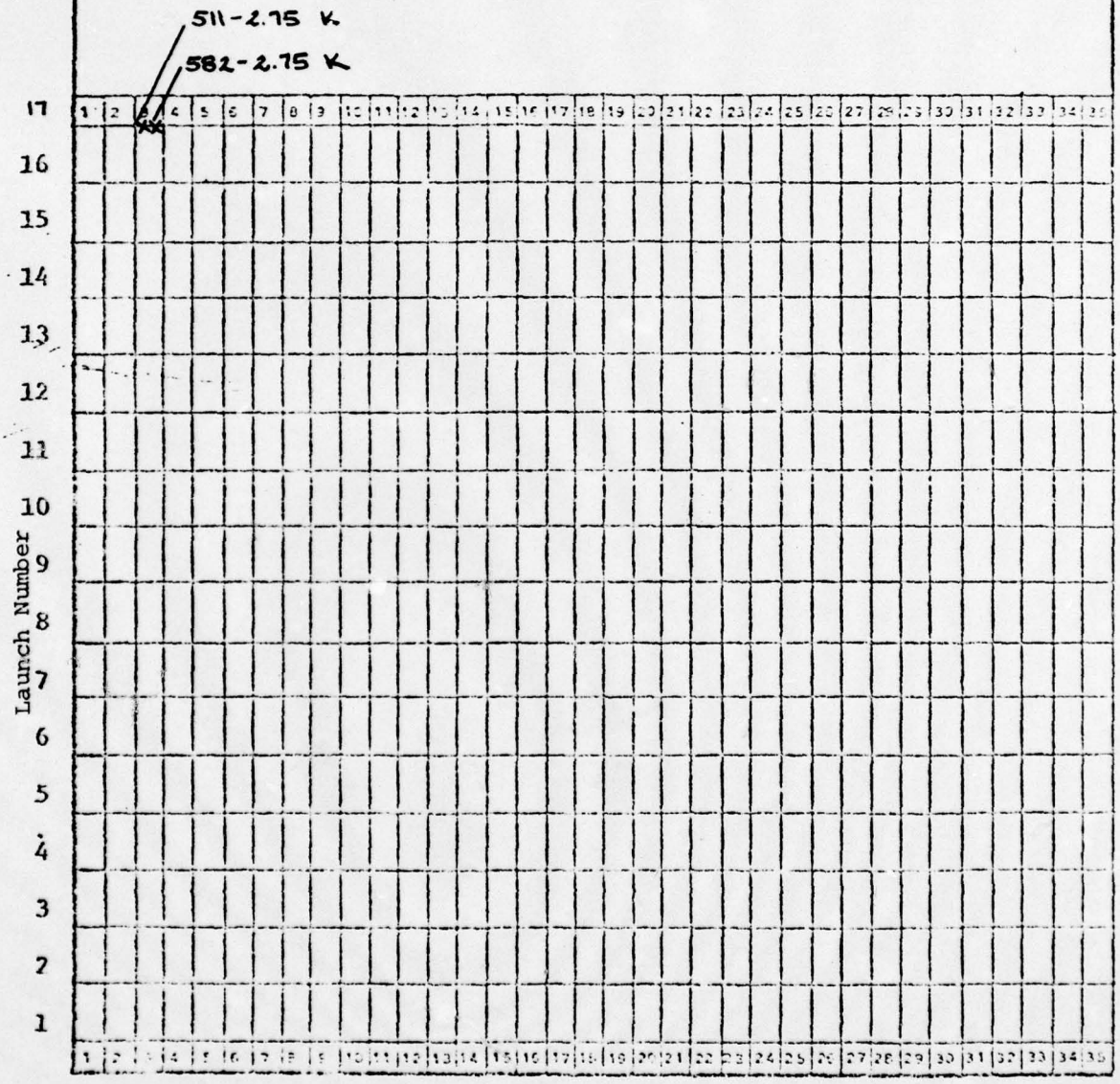

MSM

CERL DISTRIBUTION

Director of Facilities Engineering
APO NY 09827

DARCOM STIT-EUR
APO New York 09710

West Point, NY 10996
ATTN: Dept of Mechanics
ATTN: Library

Chief of Engineers
ATTN: DAEN-ASI-L (2)
ATTN: DAEN-FEU
ATTN: DAEN-FESA
ATTN: DAEN-FEZ-A
ATTN: DAEN-MCZ-S
ATTN: DAEN-RDL
ATTN: DAEN-PMS (6)
for forwarding to
National Defense Headquarters
Director General of Construction
Ottawa, Ontario K1AOK2
Canada

Canadian Forces Liaison Officer (4)
U.S. Army Mobility Equipment
Research and Development Command
Ft Belvoir, VA 22060

Airports and Const. Services Dir.
Technical Information Reference
Centre
KAOL, Transport Canada Building
Place de Ville, Ottawa, Ontario
Canada, K1AON8

Ft Belvoir, VA 22060
ATTN: Kingman Bldg, Library

Ft Monroe, VA 23651
ATTN: ATEN

Ft McPherson, GA 30330
ATTN: AFEN-FED

USA-WES
ATTN: Concrete Laboratory
ATTN: Library

6th USA
ATTN: AFKC-LG-E

US Army Science & Technology Center
- Far East Office

US Army Engineer District
Buffalo
ATTN: Library
Pittsburgh
ATTN: Library
Philadelphia
ATTN: Library
ATTN: Chief, NAPEN-D
Baltimore
ATTN: Chief, Engr Div
Norfolk
ATTN: Chief, NAOEN-D
Wilmington
ATTN: Chief, SAWEN-D
Charleston
ATTN: Chief, Engr Div
Savannah
ATTN: Library
ATTN: Chief, SASAS-L
Jacksonville
ATTN: Library
ATTN: Const. Div
Mobile
ATTN: Chief, SAMEN-C
ATTN: Chief, SAMEN-D
Nashville
ATTN: Library
Memphis
ATTN: Chief, LMMED-DM
ATTN: LMVE/B. D. Gray (3)
Vicksburg
ATTN: Chief, Engr Div
Louisville
ATTN: Chief, Engr Div
St Paul
ATTN: Chief, ED-D
St Louis
ATTN: Library
Kansas City
ATTN: Library (2)
Omaha
ATTN: Chief, Engr Div

US Army Engineer District
New Orleans
ATTN: Library
ATTN: Chief, LMNED-DG
Little Rock
ATTN: Chief, Engr Div
Tulsa
ATTN: Library
Albuquerque
ATTN: Library
San Francisco
ATTN: Chief, Engr Div
Sacramento
ATTN: Chief, SPKEL-D
Japan
ATTN: Library
Portland
ATTN: Chief, DB-6
Seattle
ATTN: Chief, NPSCO
Walla Walla
ATTN: Library
ATTN: Chief, Engr Div
Alaska
ATTN: Library
ATTN: NPADE-R

US Army Engineer Division
Europe
ATTN: Technical Library
New England
ATTN: Library
ATTN: Chief, NEDED-T
North Atlantic
ATTN: Chief, NADEN-T
South Atlantic
ATTN: Chief, SADEN-TS
ATTN: Library
Huntsville
ATTN: Library (2)
ATTN: Chief, HNDED-CS
ATTN: Chief, HNDED-SR
Lower Mississippi Valley
ATTN: Library
ATTN: LMVED-R/J. Graham(6)
Ohio River
ATTN: Library
ATTN: Chief, Engr Div
North Central
ATTN: Library
Missouri River
ATTN: Library (2)
Southwestern
ATTN: Library
ATTN: Chief, SWDED-TM
Pacific Ocean
ATTN: Chief, Engr Div
North Pacific
ATTN: Chief, Engr Div

Facilities Engineers
Ft Campbell, KY 42223
USAECOM
Ft Monmouth, NY 07703
DFAE, USAIC
Ft Benning, GA 31905
TRADOC
Ft Knox, KY 40121
Ft Sill, OK 73503
Ft Bliss, TX 79916
HQ, 1st Inf Div & Ft Riley
HQ, 5th Inf Div & Ft Polk
HQ, 7th Inf Div & Ft Ord

AF Civil Engr Center/XRL
Tyndall AFB, FL 32401

Naval Air Systems Command
ATTN: Library
WASH DC 20360

Naval Facilities Engr Command
ATTN: Code 04
Alexandria, VA 22332

Port Hueneme, CA 93043
ATTN: Library (Code L08A)

Washington, DC
ATTN: Transportation Research Board
ATTN: Library of Congress (2)
ATTN: Dept of Transporation Library

Defense Documentation Center (12)

Engineering Societies Library
New York, NY 10017